DNA methylation profiles of cytokine and transcription factor genes in immune cells: applicability as diagnostic biomarkers

Dissertation

zur

Erlangung des Doktorgrades (Dr. rer. nat.)

der

Mathematisch-Naturwissenschaftlichen Fakultät

der

Rheinischen Friedrich-Wilhelms-Universität Bonn

vorgelegt von

Dipl.-Ing. Claudia Ivascu

Berlin

Bonn, im August 2007

Angefertigt mit Genehmigung der Mathematisch-Naturwissenschaftlichen Fakultät der Rheinischen Friedrich-Wilhelms-Universität Bonn

Wissenschaftliche Betreuung:

Dr. Florian Eckhardt

Brahms AG
Neuendorfstrasse 25
D-16761 Hennigsdorf

Referenten:

1. Referent: Prof. Dr. Klaus Olek

Labor für Abstammungsbegutachtungen
Marie-Curie-Straße 1
D-53359 Rheinbach

2. Referent: Prof. Dr. Norbert Koch

Institut für Genetik
Rheinische Friedrich-Wilhelms-Universität Bonn
Abt. Immunbiologie
Römerstraße 164
D-53117 Bonn

Tag der mündlichen Prüfung: 18.12.2007

Diese Dissertation ist auf dem Hochschulschriftenserver der ULB Bonn
http://hss.ulb.uni-bonn.de/diss_online elektronisch publiziert.

Erscheinungsjahr: 2008

Parts of this work have been published in the following scientific journals:

Ivascu C, Wasserkort R, Lesche R, Dong J, Stein H, Thiel A, Eckhardt F
DNA methylation profiling of transcription factor genes in normal lymphocyte development and lymphomas
International Journal of Biochemistry and Cell Biology. 2007;39(7-8):1523-38.

Ivascu C*, Dong J*, Chang HD, Wu P, Angeli R, Maggi L, Eckhardt F, Tykocinski L, Haefliger C, Möwes B, Sieper J, Annunziato F, Radbruch A, Thiel A
IL-10 is excluded from the functional cytokine memory of human CD4+ memory T lymphocytes
Journal of Immunology. 2007 Aug 15;179(4):2389-96., *equal contribution

The following work was carried out from July 2004 – September 2006 at the Epigenomics AG, Kleine Präsidentenstr. 1, 10117 Berlin, Germany
Parts of this project were realised during a cooperative project with the group of Dr. Andreas Thiel, Dept. of Clinical Immunology, German Rheumatism Research Center (DRFZ), Berlin.
Dr. Jun Dong at the DRFZ has designed and performed experiments regarding isolation of the cell subsets from human blood samples, cell separations by FACS and chromatin immunoprecipitation.

Acknowledgments

Firstly, I would like to thank Prof. Dr. Klaus Olek for the supervision of my doctorate thesis from the initial steps in the Rheinbach laboratory until its completion at the Epigenomics AG and the German Rheumatism Research Center (DRFZ) in Berlin. I am very thankful for many scientific discussions and the support during the entire time.

I thank Prof. Dr. Norbert Koch for kindly accepting to be the second referee of the present work and doctorate procedure. At the same time, I thank Prof. Dr. Karl-Heinz Scheidtmann and Prof. Dr. Johannes Oldenburg for accepting to be examinators and thus part of the doctoral comitee.

The completion of this thesis was only possible with tremendous support from my scientific advisor at the Epigenomics AG, Dr. Florian Eckhardt. I am thankful for fruitful scientific debates, for guidance and perseverance in interpreting scientific data and for the willingness to familiarize with immunology in order to supervise this work. I have learned a lot from him.

I thank the executive and research board of the Epigenomics AG, especially Dr. Ralf Lesche and Dr. Alexander Olek for offering me the possibility to conduct my studies in this exciting field of science and for supporting the cooperation work with the DRFZ.

At the same time, I thank Dr. Jun Dong and Dr. Andreas Thiel at the DRFZ for the the intensive and scientifically enriching cooperation.

The “science” community of the Epigenomics AG deserves sincere thanks for many enlightening and encouraging discussions and for the long hours spend together in the lab: thanks to my friend Anne Fassbender, to Dr. Philipp Schatz, Dimo Dietrich, Rene Cortese, Dr. Reinhold Wasserkort, Dr. Reimo Tetzner, Susanne Auls, Sybille Krüger and Karen Freyberg.

Thanks to Melissa Maldonado, Debjani Roy, Florence Lindhaus, Dr. Philipp Schatz and Dr. Harald Lange for carefully reviewing the manuscript and for several useful suggestions.

Thanks to my boyfriend Jan for the years of encouragement, the strong believe in me and for several enlightening discussions about the medicine part to be found in this work.

Finally yet importantly, I would like to thank my parents and my sister Andrea for their constant love and support ever since I can remember.

1. Summary

The past years have seen an enormous scientific interest in the field of DNA methylation. Numerous studies have documented the functional significance of DNA methylation in the regulation of gene expression and the maintenance of local chromatin structure. A large body of evidence underlines the implication of aberrant DNA methylation in nearly all types of human cancers.

The focus of the current work was to investigate the role of DNA methylation in the human immune system at candidate immune-relevant genes by emphasising two key biological aspects.

First, the role of DNA methylation as an epigenetic mark, possessing the function to memorize the expression phenotype, was analyzed within key cytokine genes. Large-scale methylation profiling experiments of these genes were carried out in designated CD4+ memory T-cells subsets. DNA methylation in the *IL10* gene, encoding the anti-inflammatory cytokine IL-10 and in the *IFNγ* gene, encoding the pro-inflammatory cytokine IFN-γ were of special interest due to the key role of these molecules in the immune response.

Cell type specific differentially methylated regions were found in the genes encoding the cytokines IL-13 and IL-4 in DNA sequences that were previously shown to harbor regulatory elements. This finding suggests a role for DNA methylation in the expression regulation of these genes.

As for the gene encoding the cytokine IFN-γ, low levels of DNA-methylation were measured in human *ex vivo* IFN-γ expressing cells at several CpGs located proximal to the transcription start site and within an enhancer element 5.0 kb upstream. At the same time, IFN-γ non-expressing cells were shown to be strongly upmethylated at the same CpG sites. The specific role of this methylation pattern as a heritable epigenetic mark for rapid expression induction was demonstrated through experiments carried out *in vitro*. Further *in vitro* cultivation experiments were performed to investigate the dynamics between site-specific demethylation and expression induction in the *IFNγ* gene.

In contrast, DNA methylation does not seem to play any role in the regulation of the *IL10* gene. With the exception of two CpGs located in the proximal promoter, slightly demethylated in IL-10 producing cells, no differential methylation was measured between IL-10 expressing and non-expressing cells. The two questionable CpGs do not harbour the epigenetic memory mark for expression since in vitro cultivation of IL-10+ cells under expansive conditions rapidly results in the loss of IL-10 expression without measurable methylation changes at these sites. Further epigenetic analysis at the level of histones revealed covalent modifications like hyperacetylation and trimethylation that are associated with an open chromatin status in IL-10 producing cells as compared to their non-expressing counterparts. These findings led to the conclusion, that the *IL10* gene is excluded from the functional cytokine memory in human Th cells, preventing the generation of memory cells with an inherited program to secrete IL-10, possibly to ensure a limited effect of IL-10 in downregulation of adaptive pathogen-specific immunity.

As a second biological aspect, variations in the level of DNA methylation during development and maturization of the B- and T-cell lineage were monitored in key transcription factors. A set of cell types, resembling major steps of the human hematopoietic development were employed for this analysis.

It could be shown that variations in the local methylation of several transcription factor genes (*SPI1, TCF7, c-maf, Etv5, TBX21* and *GATA3*) is an accompanying feature during development and lineage maturation. For some genes (*SPI1, Eomes* and *Etv5*), an inverse correlation between promoter methylation and the respective gene expression could be demonstrated, suggesting an implication for DNA methylation in the expression of these genes.

Some of the hereby-discovered regions of differential methylation between individual cell types were tested for their use in diagnostic applications such as rheumatoid arthritis, endometriosis and lymphoma.

Specific differentially methylated CpGs in the *IFNγ* gene were successfully used to measure balance shifts of T-helper cell compartments in the peripheral blood of patients with rheumatoid arthritis. By means of the same marker, no differential methylation was found in the endometrium of women with endometriosis as compared to non-endometriosis controls.

Methylation information from specific factors (*SPI1, TCF7, c-maf* and *eomes*) was applied to show aberrant methylation patterns in a B-cell malignancy of the lymph node when compared to healthy tissue. Thus, transcription factors may represent a novel class of aberrantly methylated genes in hematopoietic cancer. In addition, the used candidate gene approach is a valid one for identifying novel tumor biomarkers.

.

2. Introduction

2.1. Role of DNA methylation in the mammalian organism

2.1.1. DNA methylation in humans: patterns and functions

In contrast to classical genetics investigating the inheritance and changes of the genetic code, epigenetics refers to all mechanisms that are not encoded within the genomic sequence and confer to specialized cells a particular and heritable spectrum of gene expression (1), (2). Three key epigenetic mechanisms are described as being responsible for the propagation of the gene transcription and repression information (3): histone modifications like histone alkylation, RNA associated gene repression and DNA methylation (4).

The most stable epigenetic modification of mammalian DNA is the methylation at the 5' position of cytosines found almost exclusively in the context of 5'–cytosine guanine–3' (CG) dinucleotides (5), (6).

The occurrence of CpG dinucleotides in the human genome is only 5–10% of the statistically predicted frequency (7). This underrepresentation is likely due to the high mutation frequency of methylated cytosines as they undergo spontaneous deamination and are thereby converted to thymine. The result is a point mutation at the respective site. Series of spontaneous deamination in the course of evolution are thought to be the cause of CpG duplets depletion in the genome.

The non-random distribution of CG dinucleotides in the genome is of great functional significance. When scanning the genomic sequence for CG dinucleotide pairs, regions with higher proportions of CG dinucleotides than would be expected by chance, are found. These regions are referred to as CpG islands (CGI) and constitute between 1% and 2% of the total genome. The vast majority of CGIs are unmethylated (8), (9) although this finding depends to some extent on the specific definition of a CGI. At present, the widely accepted CGI definition proposed by Gardiner and Frommer requires a sequence length of at least 500bp with a GC content of at least 55% and a ratio between observed and expected CpG dinucleotides of 0.65 (10). The majority of CGIs are located within gene promoters while non-CGI containing promoters tend to be depleted in CpGs (11). Promoter CGIs are frequently, but not exclusively, associated with housekeeping genes and are usually, but not always, methylation free. Several CGIs are located within genes that have a tissue restricted expression pattern. CpGs outside of CpG islands, with 70% to 80% of the total genomic CpG duplets, are largely methylated (12) and are typical of the densely packed, transcriptionally inactive chromatin. Among them are repetitive elements, transposons, and the inactivated X – chromosome.

CpG methylation is maintained by a series of DNA methyltransferases (DNMTs) with different functionalities. Most d*e novo* methylation events occur at early embryonic stages, following the drastic, genome wide methylation decrease observed after fertilization. They are induced by the Dnmt3A and Dnmt3B, two *de novo* methyltransferases which are highly expressed at this stage (13).

However, the pattern after which *de novo* DNA methylation is positioned in the genome in the early phase of embryonic development is still elusive. It has been suggested, that *de novo* methylation in the early embryo is induced preferentially at genomic regions with silent chromatin contributing to the stabilisation of the silencing (6). Simultaneously, transcriptionally active promoters at early embryonic stages remain unmethylated leading thus to the unmethylated CpG islands found in the adult somatic tissue (14).

The maintenance of an aquired methylation pattern during somatic cell division is thought to follow a semiconservative mechanism: the methylation information is copied from the parental strand to the daughter strand by the Dnmt1 (15). This methyltransferase was shown to have a high affinity for hemimethylated substrates as they occur after DNA replication.

The mechanisms underlying the reverse process of DNA demethylation have not yet been elucidated. In principle, it can be achieved passively after abolishing maintenance methylation in the course of cell division. Two classes of enzymes may account for an active demethylation process: DNA demethylases and DNA glycosylases. Although the removal of the CH_3 group by breaking the covalent carbon bound is energetically unfavourable, evidence of DNA demethylase activity is provided *in vitro* for both hemimethylated and fully methylated dsDNA substrates (16). The activity of a DNA glycosylase removing the methylated cytosine from a m^5CpG pair when methylation is present on both strands has been described as the first of a two step process followed by the replacement of the excised base through DNA repair enzymes (17) (18).

DNA methylation accounts for several effects in healthy tissue. An increase in methylation results in stable transcriptional silencing as evidenced in the X chromosomal inactivation, genomic imprinting, the stabilisation of chromosomes by silencing of transposable elements (19), (20), and the regulation of tissue restricted gene expression. Further, DNA methylation plays a crucial role during embryonic development (21). In the following paragraphs, some examples of known DNA methylation effects are highlighted.

X chromosome inactivation

X-inactivation in females is a process by which one of the two copies of X-chromosome present in female mammals is inactivated. The choice of which X chromosome will be inactivated is random but once an X chromosome is inactivated, it will remain inactive throughout the lifetime of the cell.

In contrast to the active X the inactive X chromosome (Barr body) has high levels of DNA methylation, low levels of histone acetylation, low levels of histone H3 lysine-4 methylation, and high levels of histone H3 lysine-9 methylation. Each of these epigenetic marks is associated with heterochromatin formation and gene silencing and mediates the inactivation of the chromosome. The X-inactivation center (XIC), a region on the X- chromosome encodes for two non-translated mRNAs: the *Xist* and the *Tsix* mRNA, transcribed antisense to Xist. *Xist* RNA accumulates along the X chromosome containing the active *XIST* gene and proceeds to inactivate almost all of the other hundreds of genes on that chromosome. Following this physical deactivation, large parts of the chromosome are silenced by DNA methylation. The *Xist* gene on the active X chromosome is silenced by DNA methylation (22).

Tsix mRNA is a negative regulator of Xist: it acts by preventing its abundant accumulation on the active X chromosome (23).

Genomic imprinting

DNA methylation plays a crucial role in genomic imprinting, a phenomenon in mammals where the father and mother contribute different epigenetic patterns for specific genomic loci in their germ cells resulting in an allele-specific gene expression for some genes.

Imprinting is mostly achieved through DNA hypermethylation at one of the two parental alleles of a gene. This is already affectuated in the gamete or the zygote with the consequence of monoallelic expression of the gene (24). Differential expression can occur in all cells, or in specific tissues or developmental stages. About 80 genes are currently known to be imprinted, and this number is continually increasing. Prominent non – cancerous imprinting disorders are the Beckwith-Wiedemann, the Prader–Willi and the Rett syndrome (25).

Conversely, loss of imprinting (LOI) is the disruption of imprinted epigenetic marks through gain or loss of DNA methylation, or simply the loss of normal allele-specific gene expression (26). LOI deserves special attention since it is a frequent event in tumor development. There, acquired defects in the imprinting of e.g. growth-promoting genes lead to activation of the normally silent allele and result in abnormally high expression of the gene product. Consequently, the cell gains a growth advantage. A prominent example of such aberrant activation is the insulin growth factor 2 gene *IGF2* / *H19* locus mapping to 11p15.5 where defective imprinting of the *IGF2* gene is the most common LOI event across a wide range of tumor types, including colon, liver, lung, and ovarian cancer, as well as Wilms' tumor (27), (28).

Silencing of repetitive elements

Cytosine methylation inactivates the promoters of most viruses and transposable elements, including retroviruses and Alu elements. Thus, unconstrained transposition possibly leading to chromosome instability and large expression of irrelevant promoters is efficiently blocked (29), (30), (31).

Hypomethylation, defined as the decreased level of DNA methylation at a certain genomic region, is frequently seen in the promoters of the parasitic elements in cancer cells as a consequence of global hypomethylation. The methylation dependent reactivation of these elements is a driving force towards the genetic instability seen in cancer cells (32).

Tissue specific methylation

An increasing number of genes are described as being methylated in a tissue specific manner. Often, the methylation pattern can be correlated to their expression status in the respective tissue. In addition, recent studies, including the work presented here, have revealed several tissue specific methylation patterns outside of gene and proximal promoter regions and of yet unknown functionality (33), (34).

A large number of examples are available demonstrating that CpG islands contain tissue-dependent and differentially methylated regions (T-DMR) which are potential methylation sites in normal cells and

tissues. It was hypothesised that during tissue differentiation and development, transcriptionally relevant regions in the genome become selectively de- or upmethylated to enable the transcription of a restricted set of genes within a given tissue. This can occur during both, embryonic tissue differentiation and adult stem cell differentiation (hematopoiesis, bone marrow stem cell differentiation) (35), (36). Prominent examples are the germline specific genes like the melanoma antigen gene family MAGE (*MAGE-A1* and *LAGE-1*) encoding tumor specific antigens. The promoters of these genes consist of CGIs which are essentially unmethylated in germline cells but become strongly methylated in somatic tissue (37). Song *et al.* have identified T-DMRs in the mouse located in the 5' regions of transcription factor genes and demonstrated the inverse correlation between methylation and expression for several tissues (brain, kidney, liver, testis, colon and muscle) (38). Further, large scale methylation studies involving entire chromosomes have revealed several T-DMR loci and correlated their methylation patterns with transcription in several tissues (39), (33).
Weber *et al.* have recently demonstrated that especially weak CpG island promoters, with a relatively low level of CpGs, are predisposed to de novo DNA methylation during development and that these types of promoters are most frequent in tissue specific expressed genes (14).

DNA methylation in embryonic development
Experiments in mice have demonstrated radical changes in the genome – wide methylation level during gametogenesis, fertilisation and early embryo formation.
During gametogenesis, a genome – wide DNA methylation erasure process followed by a re-methylation, has been described (40). After fertilisation, the genomes inherited from both sperm and oocytes undergo another cycle of erasure of most of their associated DNA methylation. While the paternal genome is actively demethylated, the methylation on the maternal genome is removed passively during cell division processes. It is not before the gastrulation (implantation) of the zygote and the differentiation of the initial embryo cell layers that lineage-specific patterns of *de novo* methylation are established (41), (42).

2.1.2. Role of DNA methylation in the regulation of gene expression

The most important role of DNA methylation is the regulation of gene expression. There is abundant evidence that DNA methylation in the promoter region of genes correlates directly with transcription activity (43). An important line of evidence in demonstrating the suppressive potential of DNA methylation was provided using the cytosine analogue 5–aza-2'-deoxycytosin in cell lines. This cytosine substitute is efficiently incorporated into the cellular DNA but cannot be methylated due to the presence of a nitrogen atom at the 5' position of the pyrimidine ring. Repressive states of several gene promoters could be reversed followed by activation of transcription of the associated gene (44).
The mechanisms through which the methylation mediates transcriptional repression are both direct and indirect. Two biologically relevant mechanisms have thus far been described as being interdependent events leading to silencing at a certain genomic locus (Figure 2-1).

1.) Direct transcription repression is thought to occur by inhibiting the binding of transcription factors to their recognition sites in the respective promoters. This is presumably accomplished by protruding into the major DNA helix groove (45). Several transcription factors, including c-Myc/Myn, AP-2, cAMP dependent CREB, E2F and NF-κB, recognise sequences that contain CpGs, many of which were shown to be methylation sensitive (46), (47).

2.) Indirectly, methylated DNA recruits methyl cytosine binding proteins (MeCPs) which have been shown to bind to methylated CpG dinucleotides in any sequence context and to prevent further transcription factor binding. In addition, MeCPs mediate repressive chromatin remodelling by associating with large protein complexes containing co-repressors and histone deacetylases leading to heterochromatin formation in the respective DNA region (48).

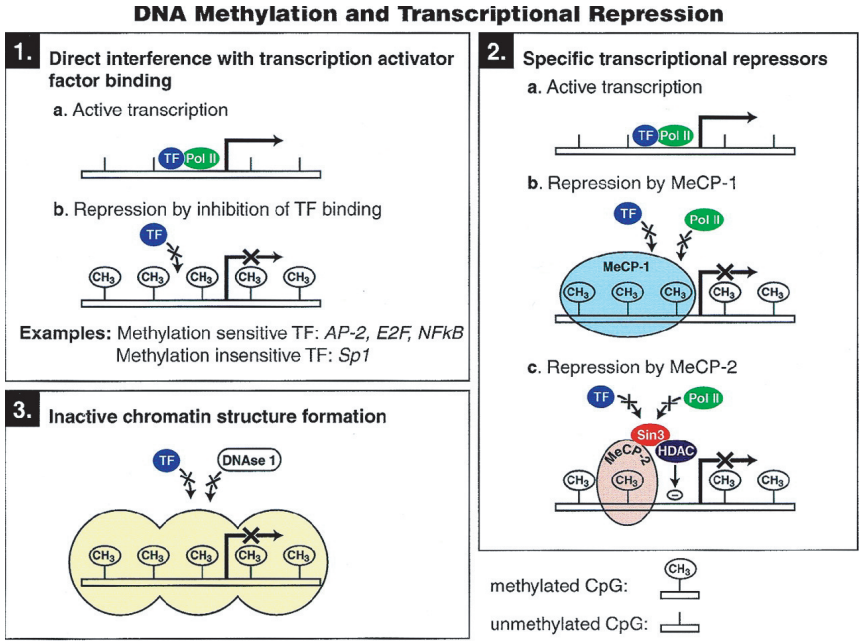

Figure 2-1 Proposed mechanisms of transcription repression mediated by DNA methylation. The left column shows the direct repression mechanisms through sterical inhibition of transcription factor binding. The right column shows the indirect mechanisms, where methylated DNA recruits methyl binding proteins and histone deacetylases thereby inducing a repressive chromatin status (Singal et. al 1999).

2.1.3. DNA methylation in T-lymphocytes: role as epigenetic memory

The immune system is a fertile field for studies of epigenetic regulation of cell fate and function as it allows for the obtainment of pure cell populations from nearly every step during adult blood cell development. There is evidence for epigenetic regulation of several key immune processes including lymphocyte development, antigen presentation, differentiation, cytokine expression, effector function, and memory.

One of the most intriguing questions is that of differentiation: how does a precursor cell give rise to daughter cells with a different set of expressed genes and further, by means of which mechanism is the daughter cell capable of remembering the inductive event leading to its phenotype? Epigenetic mechanisms, including DNA methylation, seems to partially answer this question. Current evidence that DNA methylation acts together with additional epigenetic processes to limit the probability of aberrant gene expression and to stabilize, rather than to initiate, cell fate decisions during lineage commitment has been provided.

Human B-lymphocytes develop in the bone marrow. In contrast, T-lymphocytes travel undifferentiatedly to the thymus, later to lymph nodes and the body tissue. There, the final maturization takes place in the presence of MHC attached antigens. Both lymphocytes, B- and T-cells are generated in the adult organism from a common progenitor, the CD34+ hematopoietic stem cells located in the bone marrow and require a number of specific extracellular stimuli at each step to accomplish lineage commitment (36). Development to mature T-lymphocytes requires several intermediate steps during which rearrangements at T-cell receptor genes take place in early stages, followed by a “naive” cell status prior to antigen encounter and the selective induction of a restricted set of poised cytokine genes and stable silencing of other cytokines. Figure 2-5 schematically illustrates the individual differentiation steps that lymphocytes undergo during differentiation and maturization in their distinct lineages.

T-lymphocytes differentiate first into cytotoxic CD8+ cells and CD4+ T-helper cells, the latter developing further into “effector” cells. These are categorised based on the secretion of non-overlapping patterns of cytokines such as IFN-γ (T-helper 1) or IL-4, IL-13 and IL-5 (T-helper 2) (49).

DNA methylation is involved in the regulation of the two co-receptor genes *CD8* and *CD4*. Progressive DNA demethylation occurs during differentiation from CD4-CD8- into CD8+CD4+ double positive thymocytes at the *CD8* locus (50), (51) while in the parallel lineage the *CD4* locus becomes demethylated leading to CD4+ thymocytes (52). Demethylation and expression induction occurs in activated CD8+ T-cell clones within the IL-3 promoter, with most of the demethylation occurring at a specific CpG site 164bp upstream of the transcriptional start (53).

In naive CD4+ cells, the effector cytokines IFN-γ and IL-4 exist in a restrictive chromatin structure but are not completely transcriptionally silenced. Activators such as lineage specific transcription factors can bind and induce low transcription activity. As the cells mature and differentiate into the two T-helper cell subsets, regulatory elements in both genes, *IFN-γ* and *IL-4* become demethylated. In parallel, strong expression of the genes is induced and they remain in a heritable status of expression. This status appears to be “locked in”, since absence of the associated transcription factors in the mature cells does not result in transcriptional silencing of the respective cytokine. (54), (55), (56). Recently, demethylation at a single CpG site in the promoter of the *IL-2* gene was demonstrated to be responsible for stably maintained IL-2 expression in activated T-cells (57). All of the above-described phenomena require iterated cell divisions through which the methylation signals at the specific sites are removed through the passive mechanism of repressed maintenance methylation.

Although not the exclusive mechanism, DNA methylation obviously contributes to the establishment and memorization of transcriptional thresholds that vary between genes and T cell types.

2.1.4. DNA methylation in cancer

The first indication, that DNA methylation is directly implicated in cancer formation was published already in 1979 (58). A few years later, Gama-Sosa *et al.* showed that the overall 5–methylcytosine content is strongly reduced (20 – 60% less) in tumor cells as compared to their normal counterparts, leading to the first connection between DNA methylation and cancer: *global DNA hypomethylation in cancer* (59). Global hypomethylation is defined as the genome wide reduction of the methylation content. It can lead to the transcriptional reactivation of intragenomic parasitic DNA otherwise repressed by DNA methylation, a common finding in tumorigenesis (60), (19). This phenomenon appears to begin very early in affected cells and thus to precede frank tumor formation (61). The direct effect of oncogene reactivation in the development of tumors has not yet been proven. Examples of demethylated oncogenes in neoplasia are the *bcl-2* gene in B-cell chronic lymphatic leukaemia and the *k-ras* proto-oncogene in lung and colon carcinomas (62), (63).

In parallel to the genome wide loss of methylation, several genes (including many critical to the tumor phenotype) display an increase in methylation during tumorigenesis. This process leads ultimatively to epigenetic silencing of expression and loss of protein function.

A widely studied effect of DNA methylation in cancer, with implication to both diagnostics of cancer and therapy, is the *hypermethylation of tumor-suppressor genes*. Hypermethylation, the increase of methylation level at certain (usually CpG island associated) promoters, is considered to be a common hallmark of all types of human cancer, affecting genes involved in several cellular pathways. Affected pathways are: the DNA repair, the cell cycle, the cell adherence, apoptosis, detoxification and hormonal response pathways (64), (65). Recent publications have revealed genes that belong to the non–classical pathways such as developmentally active transcriptional regulator as targets for hypermethylation in several types of cancers (66).

The transcription factors analyzed in this work represent a new class of genes previously not associated with hypermethylation in tumors.

Interestingly, during tumor formation, specific CpG islands become hypermethylated in an otherwise globally hypomethylated surrounding of a cancerous cell. This specific *de novo* methylation is thought to be either directed at target DNA sequence motifs (67) or the consequence of clonal selection of the hypermethylated phenotype in response to an advantageous surrounding.

In the last few years, an increasing number of genes have been characterized as genes in which associated promoter CpG islands are hypermethylated in cancer. DNA-methylation mapping has revealed unique profiles of hypermethylated CpG islands that are specific for each type of neoplasia. For example, the *GSTP1* gene promoter hypermetyhlation occurs in 70-80% of prostate cancer cases, while hypermethylation of the *BRCA1* gene is typical for breast and ovarian tumors but does not occur in any other tumor type (68).

Further, loss of DNA methylation at imprinted or tissue specific genes (LOI) leading to the activation of an otherwise silent allele is a well established mechanism of gene activation in certain types of cancer, as recently reviewed (25).

Recently, it has been demonstrated that microRNAs that have tumor-suppressor function can also undergo DNA-methylation-associated silencing in tumor cells (69), (70). This finding might indicate an additional contribution of DNA hypermethylation events to cancer development.

2.2. DNA methylation measurement

2.2.1. Measurement principles

DNA methylation is a binary event at the level of a single stranded DNA stretch: a given cytosine residue within a CpG dinucleotide complex is either methylated or unmethylated. However, a genomic DNA sample is heterogeneous for two reasons. First, a double stranded DNA molecule can display hemimethylation at a specific CpG: one strand is methylated, the palindromic cytosine is unmethylated. Second, the individual cells within a given sample usually consist of a heterogeneous mix of DNA molecules. Therefore, analysis of the DNA methylation distribution in a given sample can be performed at different levels, depending on the desired level of information. One can analyse: (1) the methylation content, (2) the methylation level or (3) the methylation pattern of a genomic sample (71). Figure 2-2 displays the different approaches for determining the desired methylation information from a given sample.

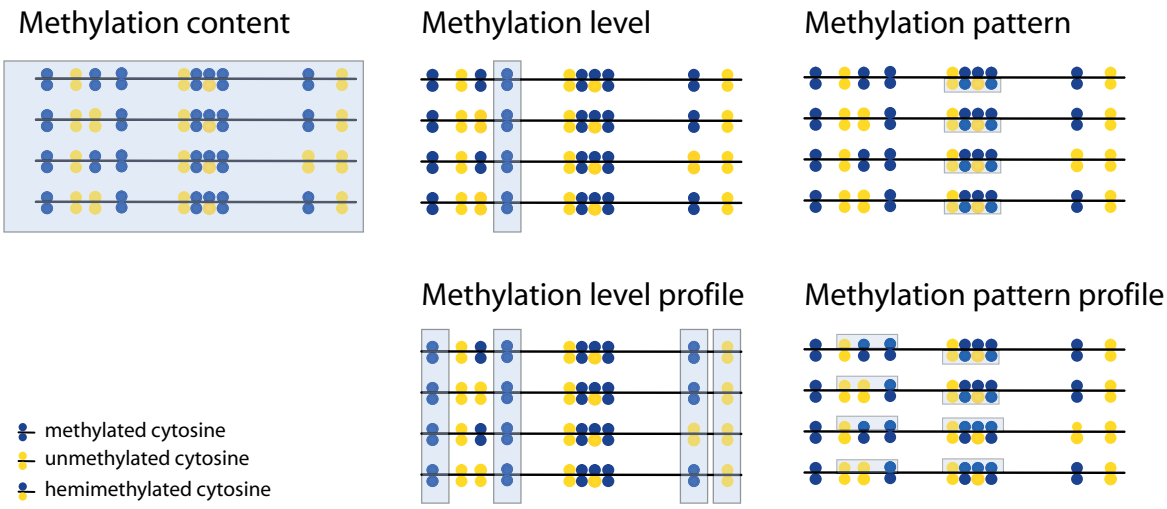

Figure 2-2 DNA methylation analysis principles. Horizontal bars represent double stranded DNA with the methylation mark either on both strands or on the single strand as hemimethylated DNA locus. The grey shaded areas represent the CpGs participating in the described measurement principle. Methylation content represents the total amount of methylated CpG in the genome; methylation level refers to the average methylation frequency at a single CpG while methylation pattern refers to a series of consecutive CpGs located in cis on a single DNA strand. (Laird, 2003).

As suggested by its name, the methylation content delivers information on the total methylation amount of the nucleic acid within the analyzed sample. This type of information is useful for the determination of e.g. global hypomethylation in cancer and stem cells or the general comparison of methylation contents within different species. However, no site-specific methylation information can be derived from the methylation content. More useful with regard to the functional relevance of DNA methylation and its application in medical diagnostics is the determination of the methylation level or the methylation

pattern of a given genomic sample. Methylation level refers to the frequency of methylation at an individual CpG dinucleotide in the genome and may be important for quantifying differences at regulatory sequences. Further, the methylation patterns deliver detailed methylation information on a set of CpGs located within a DNA stretch of several hundred base pairs. Both methylation level and the methylation pattern can be generated as “profiles” whereby the methylation status across many sites in the genome, either at individual CpGs or within distinct sequence stretches, is collected. This is very useful when a panel of distinct markers is being employed for e.g. molecular classification of cancer subclasses. All analyses performed in the current study are profiles of DNA methylation levels of candidate genes. The direct bisulfite sequencing technique that was used (described in detail in the next chapter) allows for the parallel determination of DNA levels of series of CpGs located within a sequence stretch covered by a PCR fragment. The methylation level of each individual CpG site is determined independently.

2.2.2. Detection methods

2.2.2.1. Genome wide methylation content

As already described, DNA methylation can be assessed independent of a specific sequence (genome wide methylation content) or sequence specific (methylation level and patterns). The genome wide methylation content can be determined by chromatographic methods like thin layer chromatography (72), HPLC (73), capillary electrophoresis (74) or by immunological techniques with e.g. anti 5-methylcytosine antibody (75).

2.2.2.2. Sequence specific methylation analysis

Markers that are differentially methylated between samples of different origin are almost exclusively site and sequence specific methylation signals. They are expected to enable, either as a single markers or as part of a marker panel, clinical diagnostics based on DNA methylation in the near future. The currently available techniques can be roughly divided into two categories: restriction enzyme and bisulfite conversion based methods.

Methylation sensitive enzymes

A large set of methylation sensitive restriction enzymes is currently available for methylation detection. With few exceptions, most enzymes digest exclusively unmethylated DNA at their specific restriction site leaving methylated DNA intact. The identification of differentially methylated regions based on the generated restriction fragments can be performed on a genome wide scale. This is possible either through random amplification (methylation specific arbitrarily primed PCR, MS-APCR) or by ligation of DNA linkers and subsequent amplification. Comparison analysis between different samples is performed by techniques such as 2D-gel electrophoresis (restriction landmark genomic screening,

RLGS), subtractive hybridisation followed by sequencing (methylated CpG island amplification-representational difference analysis, (MCA-RDA) or microarray hybridisation (differential methylation hybridization, DMH) (76), (77) (78), (79), (80).
Disadvantages of all methods relying on methylation sensitive restriction are the incomplete enzymatic digestion and the necessity of a restriction site for detecting differences at a specific desired site.

Methylation analysis of bisulfited DNA

Sequence specific methylation measurement has been revolutionised by the introduction of sodium bisulfite conversion of DNA combined with PCR amplification techniques (81). The methylation information is thus converted to DNA sequence information: the reaction catalyses the specific deamination of unmethylated cytosine to uracil. In the subsequent PCR amplification, the uracil is replaced by thymine leading to a sequence polymorphism measurable by conventional genomic methods (Figure 2-3).

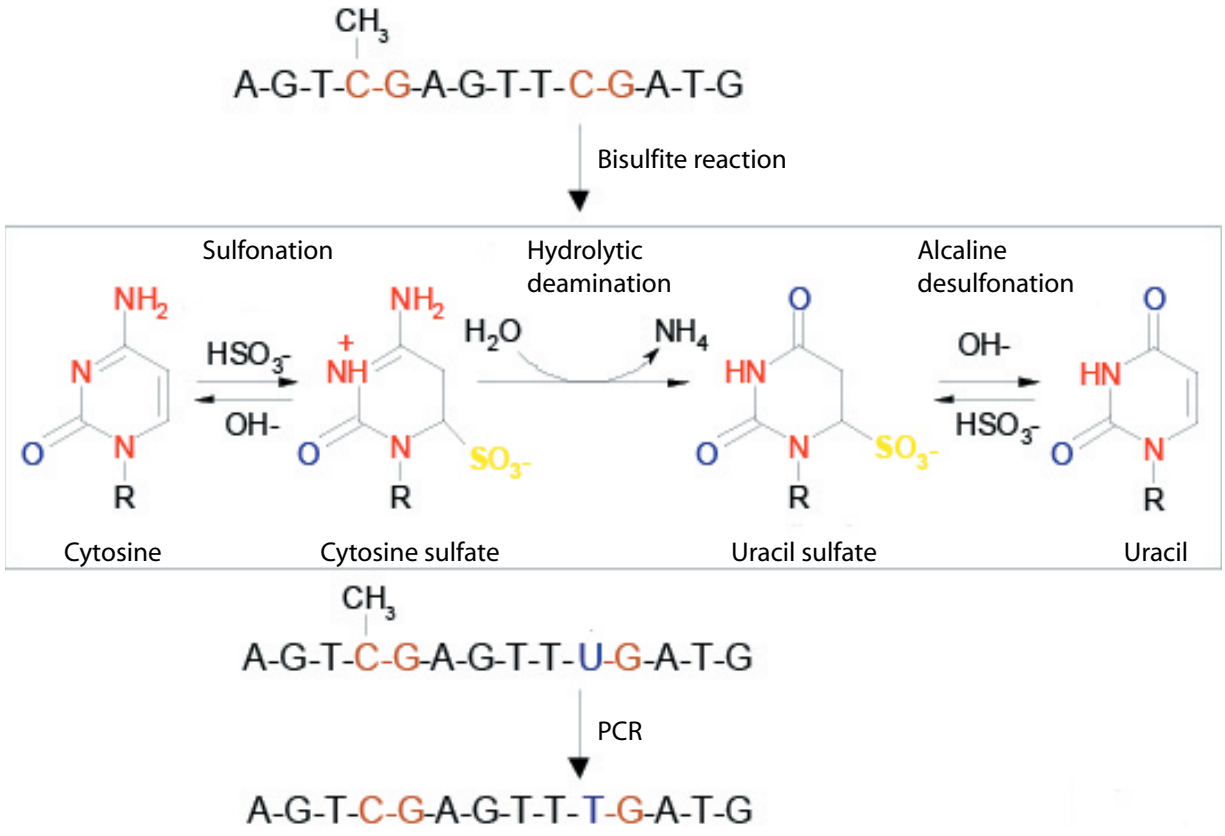

Figure 2-3 Bisulfite conversion of DNA. In the presence of sodium bisulfite, unmethylated cytosine is irreversibly converted to uracil through a series of intermediate products.

Conversion of the cytosine base is only possible in single stranded DNA. Thus, genomic DNA must be denatured prior to the bisulfite reaction. Upon completion of the reaction, the two initially complementary DNA strands loose complementarity since previously unmethylated non-CpG cytosines are all converted to uracils. The strands are referred to as bisulfite 1 and bisulfite 2 strands. Both

strands carry the methylation information and both can be amplified to measure methylation levels. For subsequent amplification of bisulfite DNA sequence specific primers are employed. Depending on the applied detection principle used, the primers can either be located to cover CpG positions and thus to discriminate between methylated and non-methylated DNA already during the amplification step or within CpG depleted regions. With regard to the latter, the higher the content of non-CpG cytosines in the primer sequence, the better the selection for efficiently converted DNA.

By converting genomic to bisulfite DNA one can determine methylation levels and methylation patterns as well as the profiles of both (Figure 2-2) and analyse them by several of the available methods.

Restriction enzyme assays are used to specifically digest previously amplified bisulfited DNA, followed by fragment analysis by gel or capillary electrophoresis (combined bisulfite restriction analysis, COBRA) (82).

Several real-time PCR applications are available for the quantitative analysis of methylation. MethylLight, for example makes use of sequence specific Taqman probes, which carry a fluorescence dye at the 5' end, and a quencher at the 3' end. If hybridisation is successful, the 5'-3' exonuclease activity of the polymerase hydrolyses the probe and releases the dye thereby generating a detectable signal (83). Although this method is suitable for high throuput, the CpG density which can be analyzed is relatively low.

Currently available methods developed for the analysis of DNA methylation have been reviewed by Laird, 2003 (71).

A powerful high throughput technique enabling the simultaneous measurement of methylation levels at several CG dinucleotides is the direct bisulfite sequencing. The method has been heavily used in the current work. It involves the sequence specific amplification of bisulfited treated DNA and the immediate sequencing of the generated PCR products, without laborious subcloning procedures. The sequencing workflow, material ressources and costs are reduced and the sequencing throughput can be significanty increased. To quantitatively determine the mixed methylation signal resulting from heterogeneously methylated DNA special software was employed (84).

The procedure of direct PCR product bisulfite sequencing involves a series of consecutive steps. The methylation level at a specific CpG site of an individual genomic DNA sample is transformed to a cumulative signal where methylated cytosines are detected as cytosines and unmethylated cytosines as thymine. The laboratory procedure involves the bisulfite treatment of the previously purified genomic DNA, the amplification of the desired genomic region by means of sequence specific primers, the sequencing and subsequent analysis and data representation by means of a methylation heat chart. The method steps from a heterogeneously methylated DNA sample to the quantitative methylation data representation are schematically shown in Figure 2-4.

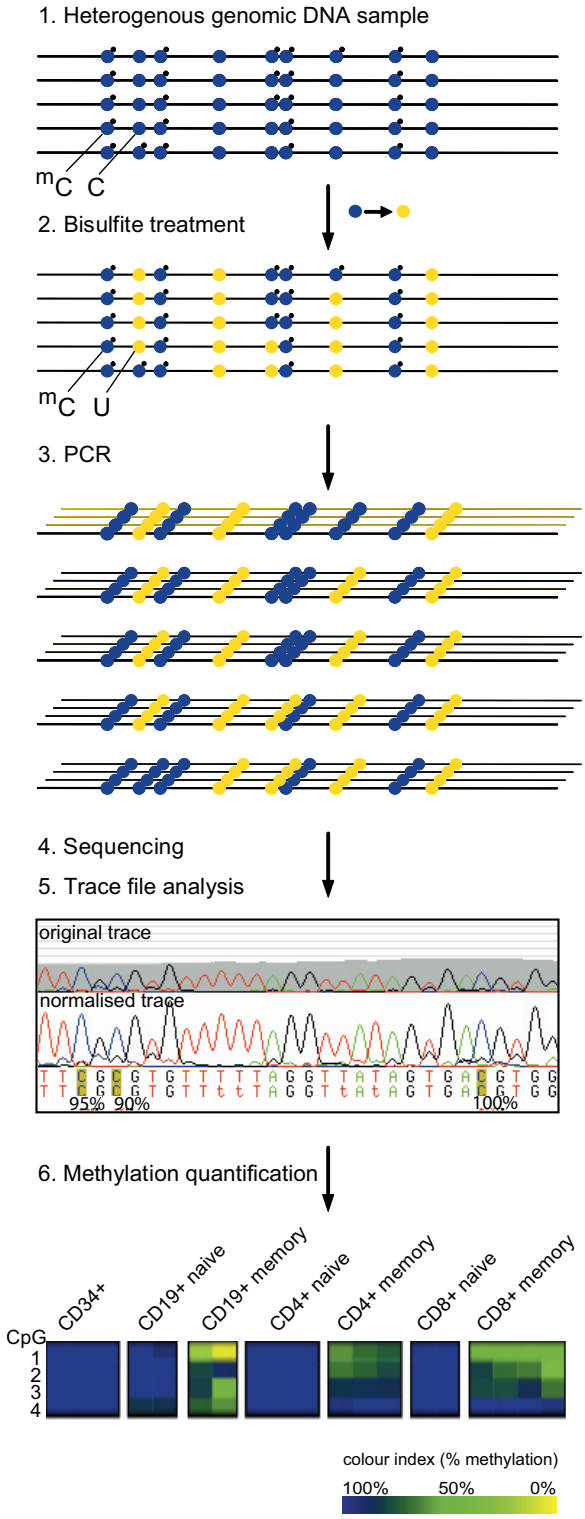

Figure 2-4 Bisulfite sequencing workflow showed schematically for a heterogeneously methylated genomic sample. After bisulfite treatment (2), methylated cytosines remain cytosine while unmethylated cytosines are converted to uracil. Sequencing of the previously amplified genomic region (3 + 4) reveals overlapping C and T signals at each individual CpG position (5). Quantification of the peak areas after normalisation allows for the methylation quantification, which is subsequently colour coded and represented in a methylation heat chart (6).

2.3. Cytokines and transcription factors in the immune system

2.3.1. The cytokines interleukin 10 (IL-10) and interferon-γ (IFN-γ)

IL-10

IL-10, *alias* cytokine synthesis inhibitory factor (CSIF) is an important regulatory cytokine with an overall immunosuppressive effect on the immune response. Many cell types including T-cells, monocytes, macrophages and dendritic cells, produce IL-10. Also, several subsets of regulatory T-cells (Treg) express IL-10. Tregs are suppressor T-cell types that have regulatory effects on the humoral and the cell-mediated immune responses and play an important role in the avoidance of allergic reactions and autoimmune disease (85).

IL-10 exerts its inhibitory action on macrophages and dendritic cells, thereby regulating effector cell activation. However, it also has stimulatory effects on B and T-cells (86). *IL-10*-deficient mice develop severe chronic enterocolitis (87) while tissue or cell-specific overexpression of IL-10 leads to impaired immune responses (88), (89). Animal and human studies revealed that IL-10 is produced during pregnancy by the trophoblast, thus suggesting an important antiabortive role during pregnancy (90), (91).

The expression of *IL10* is under the control of several transcription factors such as Stat3 (92), Sp1 (93) and Sp3 (94), NF-κB (95), Smad-4 (96), c-Maf (97) and Jun proteins (98). However, there is still lack of understanding about the epigenetic events that regulate IL-10 expression in humans and there is only scarce information on the DNA methylation status of the promoter region. Recent data obtained on the *IL10* gene accessibility with respect to DNase I hypersensitivity sites (HSS) have suggested chromatin remodelling of the gene locus in mice (99), (95), (100). This is of special interest, since the murine and human *IL10* promoter show regions of high sequence similarity, refered to as conserved non-coding sequences (CNS) which have been shown to maintain regulatory functions. The *IL10* promoter does not harbour a CpG island.

In the present study an extended region 5' upstream of the transcriptional start site and intragenic sequences of the *IL10* gene are profiled for DNA methylation in subsets of human T-helper cells isolated directly *ex vivo*. Further, additional epigenetic marks such as histone modifications are analyzed at the *IL10* locus. The DNA methylation status was assessed during several rounds of in vitro cultivation.

IFN-γ

IFN-γ is a key cytokine produced primarily by natural killer cells (NK), CD8+ and CD4+ T lymphocytes. IFN-γ facilitates host defense to intracellular pathogens and stimulates growth and differentiation of T- and B- cells, macrophages and NK cells. Further, IFN-γ and Th1 lymphocytes were shown to prevent primary tumor development by regulating tumor cell immunogenicity (101).

IFN-γ is part of the effector cytokine network in the immune response of T-helper 1 cells. Its presence leads to the inhibition of T-helper 2 cell activation.

The regulation of this effector cytokine gene has been intensively studied over the last few years at the level of chromatin modifications, DNA methylation and DNase I hypersensitivity sites. Computational studies of interspecies DNA sequence comparison (human and mouse) revealed a highly conserved distal enhancer sequence located ~5kb upstream of the transcription start (102). This region has been shown to be DNAse I hypersensitive in Th1 cells but not in Th2 cells in the mouse. In addition, it is the binding site of two essential transcription factors: NFAT1 and the Th1 specific factor TBX21.

Another DNase I hypersensitivity site with permissive chromatin status was found at 3.5kb upstream of the transcription start. This region was shown to be the binding site of the Stat5 transcription factor and its remodelling to be dependent on IL-2 (103).

Studies on DNA methylation at the *IFNγ* locus have shown the upmethylation of several CpG sites in non-expressing Th2 cells but a demethylated status of the same sites when IFN-γ was expressed in Th1 cells. Furthermore, 5-azacytidine treatment of Th2 cells induced IFN-γ expression, demonstrating an essential role for methylation in the tissue restricted regulation of the gene (104), (105).

In this study a large stretch of the *IFNγ* promoter and several intragenic CpGs mostly located in highly conserved sequence domains, were analyzed for DNA methylation in *ex vivo* human T helper cell subsets. *In vitro* experiments were performed where naive CD4+ T-cells were stimulated under different conditions to determine the optimal external stimulus and to describe the time course of site-specific demethylation. The differentially methylated regions were used to quantify Th cell balances in CD4+ memory cell subsets of patients with rheumatoid arthritis and to compare them to healthy individuals. Further, the methylation status of these regions was assessed in the DNA obtained from endometrial biopsies of patients with endometriosis.

2.3.2. Transcription factors

The importance of proper orchestration of transcription factors (TFs) expression in normal hematopoietic development has been highlighted by experiments showing that altered quantitative expression of a single TF can lead to leukaemia (106), (107). The observation that many TFs are expressed in a lineage-specific manner makes them potential candidates for epigenetic control through e.g. DNA methylation. However, little is yet known about the epigenetic mechanisms involved in the regulation of these genes.

In patients with hematological malignancies, TFs are frequently mutated or aberrantly regulated (108), (109). Thus, it may be hypothesized that aberrant promoter methylation of these genes could represent one mechanism contributing to hyperproliferation and in some cases to malignant transformation.

Transcription factors (TFs) and their interactions within signalling pathways are key in the regulation of lineage commitment as well as the maturation of human hematopoietic cells, and act at various stages (110), (111). For example, the Wnt / beta-catenin signalling transcription factor TCF7 is required to maintain the pluripotent status of progenitor cells (112). Notch-1 is essential for intrathymic T-cell

lineage commitment and subsequent T-cell development (113). Other TFs are required to confer lineage specificity, such as Eomes for CD8+ cells, TBX21 for CD4+ T-helper 1 cells (114) and STAT6, GATA3 and c-maf for CD4+ T-helper 2 cells (49).

In this study, the role of DNA methylation during hematopoietic development was analyzed through DNA methylation profiling, focusing on a set of 13 key TF genes (Figure 2-5).

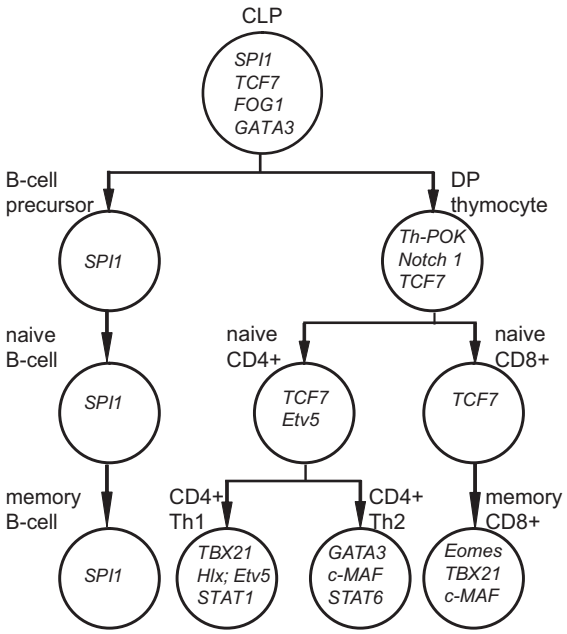

Figure 2-5 Simplified scheme of human adult lymphopoiesis. The stage-specific expression of various transcription factors analyzed in the present study is shown. For simplicity, the expression pattern of some genes and cell types has been omitted. In total, 13 transcription factors were analyzed: SPI1, c-maf, TCF7, FOG1, NOTCH1, Th-POK, GATA3, Hlx, TBX21, Eomes, Stat1, Stat6 and Etv5. Common lymphoid progenitors (CLPs) differentiate to either B-cell (left branch) or to CD4+/CD8+ double positive (DP) lymphocytes (right branch). CD4+: CD4+ lymphocytes, CD8+: CD8+ lymphocytes, Th1: T-helper 1 cells, Th2: T-helper 2 cells.

The selected TF genes included those expressed during early lymphoid development (*TCF7*, *STAT6, GATA3* and *SPI1 (PU.1)* (Gomes et al., 2002)), as well as Th2 - (*GATA3*) and Th1 specific factors (*Hlx1*, *STAT1*). Other factors such as *c-maf* and *TBX21* are expressed in both CD8+ and CD4+ lymphocytes. In addition, CD8+ specific factors were selected (*eomes*), factors which are involved in early thymocyte development (*Notch-1*) and later CD4/CD8 (*Th-POK*) lineage determination (115), (116) and co-activators such as *FOG-1* (117). *Etv5* (*ERM*) is expressed in naive and Th1 CD4+ lymphocytes (118) and was selected because of its drastic up-regulation during neoplastic B-lymphocyte development (119).

DNA methylation profiles of the above genes were assessed in healthy hematopoietic progenitor cells and in selected stages and lineages of T- and B-lymphocytes. The aim was to determine if, and at which specific CpG position the methylation information changes during development and lineage commitment. To determine if the profiled TF genes were aberrantly methylated in lymphomas, all genes were analyzed on DNA from lymph node biopsies of two non-Hodgkin lymphoma entities: a B-

cell neoplastic disorder (diffuse large B-cell lymphoma, DLBCL) and T-cell non-Hodgkin lymphoma (T-cell NHL).

2.4. DNA methylation as diagnostic tool

Interest in DNA methylation has experienced a boom in the last few years as its relevance in human malignancies has become evident. DNA methylation markers have a promising future in both clinical diagnostics and therapeutics but yet are restricted almost exclusively to cancer. In cancer research, the term “marker” or “biomarker” refers to a substance or process that is indicative of the presence of a certain cancer phenotype in the body.

The primary diagnostic applications are obvious but they can also influence the therapeutical options as several methylation markers have been described to be predictive of response to therapy through stratification of patient groups (71). As methylation is an early event in carcinogenesis the identified markers have the potential to be early indicators of existing disease and thus can be of tremendous importance in cancer diagnostics.

DNA methylation is, in contrast to gene expression, a very stable modification of the DNA. It can be measured in samples obtained by non-invasive methods such as in body fluids (blood, plasma, sputum, urine, etc.) through detached cancer cells or through the free floating DNA that is released from apoptotic or necrotic tumor cells (120), (121). However, the prerequisite for this type of sensitive measurement is a marker which is specifically hypermethylated in cancer cells but hypomethylated in “normal” cells.

2.4.1. Rheumatoid arthritis (RA)

Rheumatoid Arthritis (RA) is a crippling disease that affects 0.5 % of the population, mainly women (3:1) in the prime of their life (onset either between 35 – 45 y or after 60, sometimes at childhood age). It is a chronic inflammatory autoimmune disorder which leads to the accumulation of inflammatory T-cells in the synovial membrane of joints and ligaments. The consequence being that the immune cells induce an injury response in the joint, which in turn leads to the formation of tissue (pannus) that is invasive and has a destructive character.

The articular inflammation in RA causes activation and proliferation of the synovial lining, expression of inflammatory cytokines, chemokine-mediated recruitment of additional inflammatory cells, as well as B cell activation with autoantibody production. The measurements of cytokine levels in the synovium of RA patients has revealed a broad range of highly expressed macrophage and fibroblast cytokines such as IL-1, IL-6, IL-15, IL-18, TNF-α, granulocyte – macrophage colony stimulating factor (GM-CSF) and several chemokines.

The naturally occurring suppressor cytokines including TGF-β, IL-1Ra and IL-10 are expressed at levels that are insufficient to block the destructive process.

The role of DNA methylation has so far not been studied in RA. Since the pathological mechanism requires strong overexpression of pro-inflammatory cytokines, a defective expression control within these genes is probable.
The clinical diagnosis of RA is complex and currently cannot be performed by means of a single test. Instead, it is an evaluation of several parameters gathered from patient history, physical examination, blood tests and RA-specific molecular diagnostic testing of patient serum. A non-invasive and highly specific serum based test is needed to quickly diagnose and efficiently treat the disease.
Studies on the peripheral blood of RA patients described a disturbed Th1 / Th2 cell balance, whereby a reduction of Th1 cells as compared to Th2 cell was frequently detected (122), (123).
In the present work a DNA methylation marker was efficiently used to quantify the Th1 / Th2 cell ratio in the CD4+CD45RO+ (memory) cell compartment of peripheral blood of RA patients and healthy volunteers.

2.4.2. Endometriosis

Endometriosis is a common gynecological disease, which affects about one out of ten women of reproductive age. Characteristic of this disease is the presence of endometrial glandular tissue outside of the uterus. Despite this seemingly simple indication, it is a complex disease, which even today is only poorly understood regarding its etiology and development. The disease is responsible for various types of pelvic pain and infertility. Despite the enormous research efforts in this field, the etiology of endometriosis remains poorly understood.
The diagnostic gold standard is laparoscopy, a surgical procedure unpleasant for the patient and expensive to perform. Overall the disease remains underdiagnosed and even when finally diagnosed a delay of seven years or even longer between disease onset and diagnosis is common. The role of DNA methylation has so far not been studied in any detail in this disease.
In this study, results are presented where DNA methylation was measured at the cytokine gene loci of IFN-γ and IL-10 in patients with and without endometriosis. The sample material was endometrial biopsy tissue from women with laparoscopically confirmed or rejected endometriosis diagnosis. The results are part of a large marker scanning study aimed at developing a methylation based minimally invasive endometriosis diagnostic test.

2.4.3. Non–Hodgkin lymphoma

Malignant lymphomas are proliferative diseases that arise from the lymph nodes or extranodal lymphatic tissue. According to the variety of stages involved in the maturation and differentiation of the lymphatic cells a number of different types of lymphomas exist (124).
The name “non-Hodgkin lymphoma” was introduced to separate distinct disease entities with respect to their morphological and clinical features. The origin of the malignant cells in Hodgkin lymphoma (Reed

Sternberg cells) was for a long time a matter of discussion and it is only recently that they were assigned B-cell properties, which makes it now a clonal B-cell neoplasia (125).

Classical non-Hodgkin lymphoma are categorised by the origin of the predominant immunologic cell type found in the affected lymph nodes as determined by immunohistochemical methods. The disease categories include B-cell lymphomas, T-cell and natural killer cell lymphomas. Each subtype is further divided into precursor cell neoplasia and peripheral cell neoplasia.

In the present study biopsy samples of B- and T-peripheral cell lymphomas were analyzed. More specifically peripheral cell diffuse large B-cell lymphoma (DLBCL) and peripheral cell pleomorphic small / large T-cell non-Hodgkin lymphoma (T-cell NHL) were analyzed. Both classifications are clinically heterogenous and molecular markers which allow further stratification of patient groups with regard to therapy efficiency are being investigated (126).

As in other neoplasias, an important component of the cell biology of malignancy is inherited from its non-transformed progenitor. Each of the currently known T- and B-cell neoplasias has been traced back to particular stages of differentiation of the two lineages.

Two DNA methylation aberrancies have been detected in lymphomas: global genomic hypomethylation and CpG island hypermethylation. The vast majority of haematological neoplasms have an overall genomic hypomethylation as compared to their normal counterparts.

As described in the chapter 2.1.4, specific hypermethylation events can be assigned to lymphoma entities that do not occur in other cancers leading to a specific lymphoma “methylotype”. Figure 2-6 provides an overview of the most frequently methylated tumor suppressor genes in lymphomas.

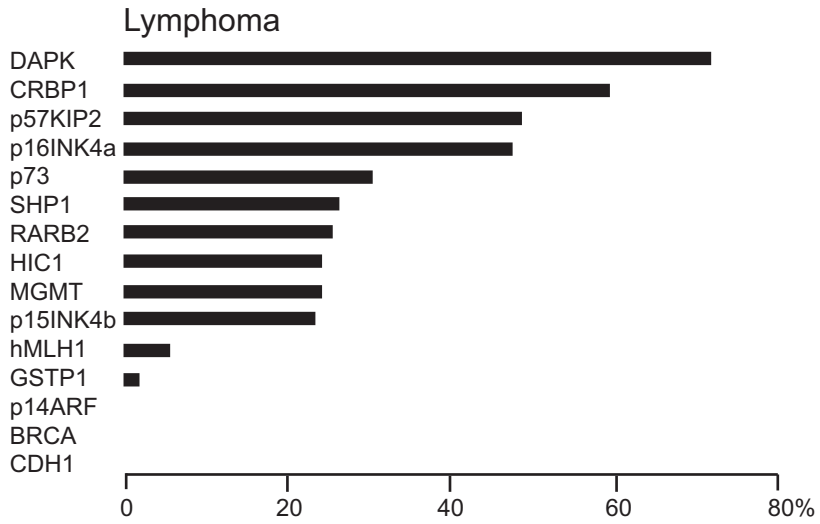

Figure 2-6 Percentage of CpG island hypermethylation of common tumor suppressor genes in lymphoma (Esteller, 2003)

Recent studies in myeloid leukaemia have suggested that aberrant expression of transcription factors are the cause of malignant cell transformation (127). Since transcription factors have a pivotal role in the establishment of hematopoietic lineages and act at very early stages of differentiation, it is plausible

that mechanisms disturbing appropriate transcription of transcriptional factors, including silencing by DNA methylation, may lead to developmental defects and cancer.
The present study is aimed at investigating the methylation patterns of specific transcriptional factor genes with regard to promoter hypermethylation in the above described lymphoma subtypes and comparing them to their normal counterparts, the cells in healthy lymph nodes.

2.5. Scope of the current project

Providing a detailed analysis of the role of DNA methylation in the immune system is the major aim of the current study. Designated candidate genes encoding important signalling molecules (cytokines) and transcriptional regulators were analyzed by methylation profiling techniques and, as for the *IL10* gene, several epigenetic features characterising the locus were analyzed.
Since diagnostic biomarker discovery was one issue in this work, the candidate genes in both gene classes, cytokines and transcription factors, were selected following a tailored biomarker candidate discovery strategy. The diagnostic performance of the identified differentially methylated regions was assessed in three major disease entities: rheumatoid arthritis, endometriosis and Non Hodgkin lymphoma.
The study was divided into two major sections: (1) cytokine and (2) transcription factor genes and the candidate genes of each class were analyzed, in part, in different cell types. Experiments were performed in order to provide answers to the following questions:

- To what extent is DNA methylation involved in the memorization and induction of transcription in the *IL10* and *IFNγ* genes?
- How is the chromatin landscape of the IL-10 gene in both IL-10+ and IL-10- cells defined?
- Is DNA methylation an epigenetic memory tag for an aquired expression phenotype?
- Is the methylation pattern of cytokine genes subject to alterations *in vitro* under expansion and / or differentiation conditions?
- Do differentially methylated regions differentiate between healthy and disease states in conditions such as rheumatoid arthritis or endometriosis?
- Is DNA methylation at transcription factors genes subject to change as cells develop and differentiate?
- To what extent does the methylation pattern of transcription factors correlate to their expression?
- Are the same regions aberrantly hyper- or hypomethylated in B-cell and T-cell neoplasms and do they represent a novel type of DNA methylation marker associated with defective transcriptional machinery in lymph node neoplasia?

3. Methods

3.1. Cell samples

3.1.1. Isolation of human CD4+ / CD8+ T–lymphocytes and CD19+ naive and memory B-lymphocytes

Buffy coats from healthy adult anonymous donors were obtained in accordance with local ethical committee approval (DRK-Blutspendedienst, Berlin und Brandenburg GmbH, Institut Berlin, Germany). Peripheral blood mononucleated cells (PBMCs) were isolated from the buffy coats by density gradient sedimentation using Ficoll-Hypaque. Cells were washed twice with 50 ml phosphate buffered saline (PBS) before CD4+ and CD8+ T-cell separation. CD4+ and CD8+ T-cells were purified from PBMCs by magnetic activated cell sorting (MACS) using CD4 and CD8 MicroBeads respectively, according to the manufacturers recommendation. The efficiency of the purification was verified by staining with FITC conjugated antiCD3, antiCD8 and antiCD4 antibodies (BD Tritest™) (10µl / $5x10^5$ cells) for 30 min on ice. Fluorescence of the labelled population was determined by a FACScalibur™ instrument using the CELLQuest™ software. The purity of each of the sorted populations was 98%.
CD19+ B-cells were purified from PBMCs by MACS using CD19 MicroBeads. The purity of the sorted population was 95% as determined by FACS using FITC conjugated antiCD19 antibodies using 10µl antibody solution for $5x10^5$ cells. Naive B-cells (CD19+CD27-) were separated from memory B-cells (CD19+CD27+) subsets by using CD27 MicroBeads.

3.1.2. Isolation and characterisation of T-helper cell subsets secreting IL-10 and IFN-γ

3.1.2.1. Isolation of T-helper memory cell subsets secreting IL-10 and IFN-γ

Highly purified human CD4+ T-lymphocytes from 30 individual healthy donors were stimulated with 5ng/ml Phorbol 12-myristate 13-acetate (PMA) and 1µg/ml Ionomycin (I) at $1x10^7$ cells per ml for 4 hours. After stimulation, cells were washed with ice-cold buffer (PBS with 0.5% BSA and 2mM EDTA), and labelled with IL-10 or premixed (1:1) IFN-γ and IL-10 specific capture matrix in cold medium for 5 minutes on ice. Subsequently, the labelled cells were diluted in pre-warmed medium (≤10^5 cells/ml) and subjected to a 45-minute cytokine secretion period at 37℃ under slow continuous rotation. The cytokine secretion was stopped by filling up the tube with cold buffer and subsequent incubation on ice for 15 minutes. Cells were harvested and surface stained with specific detection antibodies for IL-10

(conjugated with either APC or PE) or equal amounts of specific detection antibodies for IL-10 (conjugated with either APC or PE) and IFN-γ (conjugated with FITC). Subsequently, four distinct Th-cell subsets were detected and isolated: IL-10+/IFN-γ-, IL-10-/IFN-γ+, IL-10+/IFN-γ+ and IL-10-/IFN-γ- using either single or double cytometric cytokine secretion assay on a FACSDiva™. Age and gender of the 30 healthy donors as well as their distribution within the pools are shown in Table 3 in the appendix. All donors were caucasians.

3.1.2.2. Cytometric bead array (CBA) assay for assessing cytokine expression in ex-vivo T-helper cell subsets

Supernatants from 48-hour or 72-hour cultures of PMA/I stimulated Th-cell subpopulations were analyzed by the human Th1/Th2 cytokine CBA Kit, which allows the simultaneous detection and quantification of soluble IL-2, IL-4, IL-5, IL-10, TNF-α and IFN-γ in a single sample. In brief, a mixture of 10 µl of each of the six different bead suspensions specific for each cytokine (resolved in FL3 channel), was incubated with 50 µl of sample and 50 µl of PE-conjugated detection antibody (resolved in FL2 channel) for 3 hours. Acquisition of sample data was performed using a FACScalibur™ and results were analyzed using the Becton Dickinson CBA analysis software.

3.1.2.3. In vitro expansion of T-helper cell subsets

Sorted Th-cell subsets were seeded in a 96-well plate ($2x10^4$ cells/well) (without feeder cells). Different combinations of cytokines were added twice during the expansion. Cytokine profiles were assessed at day 8, after 6 hours of PMA/I stimulation (the last 4 hours with brefeldin A) and by intracellular cytokine staining for IFN-γ and IL-10 and FACS analysis.

3.1.3. In vitro expansion and differentiation of naive CD4+ T-cells

3.1.3.1. Isolation of naive CD4+ T-cells from PBMCs

PBMCs were isolated from buffy coats obtained from healthy adult anonymous donors by density gradient sedimentation using Ficoll-Hypaque. CD4+ T-lymphocytes were purified from the PBMCs by magnetic activated cell sorting (MACS) using CD4 MicroBeads. Naive Th-cell subsets were subsequently sorted from CD4+ cells using CD45RA/RO isoform MicroBeads. The purity of sorted population was 99%, as determined by FACScalibur™ using the CELLQuest™ Software.

3.1.3.2. Purification of monocytes and generation of dendritic cells

CD14+ monocytes were purified from PBMCs by MACS using CD14 MicroBeads. Sorted monocytes were cultured in the presence of 1000 U/ml GM-CSF and 500 U/ml rIL-4 for 5 days at 1.0×10^6 cells/ml

in 5 ml final volume and then matured with LPS for 2 days. Maturation was monitored by induction of CD80, CD83 and CD86 expression on cultured monocytes, as follows: cultured cell populations were washed twice with PBS and centrifuged at 1500 g (3200 rpm) for 3 minutes. After removing the supernatant, cells were resuspended and 150 mg mouse IgG was added to the cell suspension for 15 minutes to prevent non-specific binding of reagents to Fc receptors. Following the incubation period, 100ml of cell suspension was added to fluorochrome-conjugated reagents (FITC-anti CD14, PE-anti CD80, PE-anti CD83 and PE-anti CD86) and cells were incubated in the dark for 15 minutes after light vortexing. Cells were washed and fixed with 200ml 2% formaldehyde. Stained cells were analyzed by a FACScalibur

3.1.3.3. Differentiation of naive CD4+ T-cells into IFN-γ producing cells

Naive CD4+ Th cells were stimulated with either:
1. plate-bound anti-CD3 and anti-28, in the presence of rIL12 and anti-IL-4 (stimulus I)
2. plate-bound anti-CD3 and anti-28, in the presence of rIL12, anti-IL-4 and IFN-γ (stimulus II)and
3. alloDC (generated as described in chapter 3.1.3.2) (stimulus III)
for 7 days.
The cells were re-stimulated with PMA / Ionomycine for 4 hours followed by IFN-γ capture assay. IFN-γ-producers were separated from non-producers via FACS with a purity higher than 95% for each subpopulation.

3.1.4. Isolation of human IFN-γ+ CD4+ cells from patients with rheumatoid arthritis

3.1.4.1. Naive and memory cell isolation

PBMCs from nine patients were isolated from 20-50 ml heparinized blood, while PBMCs from six healthy donors were isolated from buffy-coated blood preparations by density gradient sedimentation using Ficoll-Hypaque. CD4+ T cells were purified from PBMCs by MACS using CD4 MicroBeads. Subsequently, over 95% pure naive and memory CD4+ T cells were isolated using CD45RA and CD45RO MicroBeads respectively.

3.1.4.2. Isolation of IFN-γ producing cells

CD45RO+CD4+ memory T-cells were stimulated with PMA and ionomycin for 4-6 hours, in the presence of 5 μg/ml brefeldin A for the last two hours. The stimulated cells were then fixed with 2% formaldehyde, permeabilized with 0.3% Triton-X-100 in PBS and stained intracellularly for IFN-γ.

Alternatively, IFN-γ producers and non-producers were FACS sorted after 4 hours of PMA and ionomycin stimulation and cytokine secretion assay.

3.1.5. External sample sources

3.1.5.1. Primary hematopoietic cells

Bone marrow derived hematopoietic progenitor cells (CD34+) from two female donors (caucasian, age 30y and asian, age 36y) and one male donor (caucasian, age 21y) were purchased from Cambrex Bio Science (Walkersville, Maryland, US).

3.1.5.2. Human T-helper cell clones

Human IL-10+ and IL-10- Th1 and Th2 clones were obtained from the group of Francesco Annunziato from the Center of Research Transfer, High Education MCIDNENT, University of Florence, Italy and were cultivated there as previously described (128), (129).

3.1.5.3. Lymph node biopsies

Lymph node biopsies from diffuse large B-cell non-Hodgkin lymphoma (n = 20, mean age 67 ± 7 years) T-cell non-Hodgkin lymphoma (n = 14, mean age 63 ± 9 years) and healthy individuals (n = 18, mean age 69 ± 10 years) were obtained from one of the following sources: Ardais, (Lexington, US), Phylogeny (Columbus, US), Asterand Inc. (Detroit, US) and Benjamin Franklin University hospital (Berlin; Germany). Only anonymized samples were used and ethical approval was obtained for the study. All samples were histologically examined and confirmed to have a tumor cell content of > 85% in case of positive NHL / Hodgkin disease diagnosis and to be free of malignant cells in the normal controls.

3.1.5.4. Lymphoma and leukaemia cell lines

The following human leukaemia and lymphoma cell lines were used for gene expression and methylation measurements: Jurkat clone E6-1 (T-lymphocytes derived from acute T cell leukemia, ATCC TIB-152), KARPAS-299 (lymphoma cell line of T-cell origin, DSMZ ACC 31), SU-DHL4 (lymphoma cell line of B-cell origin DSMZ ACC 495) and Z-138 (leukemia cell line of B-cell origin) (130). KARPAS-299 and SU-DHL4 were cultured in RPMI 1640 with 10% fetal calf serum (FCS) and 2mM L-glutamine. Z-138 was cultured in DMEM with 10% fetal calf serum and 2mM L-glutamine. Jurkat clone E6-1 was cultured in RPMI 1640 with 10% fetal calf serum, 2mM L-glutamine, 10mM HEPES and 1.0mM Sodiumpyruvate.

3.1.5.5. Endometrial biopsies

Tissue from endometrial biopsies of women with laparoscopically confirmed endometriosis was purchased from Cureline Inc. (Seattle, USA). The time point of extraction of each sample was the secretory cycle phase.

3.2. Direct bisulfite sequencing

3.2.1. DNA extraction and quantification

3.2.1.1. DNA extraction from peleted cells

Genomic DNA from all lymphocyte samples and the cell lines was extracted using the QIAamp DNA Mini Kit from Qiagen. Peleted cells were resuspended in 200µl PBS and lysed using the manufacturer's cell lysis buffer (AL), 40U Proteinase K and 20U RNAseA for 4h at 37℃. After the lysis , the genomic DNA was isolated and purified according to the manufacturer's recommendations. The elution of the DNA was performed with 60µl of prewarmed (50℃) buffer AE. Quantification of the eluted DNA was performed at 260nm using an Eppendorf UV spectrophotometer.

3.2.1.2. DNA extraction from lymph node biopsies

Each 20mg sample of frozen lymph node biopsy tissue was lysed by incubation with tissue lysis buffer (TLB) (Qiagen) in combination with 40U Proteinase K over night (16h). Subsequently, the genomic DNA was isolated using the QIAamp DNA Mini Kit (Qiagen) according to the manufacturers protocol. Elution of the DNA and subsequent quantification was performed as described for the peleted cells.

3.2.1.3. DNA quantification

The amount and the purity of isolated genomic DNA and bisulfite treated DNA was assessed by UV spectrophotometrical measurements at λ = 260nm (nucleic acids) and λ = 280nm (proteins).
A minimum of 50µl of genomic DNA were measured in a UV spectrophotometer in disposable cuvettes of 10 mm thickness and the concentration (ng/µl) was obtained according to the Lambert – Beer law by multiplying the optical density with the factor 50. Protein contamination was assessed by determining the ratio of the optical densities at 260nm and 280nm.
Bisulfite treated DNA was quantified using a NanoDrop® ND-1000 spectrophotometer. 1.5µl of bisulfite converted DNA was used for measurement and the obtained optical density was multiplied by the factor 33, as converted DNA is single stranded. The purity of the samples was monitored on the recorded UV-spectrum (from 160 – 300 nm). In the presence of peaks other than at 260nm, the DNA

solution was re-purified on a Microcon YM30 centrifugal filter device by washing with water and re-suspending in fresh TE-buffer.

3.2.2. Preparation of bisulfited DNA

3.2.2.1. Preparation of reference upmethylated and unmethylated DNA

For accurate quantification of the individual methylation levels at the investigated genomic loci, DNA standards of known methylation levels were generated. This was prepared by mixing defined amounts of artificially up- and downmethylated DNA and subsequent sequencing.

Unmethylated (0% methylation) DNA was generated by the molecular stand displacement method (131), using the GenomiPhi® DNA Amplification Kit according to the manufacturers instructions on isolated human genomic DNA from peripheral blood lymphocytes (Promega).

Artificially upmethylated DNA (100% methylation) was generated by enzymatic treatment of the previously generated unmethylated DNA with a DNA methylase (*Sss*I metyhlase) in the presence of S-adenosylmethionine (SAM). 10µg unmethylated DNA were incubated with 40U *Sss*I methylase and 1.24µl SAM in a final volume of 100µl for 16 hours at 37℃ in the Eppendorf 5355 Comfort thermomixer.

Both DNAs the methylated and the unmethylated were bisulfite treated, spectrophotometrically quantified by the NanoDrop spectrophotometer and mixed according to obtain DNAs of 10%, 20%, 50% 70% 80%and 90% methylation.

3.2.2.2. Bisulfite reaction

The bisulfite conversion of the analyzed DNAs was performed according to an enhanced protocol developed at Epigenomics AG (132) based on the original method reported by Frommer et. al (81).

An amount of 1µg-2µg genomic DNA dissolved in 100µl DEPC treated water was incubated with 354µl bisulfite solution containing:

0.4708 g/ml Sodium bisulfite $Na_2S_2O_5$,

0.1128 g/ml Sodiumsulfite Na_2SO_3 and

146µl dioxane solution containing 39.4 mg/ml 6-hydroxy-2,5,7,8-tetramethylchromane-2-carboxylic acid as radical scavenger.

The mixture was incubated in a DNA Engine Tetrad® thermocycler with the following cycler program: 3 min at 99℃ (denaturation of the DNA.), 1.5h at 60° C (conversion reaction), 3 min at 99℃ (second denaturation step), 1.5h at 60℃ (conversion reacti on), 3 min at 99℃ (third denaturation step) and 2h at 60℃ (conversion reaction). Subsequently, the re action mixture was diluted with 200µl water and purified by means of Microcon YM30 centrifugal filter devices.

The purification consisted of six centrifugation steps at 14.000g for 12 min each. First, the reaction mixture was centrifuged to recover the DNA on the filter membrane. Subsequently, the recovered DNA

was washed with 0.2M NaOH (400µl) solution for removal of excessive sulfite and three times with DEPC treated water (400µl). The purified bisulfited ssDNA was eluted in 50µl-75µl prewarmed TE buffer and quantified on a NanoDrop spectrophotometer.
The advantages of this bisulfite protocol are the high conversion rates, the reproducibility and the high DNA recovery after purification.

3.2.3. DNA amplification

PCR amplification was performed using primers designed specifically for bisulfite converted DNA and flanking the desired regions of interest on the individual bisulfited DNA. The primers with a minimum length of 19 bp and an annealing temperature of 55°C ± 2°C were manually designed and ordered without additional labelling at MWG Biotech. The target sequence of the designed primers contained no CpGs thus allowing unbiased amplification of methylated and unmethylated DNAs. Primer functionality was confirmed by sequencing the generated PCR product on the reference DNAs described in chapter 3.2.2.1 and a standard human genomic DNA (Promega). Primers that gave rise to an amplificate of the expected size when using genomic DNA as template were discarded, thus ensuring the specificity for bisulfite-converted DNAs. Each amplification was performed by means of a single primer pair (singleplex – PCR). A comprehensive list of all primer sequences used in the present study is given in Table 1 and Table 2 in the appendix, including the individual genomic positions, the amplicon length and the number of CpGs analyzed within the designated region.
The reaction was performed on 96 well microtiter plates in a total volume of 25µl. The reaction composition was as follows: 10ng of bisulfite converted DNA, 2.5µl 10xPCR buffer (Qiagen), 5 pmol dNTP's (each), 12.5 pmol forward primer, 12.5 pmol reverse primer and 1U of HotStart Taq polymerase. Water was added to obtain a final volume of 25µl. The cycling reactions were performed in a DNA Engine Tetrad® thermocycler. The following temperature profile was used for all amplifications: one heating step of 15 min at 95 °C (initial activation of the polymerase) and 45 cycles with 20 s denaturation at 95 °C, 45 s at 55 °C (pri mer annealing) and 30 s at 72 °C (chain polymerisation). A final step of 10 min at 72°C aft er the 45 cycles was performed to ensure complete polymerisation. The obtained PCR product was briefly analyzed by electrophoresis on a 1.5% agarose gel and used in the subsequent sequencing reaction.

3.2.4. PCR product purification and sequencing

Previous to sequencing, the PCR products were purified in order to remove excess dNTPs and primers. For purification, 5.0µl of the PCR product were incubated with 2.0µl of a mixture of exonucleaseI and shrimp alkaline phosphatase (ExoSAP IT) for 45min at 37°C. Excess primers are degraded by the exonuclease and excess nucleotides are dephosphorylated by the alkaline phosphatase. The enzymes were denatured by heat inactivation for 15 min at 95°C subsequent to the reaction incubation. Both incubations were performed in a DNA Engine Tetrad® thermocycler.

The sequencing reaction was performed by means of the di-deoxy method described by Sanger et al. (1977) (133). The sequencing chemistry used was the BigDye Terminator V3.1 containing fluorescence labelled ddNTPs and the DNA polymerase. The reaction was performed by mixing following components:

5.0µl of the ExoSAP IT digested PCR product (DNA content was not previously quantified)
1.0 µl BigDye Terminator V3.1 containing labelled ddNTPs,
4.0µl Sanger buffer,
5.0µl dNTP mix (0.02mM each) and
5µl sequencing primer (2mM)
in a total volume of 20µl.

The reaction mixture was incubated in a DNA Engine Tetrad thermocycler and subjected to the following temperature profile: 2 min at 96°C (initi al denaturation) followed by 25 cycles of 30 sec at 95°, 15 sec at 55°C (primer annealing) and 4 min at 60°C (elongation).

The sequencing reaction was subsequently purified to remove unincorporated dye terminators (ddNTPs) by gel filtration spin plates DyeEx™ 96 according to the manufacturers protocol. Briefly, the total reaction volume was pipetted on the gel bed and centrifuged on an Eppendorf 5810 tabletop plate centrifuge for 5 min at 910 g. Prior to analysis by capillary electrophoresis, 10µl of Hi-Di® formamide was added to each sample well to ensure proper denaturation. The electrophoresis was carried out in a 3730 ABI DNA Analyser. The length of the capillaries used was 36 cm (3730 DNA Analyzer Capillary Array) filled with the POP-7™ polymer. The electrophoretic conditions were the following: oven temperature: 60°C, injection voltage: 1.2 kV, injec tion time: 15 sec, running voltage: 8.5 kV, running time: 2450 sec. The resulting sequence traces were called by the integrated ABI KB basecaller. The quantitative methylation information at CpG positions was determined by a subsequent software based analysis (ESME).

3.2.5. Software based methylation quantitation

The analysis of all resulting tracefiles was performed by means of in-house developed software (ESME) (84) after basecalling with the intrinsic ABI basecaller.

Briefly, after regular basecalling, the bisulfite specific analysis software performs signal normalisation, corrects for incomplete bisulfite conversion and aligns the positions in the trace file to the reference sequence in the database. After these initial processing steps, the methylation levels are calculated by comparing areas of overlapping C and T signal peaks at CpG sites. The procedure allows discrimination between levels of methylation that differ by 20%. The calculated levels are depicted in a colour-coded matrix. The rows of the matrix represent the methylation level for individual CpG sites while columns represent averages of triplicate sense sequencing for various cell types.

3.2.6. PCR product cloning and sequencing

For the high resolution methylation analysis on region 5 of the *IL10* gene (chapter 4.1.3.2), PCR products generated on bisulfited DNA of individual donors were subcloned into the TA cloning Kit (Invitrogen) following the manufacturers recommendation. Individual E. coli clones were picked, re-cultured in LB medium and plasmid DNA extraction was performed using the plasmid mini Kit (Qiagen), again following the manufacturers instructions.
The cloned PCR product was sequenced from the plasmid as template, without prior amplification by means of the same primer assay as used for its generation. Sequencing and trace file analyis were performed as described in the chapter 3.2.4.
Donors used for the amplification and cloning of the IL10 region 5 DNA are listed in the Table 5 (7.5.2)

3.3. Real time mRNA expression quantification assays

3.3.1. mRNA extraction and cDNA preparation

Total mRNA from the four analyzed cell lines was isolated by means of the RNeasy Kit according to the manufacturer's protocol.
The isolated mRNA was converted to cDNA by means of the Omniscript Reverse Transcription Kit. The reverse transcription reaction was performed in a total volume of 20µl with 0.25 µg/µl total RNA, 1µmol/µl polyT primer, 10µmol/µl random hexamers, 0.5 mM dNTP's, 0.5 U/µl RNAse Inhibitor and 0.2 U/µl Omniscript reverse transcriptase. The reaction mixture was incubated for 1h at 37℃ in a DNA Engine Tetrad® thermocycler and the generated cDNA was used for subsequent amplification without previous clean up or quantification.

3.3.2. Real time PCR for quantitative expression measurement

Primer assays were manually designed for quantitative amplification of the generated cDNA. Each assay contained primers located on consecutive exons and spanning a large intron to ensure amplification of only cDNA and not genomic DNA contaminants. The used primer sequences are given in Table 3 (chapter 7.3, appendix).
The real time PCR assays were performed by means of the SYBR® Green PCR master mix chemistry in an ABI Prism 7900HT Sequence detection system.
The total reaction volume was 15µl comprising 7.5µl of the SYBR® Green PCR master mix, 1.5µl of the individual cDNA dilution (1:100) and a final concentration of 0.4µM primers. The temperature profile was the following: initial activation of the polymerase at 96℃ for 10 minutes followed by 40 cycles with the profile: 95℃ for 15 seconds, 60℃ for 1 minute , 72℃ for 30 seconds. Fluorescence intensities

were measured in each cycle during the annealing and extention step (from 60℃ – 70℃). Analysis of the real-time PCR was performed by means of the ABI SDS 2.2 software.
Relative mRNA expression was calculated as described by Muller et al. (134) using the glycerol aldehyd-3-phosphate dehydrogenase gene (GAPDH) amplification as reference for normalization. Expression of each gene was calculated by averaging the normalized expression values of three independent measurements. Mean values were plotted against averaged methylation levels for regions with significant differential methylation between the analyzed cell lines (Figure 4-15).
The expression quantification as determined by the Q-gene software developed by Muller et al. is described in the chapter 3.5.

3.4. Chromatin immunoprecipitation

Sorted IL-10-secreting and nonsecreting cells were fixed with 1% formaldehyde for 10 min at room temperature. The fixation was stopped with 0.125 M glycine. The chromatin was sheared to obtain fragment lengths of approximately 200–1000 bp by sonication with five pulses of 10 seconds at 30% power on a Bandelin sonicator. The chromatin was incubated with antibodies directed against hyperacetylated histone H3 (H3Ac) or Lysine 4 trimethylated histone H3 (H3K3me3) overnight, followed by incubation with ProteinA-MicroBeads for 2-hours. Washing steps were performed on µ columns with high salt, low salt, LiCl, and TE buffer sequentially. Chromatin precipitate was eluted with 1%SDS, 0.1M $NaHCO_3$. Crosslinks were reversed by incubation at 65 ℃ for 4-hour in the presence of 0.2 M NaCl, and the DNA was purified with NucleoSpin Extract II. The amount of immunoprecipitated DNA was determined by real time PCR with LightCycler instrument 2.0 using FASTStart SYBR Green Master Mix. The relative amount of DNA was calculated with the formula $2^{(\text{crossing point input - crossing point input})}$.
The primer sequences used for the amplification of the crosslinked DNA are given in Table 4 (chapter 7.4, appendix).

3.5. Statistical methods

3.5.1. Kruskal Wallis test, Wilcoxon test and Bonferroni correction

For statistical analysis, methylation levels of adjacent CpGs within a region were averaged for each individual sample.
For more than two groups comparisons (as applied in chapter 4.2.1), the resulting means were tested for significance (< 0.05) by using the non-parametrical Kruskal Wallis rank sum test. This test allows the analysis of variance (comparison of means) between more than two groups, without assuming a normal population. Each averaged methylation was considered an independent measurement. Due to the low sample numbers in the single tested groups, the resulting p – values were left uncorrected. The significance level applied was 0.05.

For two group comparisons, as applied in chapter 4.3.3, the averaged methylation levels between the two cancer entities and normal lymph node DNA were compared using the Wilcoxon rank statistics followed by Bonferroni correction. The Wilcoxon test is too a rank sum test for comparison of means between two independent sample groups which does not require information about the data distribution.
The Bonferroni correction is a conservative adjustment of the significance level to account for multiple comparisons when more than one hypothesis is tested on the same data. In order to avoid falsely positive tested hypothesis, the p – value is multiplied with the number of tested hypotheses thus increasing its individual value for each hypothesis.
If not otherwise specified, a Students t-test was used to interrogate statistical significance. All reported p–values are twosided and all confidence intervals are quoted at the 95% level.

3.5.2. Box-whisker plots

In order to visualize different types of populations in one plot, averaged methylation data for different biological questions were displayed as box whisker plots.
A given dataset is segmented into two measures of dispersion (quartiles), a measure of central location (median), the maximal value and the lowest data value. These measures are plotted such, that the lower whisker represents the lowest observation followed by the data belonging to the lower quartile (Q1), the median and the upper quartile (Q3) all being depicted in the box. Thus, the box represents 50% of the data. The largest observation is shown graphically in the upper whisker. In addition, the boxplots indicates which measurements are considered unusual (outliers) by the dots below the lower whisker or above the upper whisker. The box plots in this study were generated by the software Microsoft Excel 2003 software.

3.5.3. Q-gene software for mRNA analysis

The Q-gene software was used to calculated mean normalized expression of the transcription factor genes in the cell lines (Figure 4-15) and was developed by Muller et al. as a Microsoft Excel based software application(134). The software requires three independent measurements (raw c_0t values) for each mRNA and from the selected reference gene. It then calculates the mean normalized expression by averaging the three independently calculated normalized expressions stemming from the triplicate measurements. Thereby, the PCR efficiencies of the reference gene and the target gene are not considered equal. The standard error is calculated by means of the Gaussian differential equation and is included in the graphical output.

4. Results

4.1. Epigenetic control in the immune system: DNA methylation of cytokine and transcription factor genes in T-helper cell subsets

4.1.1. Isolation of CD4+ memory cells secreting IL-10 and / or IFN-γ

To isolate *ex vivo* different human T-helper (Th) cell subsets secreting IL-10 or IFN-γ or both, CD4+ lymphocytes from the peripheral blood of 30 individuals were isolated as described in the methods section (chapter 0). A double cytokine secretion assay was performed to select for cells expressing IFN-γ and / or IL-10. After stimulating CD4+ T-cells with P/I, following intracellular cytokine productions were induced and the different cell types could be isolated: IL-10$^+$IFN-γ$^-$ (1-5% of total cells, IL-10 positive), IL-10$^+$IFN-γ$^+$ (0.6-3% of total cells, Double positive), IL-10$^-$IFN-γ$^+$ (5-15% of total cells, IFN-γ positive) and IL-10$^-$IFN-γ$^-$ (80-90% of total cells, Double negative) (Figure 4-1 A), shown for one randomly selected donor). Each individual cell type was FACS sorted to a purity > 95% (Figure 4-1 B). As they are characterized by expression of the CD45RO isoform, IL-10 positive, IFN-γ positive and the Double positive cells resembled antigen-experienced memory Th-cells properties. The double negative cells are CD4+ naive-like cells, expressing the CD45RA isoform. In order to confirm the supposed cytokine secretion pattern of the isolated Th-cell subsets, the purified cells were cultured for 48-hr or 72-hr and supernatants were analyzed for various cytokine productions (IL-4, IL-5, IL-10, IFN-γ and TNF-□) by a cytokine bead array (CBA). IL-10$^+$IFN-γ$^-$ Th-cells produced only IL-10 but no IFN-γ, while IL-10$^-$IFN-γ$^+$ Th-cells produced only IFN-γ, but no IL-10. As expected, Treg1-like IL-10$^+$IFN-γ$^+$ Th-cells secreted both cytokines, whereas IL-10$^-$IFN-γ$^-$ Th-cells secreted neither one. All cells expressed the T-cell differentiation and proliferation factor IL-2 (Figure 4-1 C). The other cytokines, IL-4, IL-5 and TNF-□ are not expressed by any of the purified cell types excluding thus the co-purification of Th2 IL-10 secreting cells.

For control purposes, human Th1 and Th2 cell lines obtained from a collaborator group were included in the study and DNA methylation analysis was performed at the same loci as analyzed in the *ex vivo* cells.

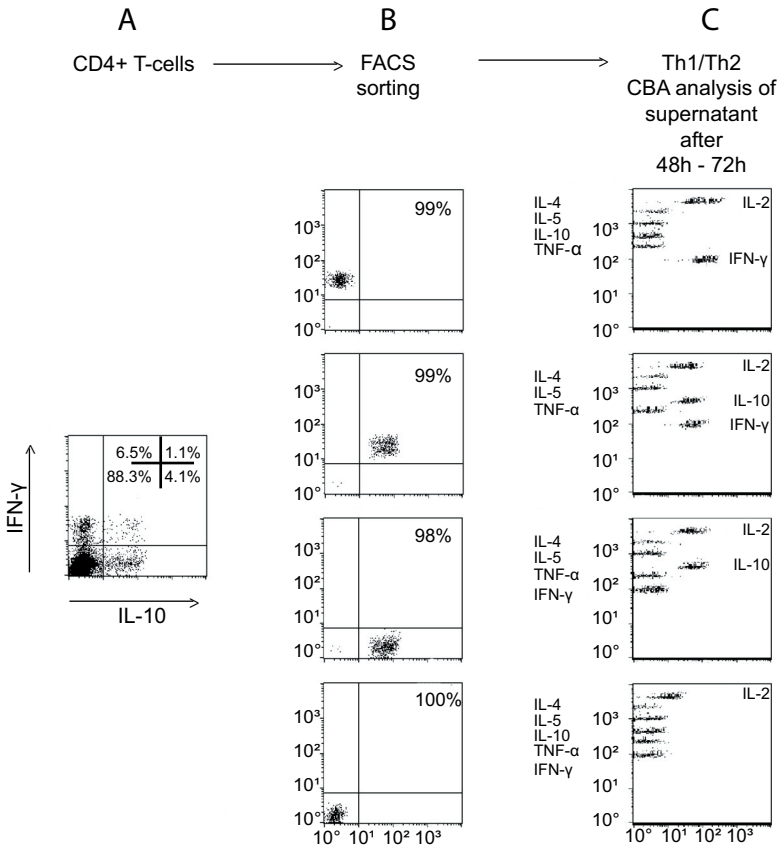

Figure 4-1 (A) Induction and analysis of CD4+ Th-cell subsets. The following Th-cell subsets were identified: IL-10+IFNγ-, IL-10+IFNγ+, and IL-10-IFNγ+ and IL-10-IFNγ-. (B) Purity analysis of CD4+ Th-cell subsets. The induced Th-cell subsets were sorted by a FACSDiva. A small fraction of each sorted subset was reanalyzed for purity on a FACScalibur. (C) Distinct cytokine profiles of CD4+ Th-cell subsets. Equal amounts of cells from each subset were cultured 48- or 72-hr. Supernatants were assessed for IL-2, IL-4, IL-5, IL-10, TNF-α and IFN-γ (from top to bottom) by a CBA and results were analyzed on a FACScalibur.

mRNA expression of IL-10, IFN-γ, GATA3 and TBX21

Subsequently, quantitative real-time PCR analysis was performed on the four cell types from five randomly selected donors to assess mRNA expression of *IL-10* and *IFN-γ* and to evaluate expression levels of transcription factors that have been associated with the regulation of *IL-10* and *IFN-γ* such as GATA-3 (135), (136) and TBX21 (137). Abundant amounts of IL-10 mRNA were measured only in IL-10 secreting subsets, IL-10+IFN-γ- and IL-10+IFN-γ+ Th-cells. GATA-3 mRNA expression was significantly higher in IL-10+IFN-γ- Th-cells in comparison to IL-10+IFN-γ+ Th-cells. This is in agreement with recently published data where the Th2 key regulator GATA-3 was identified to directly influence IL-10 expression by chromatin remodelling at the IL-10 gene locus (138). As expected, IFN-γ and increased TBX21 mRNA expression levels were restricted to IFN-γ-secreting Th-cells, except for one sample with lower expression in the IL-10+IFN-γ+ Th-cells in comparison to the other four donors (Figure 4-2).

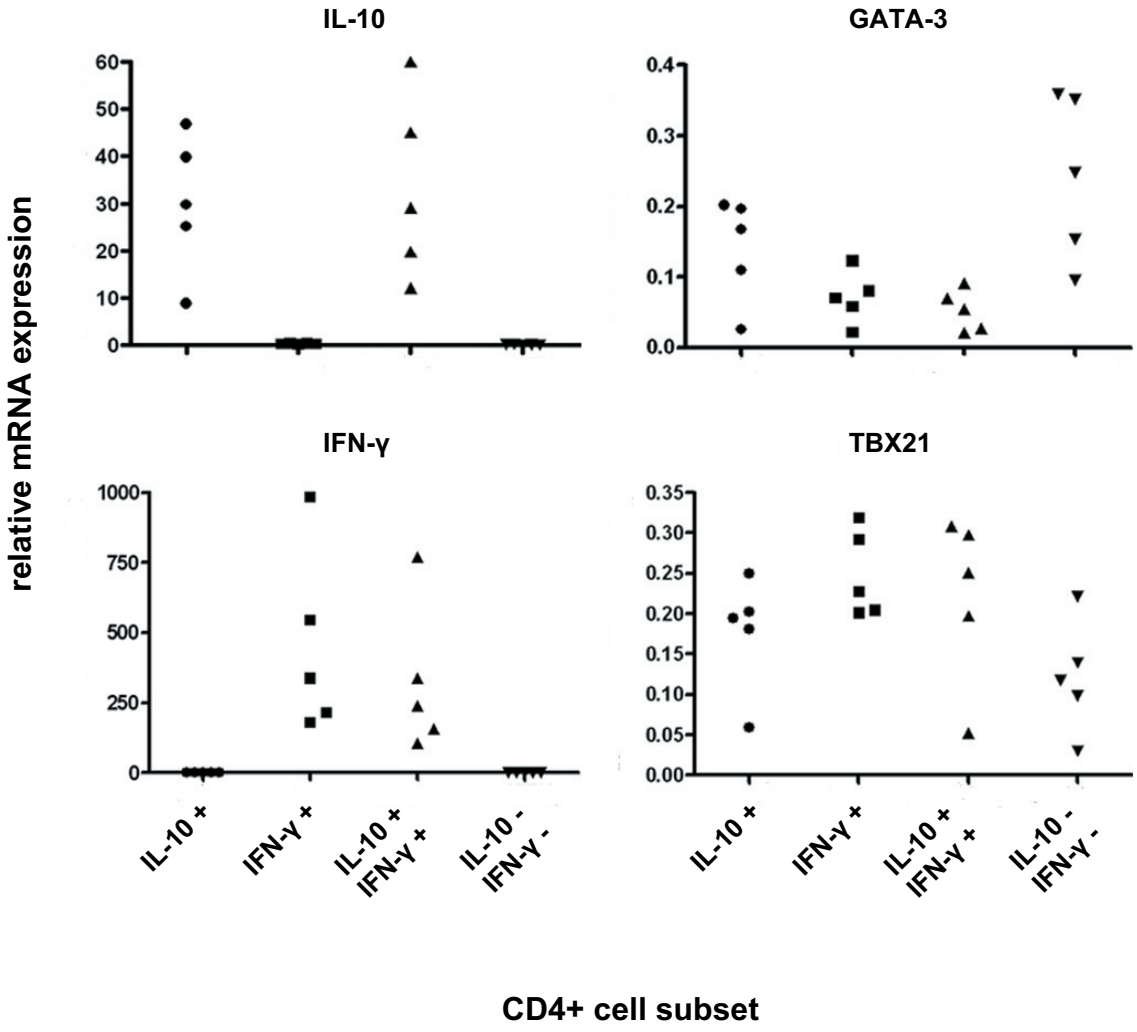

Figure 4-2 mRNA expression of IL-10, IFN-γ and the transcription factors GATA-3 and TBX21 in the isolated Th-cell subsets IL-10+/IFN-γ-, IL-10+/IFN-γ+, IL-10-/IFN-γ+ and IL-10-/IFN-γ-. Expression was quantified by real-time PCR. The data shown is derived from five independent biological samples.

4.1.2. DNA methylation profiles of *IL4*, *IL13*, *GATA3* and *TBX21* in CD4+ memory cells

In order to avoid confounding effects such as age, gender or other yet unknown differences and to enable work with the small cell numbers obtained for the IL-10+IFN-γ+ cell type, pools of 10 donors were formed resulting in a total of 12 samples (three independent biologic samples for each of the four subsets). Age and gender of the obtained donors, as well as the individual pool composition are summarized in Table 3 in the appendix. These samples were used for DNA extraction, bisulfitation, PCR amplification and direct bisulfite sequencing. As a control, clonally expanded human Th1 and Th2 IL-10+ and IL-10- cells were used and DNA methylation profiles were determined as well.

For all genes, regions encompassing several kilobases upstream of the TSS were selected for analysis with a focus on evolutionary inter-species conserved non-coding regions (CNS) containing putative

regulatory sequences (139). The species used for alignment comparison were mouse and rat. Both analyzed transcription factors, GATA-3 and TBX21 have CpG islands located at the 5' end of the gene locus in the promoter region. None of the four analyzed cytokine genes (*IL4*, *IL13*, *IL10* and *IFNγ*) displayed CpG dense regions or annotated CpG islands in their promoters.

The methylation profiles for the cytokine genes *IL4* and *IL13* and the transcription factor genes *GATA3* and *TBX21* are shown in Figure 4-3.

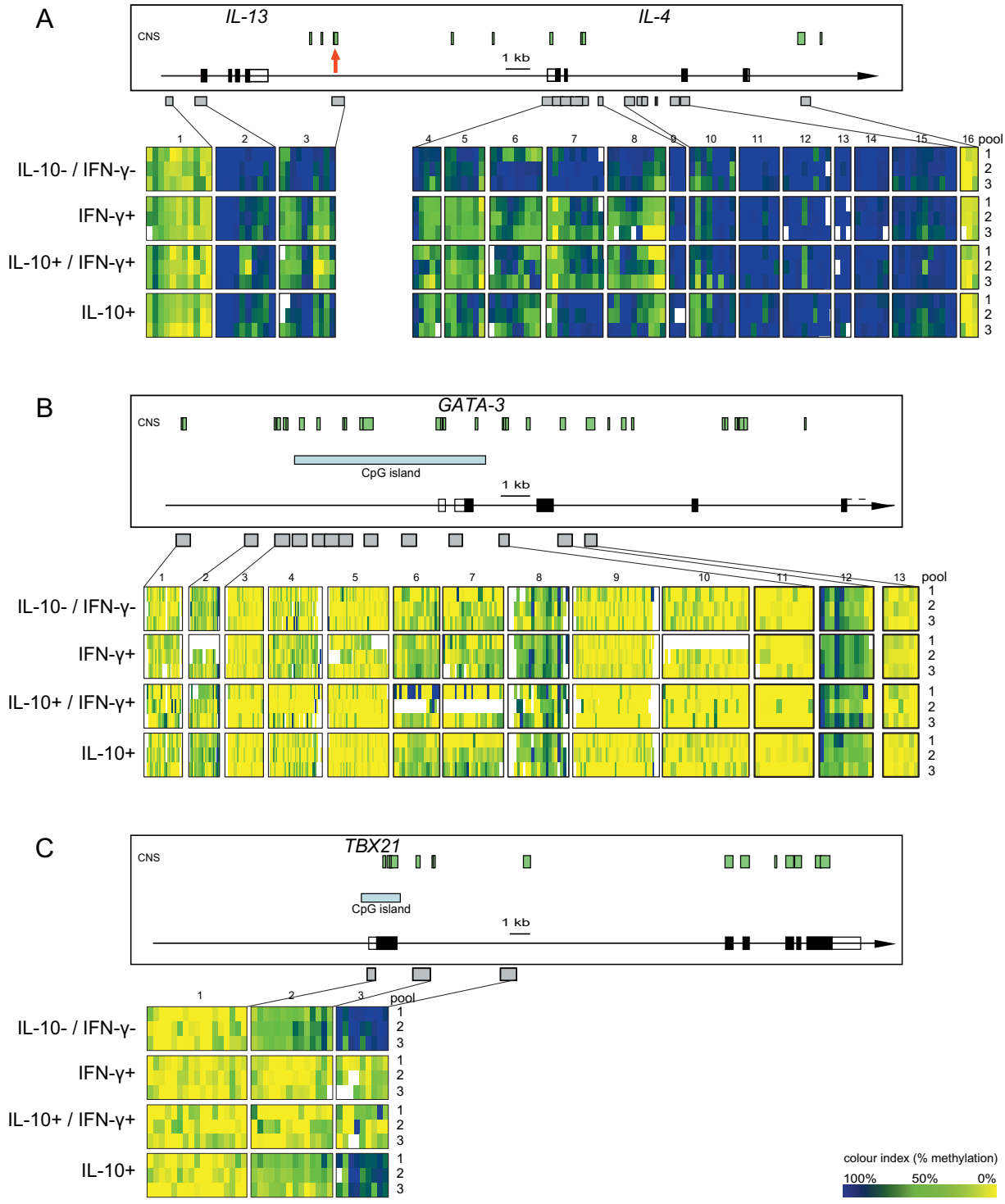

Figure 4-3 Genomic organisation and DNA methylation profiles of the gene loci *IL4*, *IL13* (A), *GATA3* (B) and *TBX21* (C) in four distinct T cell types: IL-10-/IFN-γ- naive cells, IFN-γ+ Th1 like cells, IL-10+/IFN-γ+ Treg like cells and IL-10+ cells. Three independent samples, each consisting of pooled cells of the same type from 10 healthy donors were analyzed. The analyzed genomic regions are depicted in dark grey bars below the gene location. Green boxes represent conserved non-coding sequences (CNS) as determined by interspecies comparison between human, mouse and rat genome (Ensembl). CpG islands, as determined by the Ensemble (release 44) are shown as light grey bars. Black boxes represent exons; non–filled boxes stand for untranslated regions.

The Th2 specific cytokine genes *IL4*, *IL5* and *IL13* are clustered in a 160 kb region on the short arm of human chromosome 5 (Figure 4-3 A, *IL5* locus not shown). The expression of IL-4 and IL-13 was shown to be coordinatively regulated in Th2 cells by a locus control region (LCR) located downstream of the *IL13* gene (Figure 4-3 A, red arrow) (140). A LCR is a sequence element outside of coding regions that confers tissue specific high level expression of the linked genes, presumably by overriding suppressive effects of the flanking DNA sequences (141).

Analysis of the *IL4* and *IL13* loci revealed differential methylation between IL-10-/IFN-γ- naive cells on the one side and IFN-γ+, IL-10+/IFN-γ+ and IL-10+ cells on the other side within the LCR (Figure 4-3 A, region 3). While naive cells display levels of >90% methylation for all CpGs in the region, the remaining three cell types have significantly decreased levels of ~50% ($p<0.004$), with exception of two CpGs located in the middle of the analyzed fragment. Similar patterns were observed for several regions located intragenic of IL-4 (Figure 4-3 A, region 4-8). However, for regions 6, 7 and 8, IL-10+ cells tend to have a higher degree of methylation when compared to IFN-γ+ and IL-10+/IFN-γ+ cells.

A methylation level of 50% is indicative of allele specific methylation, whereby one allele is silenced by a 100% methylated locus and the other shows hypomethylation and permissive chromatin state. The methylation data presented here is in line with the previous finding that both genes, *IL4* and *IL13*, are expressed preferentially from one chromosome rather than at random (142).

CpGs located approximately 1.5 kb upstream of the *IL13* gene are hypomethylated in all four analyzed cell types (<20%) while the proximal 5' promoter region and parts of exon 1 display high levels of methylation, greater than 80% (Figure 4-3 A). Two CpGs within this latter region are demethylated in the double positive IL-10+/IFN-γ+ cells. All downstream intragenic regions of the *IL4* gene (regions 9–15) are strongly methylated in all analyzed cell types. The three CpGs located downstream at region 16 belong to a conserved element and are unmethylated in all four cell types.

GATA-3 and TBX21 are two transcriptional regulators shown to direct naive T-cell differentiation towards Th2 and Th1 effector cells respectively.

The *GATA3* gene promoter consists of a 5.0 kb large CpG island comprising a number of conserved DNA streches consistently downmethylated in all analyzed cell types (Figure 4-3 B, regions 3-7). This finding is in agreement with the general notion, that CpG island methylation is very low in normal cells. None of the analyzed regions display differential methylation between any of the different cell types although GATA-3 was shown to be differentially expressed in the analyzed cell types (Figure 4-2) suggesting no role for DNA methylation in the expression regulation of this gene.

Similar to the methylation levels detected in the CpG island of the *GATA3* gene, the CpG island of the *TBX21* is unmethylated in all analyzed cell types (Figure 4-3 C, region 1). Interestingly, the intragenic regions 2 and 3, both spanning conserved sequence elements display lower levels of methylation in IFN-γ+ cells as compared to IFN-γ- cells (Figure 4-3 C, regions 2-3). Consistently, IFN-γ+ cells were shown to have lower levels of *TBX21* expression (Figure 4-2). As TBX21 was shown to be directly involved in the regulation of the *IFNγ* gene expression and to be a key transcription factor in Th1 cells (137), (143) the presented data suggests a role for DNA methylation in the regulation of the TBX21 transcription.

4.1.3. Epigenetic modifications of the *IL-10* locus

4.1.3.1. *IL-10* DNA methylation profiling in CD4+ memory cells

Seven amplificates have been designed within the IL-10 gene encompassing 48 CpGs. Region 1, located approximately 9.0 kb upstream of the annotated TSS and covering two CpGs is followed by regions with slightly higher CpG density upstream of the TSS. Region 5, located in the proximal promoter, contains six CpGs. Regions 6 and 7 are located within the gene body in the introns 1 and 4 respectively (Figure 4-4 A). Alignments between the human, mouse, and rat IL-10 locus were performed and the extent of DNA sequence homology was computed with the web-based program VISTA (http://genome.lbl.gov/vista/index.shtml). Regions outside annotated exons with a length of at least 100bp that show sequence identity greater than 75% were considered conserved non coding (CNS) regions with putative regulatory functions. The criteria are fulfilled by regions 5 and 7 (Figure 4-4 A). The methylation analysis was performed in the previously isolated CD4+ memory cell subsets and in IL-10+ and IL-10- T-helper (Th) cell clones of both types, Th1 and Th2.

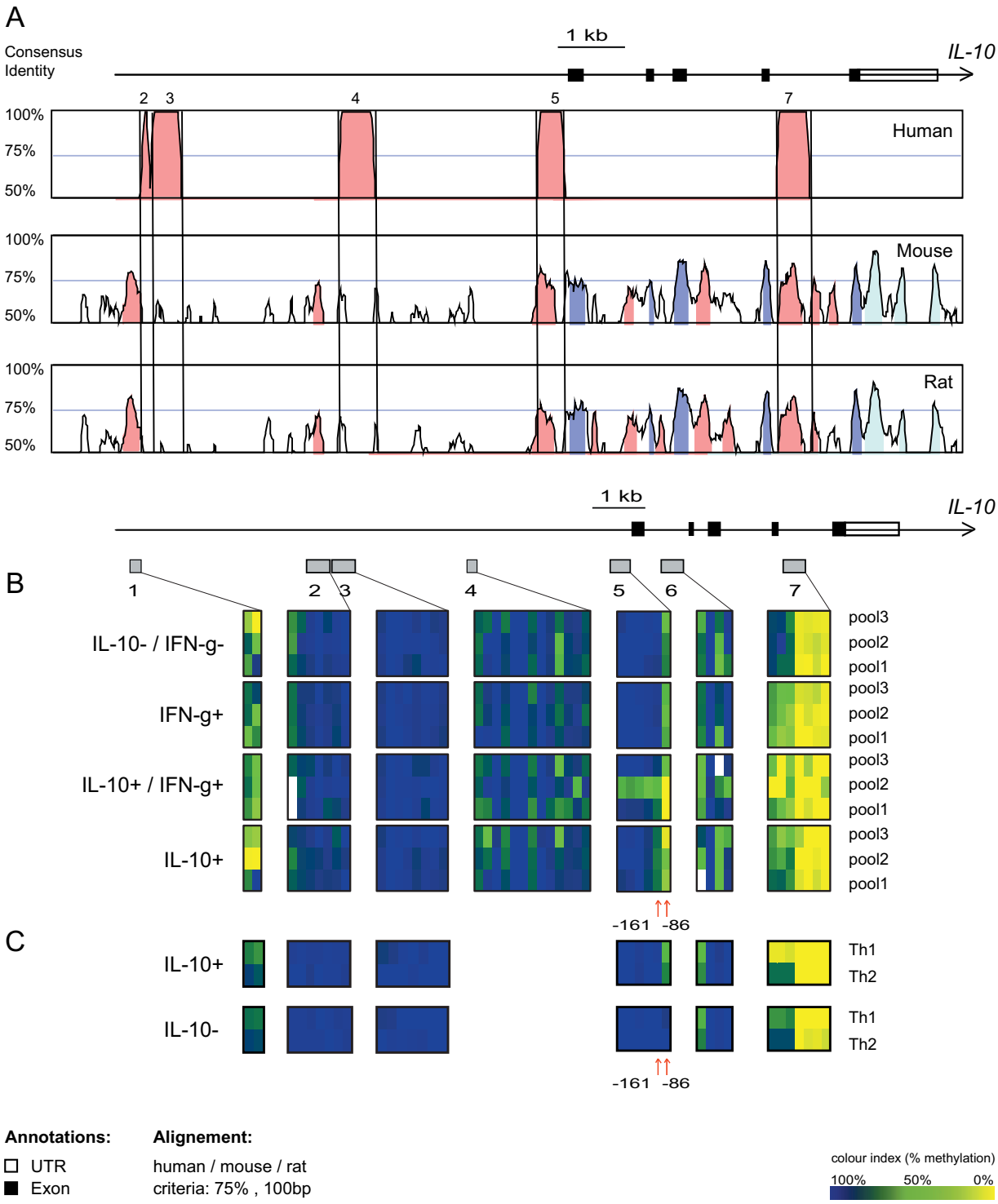

Figure 4-4 (A) Genomic organisation of the human *IL10* gene with interspecies sequence alignment between human, mouse and rat. Genomic regions with sequence similarity greater than 50% over at least 100bp are shown in the histogram plot. (B) DNA methylation profiles of the *IL10* locus in CD4+ Th-lymphocytes. The methylation heat charts represent triplicate measurements of three samples, each resulting from pooling the genomic DNA of of ten individuals. (C) DNA methylation profiles at selected regions in the *IL10* locus in IL-10+ and IL-10- Th cell clones.

With the exception of two 3' CpGs of region 5, no methylation pattern specific for IL-10-secreting Th-cells was found as compared to IL-10 non-secreting Th-cells. Two CpGs of region 1, located 9.1 kb upstream of the transcriptional start site, showed low levels of methylation in both IL-10+ and IL-10- Th-cells. CpGs of regions 2 and 3 (5.5 and 5.0 kb upstream) were almost fully methylated in all cell subsets (Figure 4-4 B). CpGs of region 4 (2.5 kb upstream) and 6 (intron 1) displayed alternating patterns of methylation, without an explicit preference assignable to a certain Th-cell subset (Figure 4-4 B). The conserved region 7 (intron 4) displayed hypermethylation of the first three CpGs in the double negative cells for all samples, while the single positive IFN-γ+ and IL-10+ cells display 50% methylation. Exceptions are two pools within the double positive cells (pool2 and pool3) with relatively low level of methylation for this specific CpGs. As pool 1 does not display the same pattern and this methylation pattern does not correlate to IL-10 expression, these three CpGs were not investigated further. The 3' CpGs of region 7 show a low level of methylation throughout all Th-cell subsets analyzed (Figure 4-4 B).

The human IL-10+ and IL-10- Th cell clones displayed similar methylation profiles as described in the *ex vivo* T-cells for all analyzed regions (Figure 4-4 C). Again, with the exception of the most 3' CpG of region 5 (Figure 4-4 C), no methylation differences were observed between IL-10+ and IL-10- cells. The adjacent CpG. However. is hypermethylated in both IL-10+ and IL-10- Th cell clones (Figure 4-4 C). In addition, the aforementioned 3' CpGs of region 5 (proximal promoter) are slightly demethylated in both IL-10+ Th1 and Th2 cell clones as compared to IL-10- Th1 and Th2 cell clones.

The CpG at position –161 (relative to the TSS) has an overall level of 100% methylation in IL-10- cells (averaged over the six pools of IL-10- cells), while the IL-10+ cells have only 75% methylation (Figure 4-4 B). Even more specifically, the CpG located 75bp downstream at position –86 is 85% methylated in IL-10- cells and approximately 25% in the IL-10+ cells (Figure 4-4 B).

These two CpGs are of special interest since they are located in a region of high sequence similarity to the mouse genome where homologue CpGs have been shown to be specifically downmethylated in the mouse Th2 cell line D10 in contrast to the Th1 cell line D5. In addition, these CpGs are located in DNAseI hypersensitivity regions in the mouse. Hypersensitivity regions are usually correlated to an open, permissive chromatin status (99). However, no such data has yet been reported for human ex vivo T-helper cells.

4.1.3.2. High resolution methylation analysis of the *IL-10* region 5

To analyse the methylation status at the 5' CpGs of region 5 at a higher resolution, sequencing of clones derived from non-pooled, randomly selected individual DNA samples was performed. For each individual cell type, two donors were selected and their bisulfited DNA was amplified specifically at the *IL10* region 5. The resulting PCR products were cloned into a plasmid and transfected into *E. coli*. Isolated bacterial clones carry thus a single version of a PCR strand with binary methylation information. A total number of 138 clones distributed on the four cell subsets were analyzed by sequencing. Table 5 (appendix) summarizes the number of clones for each single cell type together

with age and gender of the selected donors. Wilcoxon rank sum statistics followed by Bonferroni correction was performed to assess the statistical significance of the differential methylation at each single CpG position. The CpGs at positions -86 and -161 strongly differentiate between IL-10+ and IL-10- cells ($p< 0.26x10^{-10}$ and $p< 0.94x10^{-4}$). While IL-10+ cells show a clear tendency to be demethylated at these CpG positions, IL-10- cells are mostly upmethylated suggesting thus a less permissive chromatin conformation in the specific region (Figure 4-5). Thus, the low methylation status at these three CpG positions in IL-10+ cells correlates with the expression of the gene. Although other CpGs in region, located upstream of the TSS and downstream of the CpG at position -349, show demethylation in some of the clones, they do not reach statistical significance.

No significant difference was detected between the two distinct IL-10+ cell types (double positive and single positive) as well as between the two IL-10- cell types (double negative and single negative) at this specific region 5 (Figure 4-5).

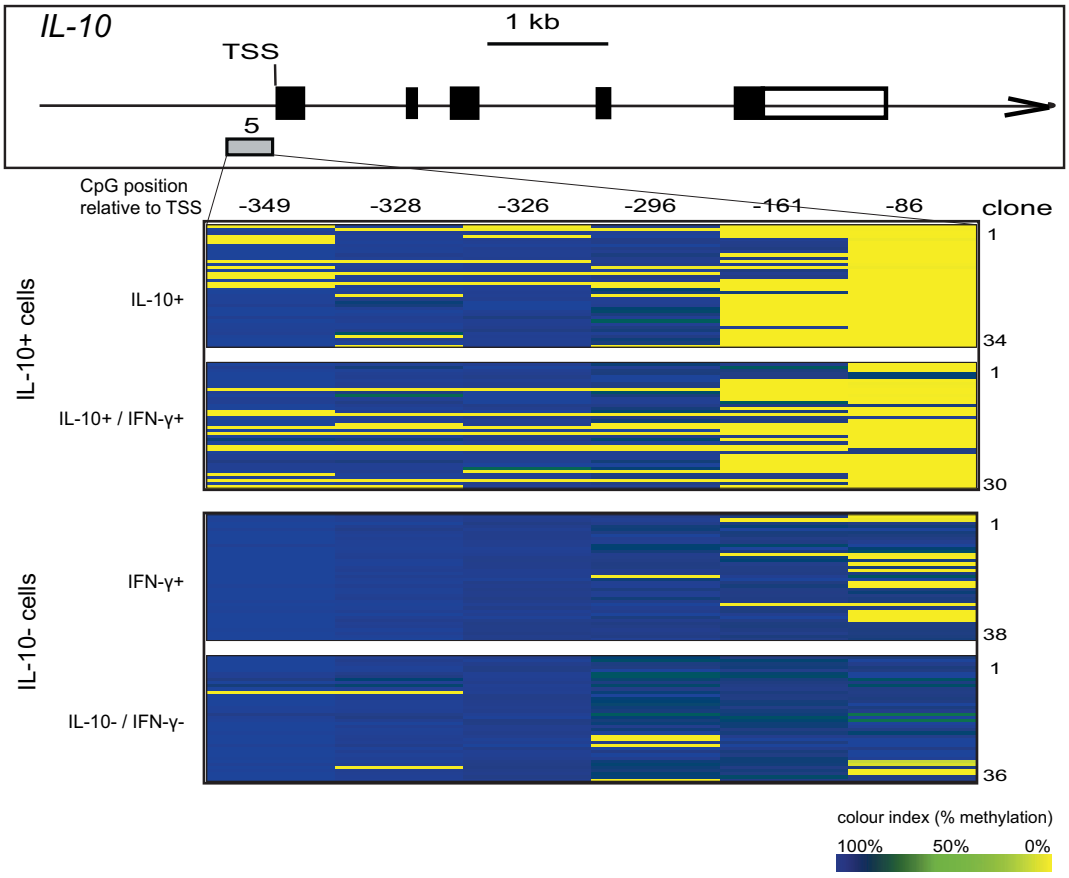

Figure 4-5 Bisulfite clone sequencing of the *IL10* region 5. Up to 38 clones derived from the PCR products of two individuals were sequenced for each cell type. The relative position of each analyzed CpG within the region is given on top of the chart.

4.1.3.3. Histone acetylation and histone methylation at the *IL-10* locus

To gain more insights into the epigenetic status of the IL-10 locus in IL-10 expressing Th cells, a chromatin immunoprecipitation (ChIP) assay was performed to analyse the histone modifications.

Certain chemical modifications of the local histones like acetylation of histone 3 or trimethylation at the lysine-4 position of histone 3 are associated with an open chromatin status thus allowing the binding of transcription factors and other transcriptional enhancers as reviewed in (144), (145).
IL-10+ and IL-10- CD4+ / CD45RO+ cells were isolated from two different donors and the ChIP assay was performed as described in chapter 3.4. The genomic regions 1, 2, 4 and 5 (Figure 4-4 A) were amplified by real time PCR after immunoprecipitation with the respective antibody and the amount of amplified DNA was normalized to the previously measured input DNA.

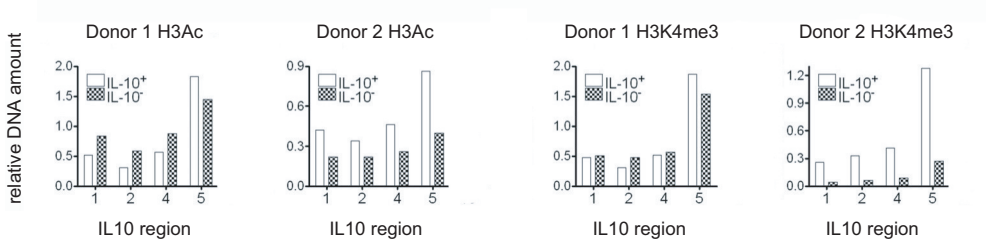

Figure 4-6 Histone acetylation (H3Ac) and histone trimethylation (H3K4me3) at indicated regions (x-axis) in the putative *IL10* gene promoter of ex vivo purified IL-10+ and IL-10- Th-cells. Immunoprecipitated DNA was quantified by real-time PCR and normalized to input DNA amounts (y-axis).

High levels of histone 3 acetylation and methylation were observed in IL-10+ cells from donor 2 within the region 5 (Figure 4-6). Less prominent, but with the same tendency is the data for region 5 in IL-10+ cells from donor 1. The regions 1, 2 and 4 deliver conflicting data between the individual donors in the histone trimethylation experiment. While IL-10+ cells of donor 2 are strongly methylated at the respective histones when compared to IL-10- cells, the difference between the two cell types in donor 1 is not statistically relevant (Figure 4-6). Also, the differences between donor 1 and donor 2 in acetylation at the regions 1, 2 and 4 are insignificant (Figure 4-6).
Since the two differentially methylated CpGs between IL-10+ and IL-10- cells are located in region 5, the observed histone acetylation and trimethylation marks are strengthening the assumption that this promoter region harbors regulatory functions for the expression of the downstream *IL10* gene.

4.1.3.4. Loss of *IL10* expression after rounds of *in vitro* cultivation

“Epigenetic memory” is defined as the inherited epigenetic status of a specialized cell type which is stably maintained after rounds of proliferation and harbours the information for the specific gene activity in the cell (35). To analyse wheather the demethylated CpGs at position -86 and -161 relative to the TSS and the modified histones in IL-10+ cells harbor the epigenetic memory for IL-10 expression, IL-10+, IL-10+/IFN-γ+ and IL-10-/IFN-γ+ cells were isolated from PBMC fractions of healthy donors and cultured in vitro for a period of two weeks. The expression of IL-10 and IFN-γ was monitored by intracellular staining and FACS analysis and the DNA methylation was measured after the expansion

period in both IL-10+ and IL-10- cell fraction. Figure 4-7 shows the frequency of cells with IL-10 expression after the in vitro cultivation period.

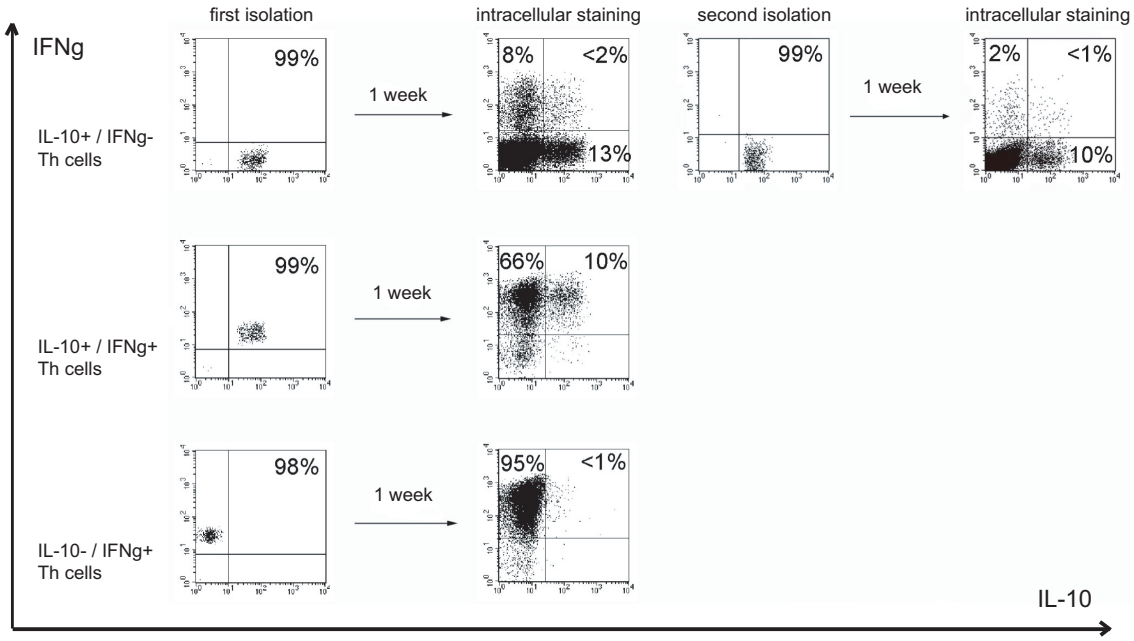

Figure 4-7 Loss of IL-10 expression after *in vitro* cultivation and re-isolation. *Ex vivo* isolated IL-10+/IFNγ-, IL-10+/IFNγ+ and IL-10-/IFNγ+ cell subsets were expanded for one week under neutral (rIL-7 plus rIL-15) conditions. After one week, a second cytokine secretion assay for IL-10 and IFNγ was performed and IL-10+/IFNγ- cells were re-isolated out of the first round sorted IL-10+/IFN-γ- cells. Re-expression of IL-10 and IFN-γ was assessed by intracellular staining following P/I restimulation for all subsets after one week and after another week of culture for re-isolated IL-10+/IFNγ- cells.

While more than 95% of the IL-10-/IFN-γ+ cells maintain the ability to produce IFNγ upon culture in vitro (Figure 4-7), less than 13% IL-10+ cells produce IL-10 after cultivation under the same conditions in the same period. After one week of in vitro cultivation, remaining IL-10 producing cells were re-isolated and kept under the same conditions for additional seven days to monitor the IL-10 expression maintenance. Similar to the first cultivation round, more than 90% of the cells had lost the ability to express IL-10 (Figure 4-7). To verify if de novo DNA methylation occurs at the CpG loci -86 and -161 during in vitro cultivation, methylation was measured within region 5 and region 3 as reference (Figure 4-8) in both cell types, IL-10+ and IL-10-.

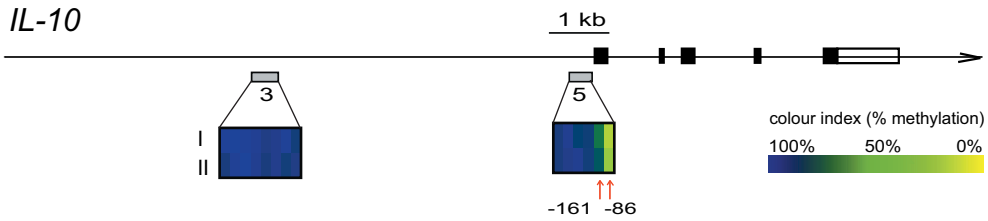

Figure 4-8 DNA methylation of the regions 3 and 5 after two weeks of *in vitro* cultivation of *ex vivo* isolated IL-10+ cells. The upper raw (I) displays the methylation pattern of cells which maintain the ability to produce IL-10, while the lower line (II) shows the methylation pattern of cells that have abandoned IL-10 production.

The previously demethylated CpGs -86 and -161 in *ex vivo* IL-10 producing cells remain demethylated in culture regardless of the IL-10 expression pattern, suggesting that the two differentially methylated CpGs do not harbor the epigenetic memory to maintain IL-10 production when cultured under conditions sufficient for expansion. Thus, IL-10 expression might not be part of a programmed cell memory but its expression is rather dependent on extracellular stimuli.

4.1.4. DNA methylation at the *IFNγ* locus

4.1.4.1. DNA methylation profiling of the *IFNγ* gene in CD4+ memory cells

For the *IFNγ* gene, amplicons were designed in five selected regions covering a total of 28 CpGs and spanning a stretch of 6.3 kb. Region 1 is positioned within a previously described IFN-γ regulatory element ~4.0 kb upstream of the annotated TSS. This element was discovered by interspecies alignment as being located within a highly conserved non coding sequence (CNS) which is associated with low methylation levels and DNAseI hypersensitivity in IFN-γ expressing T-cells in mouse (102). Regions 2 and 3 span a conserved non-coding element, in the proximal promoter (Figure 4-9). Regions 3, 4 and 5 span the exons 1 and 3 respectively (Figure 4-9).

The methylation analysis was performed on the DNA of the pooled samples as described in chapter 4.1.3. A very pronounced pattern of differential methylation was observed for all of the analyzed regions. IFN-γ expressing cells tend to have extremely low methylation levels (<10%) at all analyzed CpGs, while IFN-γ negative cells display methylation levels higher than 80% at the same CpG positions (Figure 4-9). The results are in agreement with recently published data showing that hypomethylation of the *IFNγ* promoter is correlated with the cells potential to express IFN-γ (55).

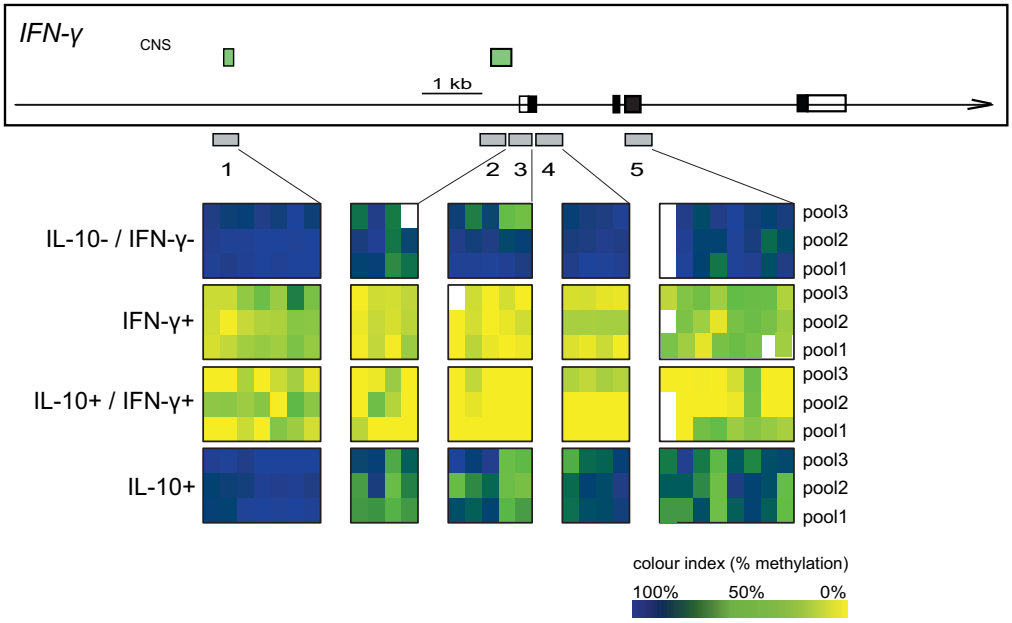

Figure 4-9 Genomic organisation of the human *IFNγ* gene and DNA methylation profiles of the *IFNγ* locus in CD4+ T-helper cells. Heat charts display the methylation levels of each individual CpG from triplicate measurements of the three independent pooled samples. CNS: conserved non-coding sequence.

4.1.4.2. Demethylation dynamics at the *IFNγ* locus after six days of *in vitro* cultivation

Based on the results obtained in the *ex vivo* cells, where it was shown that IFN-γ- phenotypes are hypermethylated in the promoter and several intragenic CpGs, *in vitro* cultivation of naive T – cells (CD4+CD45RA) was performed under different stimulation conditions that determine cell differentiation towards Th1-like cells. The aim of the experiment was to monitor the local DNA methylation status upon which IFN-γ expression is induced and to observe the interdependence between methylation and expression. Additionally, by using three different stimulation conditions, it was tested which *in vitro* stimulus is capable of inducing the lowest level of methylation in the same period of time thus resembling most closely the *in vivo* cell differentiation conditions. The applied stimuli were the following: stimulus I: anti-CD3/anti-CD28, rIL12 and aIL4, stimulus II: anti-CD3/anti-CD28, rIL12, IFN-γ and anti-IL4 and stimulus III: allogeneic dendritic cells (allo DC). At day six of cultivation, the cells were harvested and FACS-separated according to their IFN-γ expression status.

After sorting, the genomic DNA was extracted and used for DNA methylation measurement at the *IFNγ* locus. Every cultivation experiment was performed in duplicates. All five regions shown in Figure 4-9 were analyzed by bisulfite sequencing in triplicate experiments. The DNA methylation rates for individual CpGs were averaged (mean) for each of the five analyzed regions and the methylation measurements were plotted for each region (Figure 4-10).

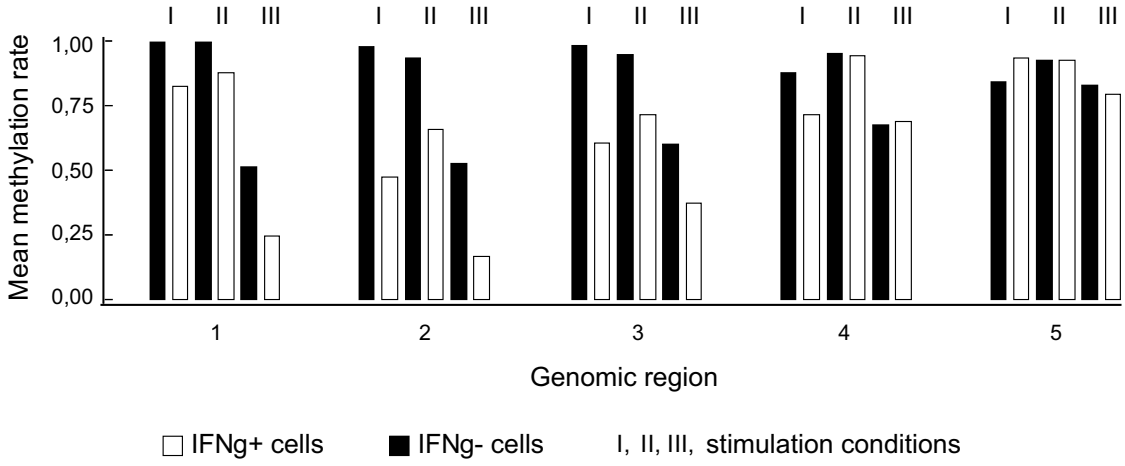

Figure 4-10 Averaged methylation levels of IFN-γ- and IFN-γ+ cells after six days of *in vitro* cultivation towards Th1 differentiation under different stimulation conditions.

Regions 1, 2 and 3 showed significantly decreased methylation levels between IFN-γ– and IFN-γ+ cells for all three differentiation conditions ($p < 0.008$, 0.001 and 0.0002 for the stimuli I, II and III respectively). While IFN-γ- cells are hypermethylated like their naive precursors, the IFN-γ+ are slightly less methylated. However, while external stimuli I and II do not differ strongly in their influence of the local methylation and induce IFN-γ expression after relatively low methylation decrease (50% – 75%), the allogeneic dendritic cells induce a significantly stronger decrease in methylation within both, IFN-γ- and IFN-γ+ cells.

The interdependence between methylation and expression, however, does not become clear after this experiment. While average methylation levels of 60% - 75% still allow IFN-γ expression (regions 1, 2 and 3 in IFN-γ+ cells), an overall of 50% methylation within the IFN-γ– cells generated by stimulus III does not allow expression yet. This can be explained in part by the role of individual CpGs within the regions of interest, especially those located on binding sites of TBX21 and CREB transcriptional regulators (54), (55). It is difficult to describe CpGs individually by the data analysis approach selected here. Instead, they need to be analyzed by a quantitative methods like methylation sensitive restriction nucleases combined with real – time PCR techniques.

In addition, it was recently described (146) that the hypermethylated IFN-γ promoter can be transactivated upon strong extracellular signalling followed by induction of IFN-γ expression which would explain the high methylation levels in IFN-γ+ cells obtained after treatment with the stimuli I and II.

The boxplots in Figure 4-11 summarize the methylation results by averaging the three significant regions (1, 2 and 3) for the individual stimuli. The mean variation (box height) of the methylation in IFN-γ- cells is less than that in the IFN-γ+ cells, suggesting that the IFN-γ- cells are a more homogenous population of cells and underlining the effect of methylation states of individual key CpGs for expression induction.

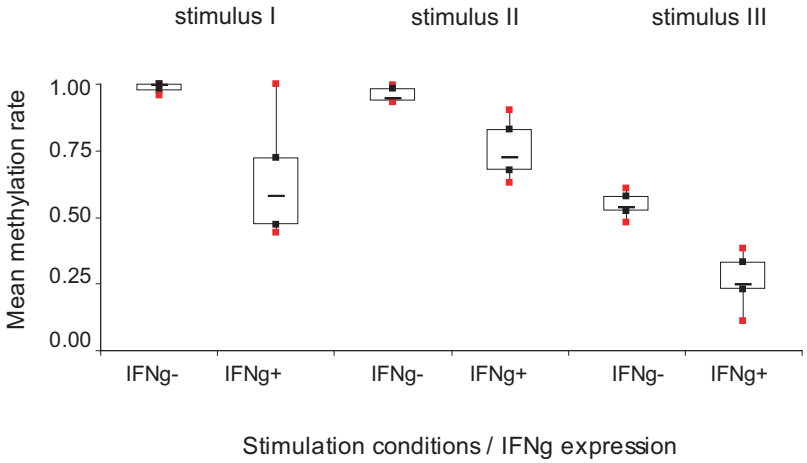

Figure 4-11 Box plots of averaged DNA methylation for all analyzed CpGs within regions 1, 2 and 3

However, despite the relatively low methylation levels obtained with the stimulus III, the methylation levels measured *in vivo* could not be reached under any of the conditions tested *in vitro*. In addition, while Th1 cells show *in vivo* hypomethylation within the entire IFN-γ locus (promoter and intragenic regions), regions 4 and 5 remain largely hypermethylated suggesting that the cells obtained after six days of cultivation *in vitro* (approximately four rounds of proliferation) do not resemble native Th1 cell methylation patterns at the *IFNγ*locus.

4.2. Epigenetic control in the immune system: DNA methylation of transcription factors in hematopoietic development

4.2.1. Methylation profiling of 13 transcription factor genes in consecutive stages of normal T- and B-cell development

For DNA methylation profiling, 13 transcription factor genes (Table 2) previously shown to be key regulators in adult lymphocyte development and lineage commitment were chosen (147), (148). Figure 2-5 shows schematically the expression of each selected TF in distinct lineages and / or at specific developmental stages (149), (112), (150), (151).

For each gene, several putative regulatory regions were analyzed (Figure 4-12) and the respective DNA methylation profiles were determined. These regions were selected by two different approaches. Firstly, for each gene, CpG-dense regions or CpG islands located within the 5' untranslated regions (UTR) were selected. Secondly, we identified highly conserved non-coding elements (CNS) containing isolated CpGs by interspecies comparison. This strategy has successfully been used before to identify regulatory elements for other genes and model organisms (139), (152). In order to identify non-promoter associated regions of differential methylation, some of the amplicons were located up to 7.0 kb upstream and 5.0 kb downstream of the annotated transcription start site (TSS).

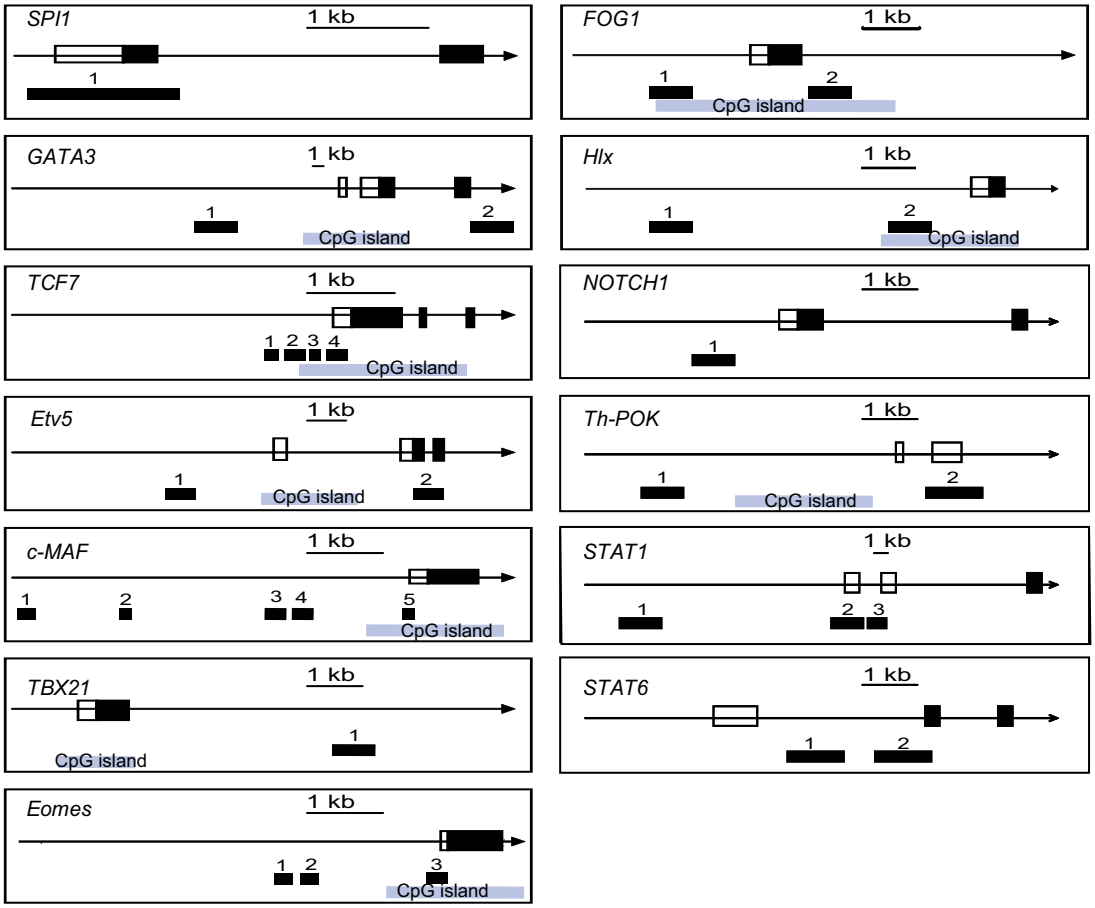

Figure 4-12 Localization of regions (black bars) profiled for DNA methylation within the genomic context for all selected genes. Non-coding exons are shown as empty boxes; coding exons are depicted as solid boxes. A scale bar (1.0 kb) for each gene and CpG islands (CGIs) as annotated by Ensembl (NCBI 36) are shown.

Methylation comparisons were performed between cell types representing consecutive stages of the human adult hematopoietic cascade (Figure 2-5): (1) bone marrow derived hematopoietic progenitor cells, (n=3), (2) CD4+ naive cells (n=3), (3) CD8+ naive cells (n=2), (4) CD19+ naive B-cells (n=2), (5) CD4+ (IFN-γ+) memory cells (n=3), (6) CD8+ memory cells (n=4) and (7) CD19+ memory B-cells (n=2).

Significant methylation differences were detected between the seven cell types in specific regions of *SPI1, GATA3, TCF-7, Etv5*, *c-MAF* and *TBX21*. For the remaining genes, *FOG1*, *Hlx*, *Eomes*, *Notch1*, *Th-POK*, *STAT1*, and *STAT6*, no differential methylation could be identified in any of the examined regions. Figure 4-13 A shows the level of differential methylation for each individual CpG in the sequence of the selected regions. Figure 4-13 B shows the average methylation of genes that displayed no differential methylation. The methylation heat charts in Figure 4-13 B are consist of averaged methylation of individual CpGs located within the analysed genomic region. This is possible, when co-methylation, or identical levels of methylation are observed between adjacent CpGs.

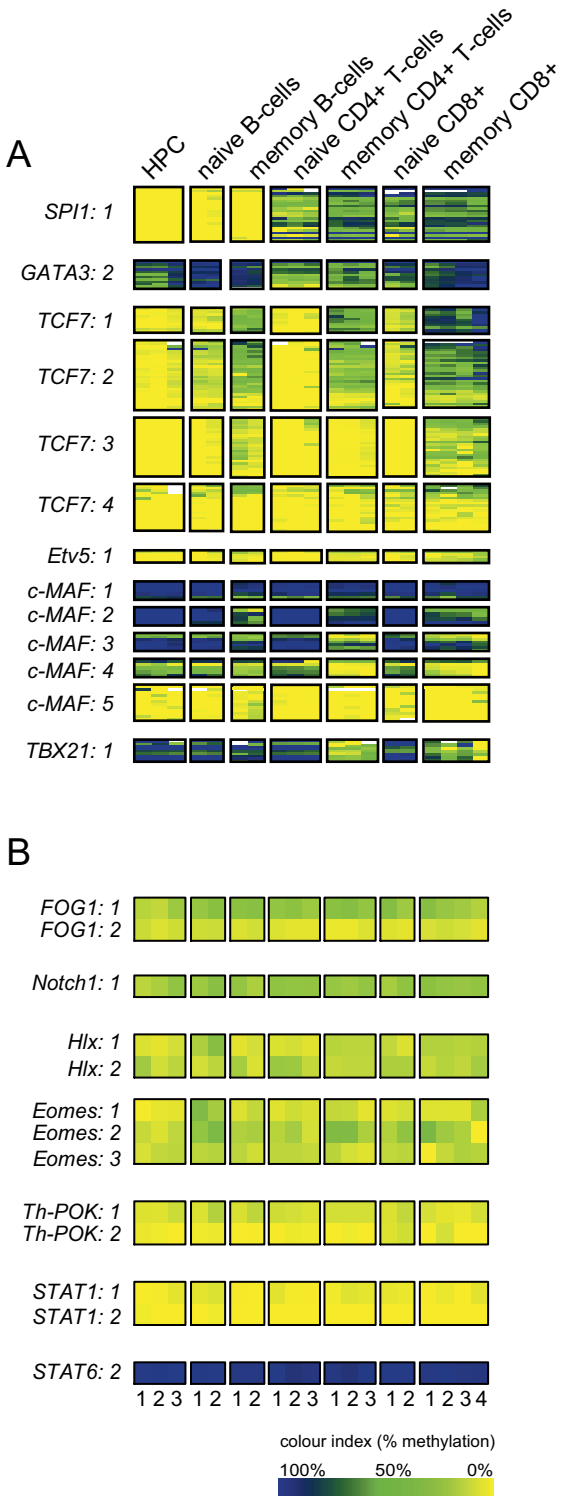

Figure 4-13 (A) CpG wise DNA methylation profiles of selected transcription factors in progenitor, T- and B-cells of different developmental stages. Selected differentially methylated regions are displayed for each gene within the analyzed cell types. (B) Averaged methylation levels of transcription factor gene regions that are not differentially methylated within the analyzed lineages and developmental stages. The gene names and the displayed regions are indicated. The colour code is given below. HPC: hematopoietic progenitor cells.

Within the *SPI1* gene locus, all 22 analyzed CpGs located within the 5' UTR, exon1 and intron1 were unmethylated (Figure 4-12 and Figure 4-13 A, average methylation level< 5%) in the progenitor cells (CD34+), naive and mature B cells. In contrast, the same region showed increased methylation (> 60%, $p \leq 0.001$) in all naive and memory cells of the T-cell lineage, indicating that this gene is specifically methylated in this lineage. More specifically, the Th2 dominant transcription factor *GATA3* (147) displayed reduced methylation levels within the analyzed region 2 (Figure 4-12 and Figure 4-13 A, $p \leq 0.02$) only in naive and memory CD4+ lymphocytes but not in CD34+ cells, CD8+ lymphocytes and B-cells.

Regions within *TCF7*, *Etv5, c-MAF* and *TBX21* displayed differential methylation patterns as well Figure 4-13. In contrast to *SPI1* and *GATA3*, the methylation of these genes was dependent on the differentiation state (naive versus memory) as opposed to the cell type itself (i.e. B-cells versus T-cells). For *TCF7*, a region of 630 bp located about 0.7 kb upstream of the TSS (regions 1 and 2, Figure 4-12) was consistently higher methylated (>60%, $p \leq 0.001$) in all B- and T- memory cells compared to progenitor cells and naive B- and T-lymphocytes (Figure 4-13 A). Within the memory lymphocyte group, a gradual, lineage dependent increase in methylation was detected, with CD8+ memory lymphocytes showing the highest methylation level and an increase in DNA methylation towards more downstream regions for this cell type (region 3, Figure 4-12 and Figure 4-13 A). A similar, but less pronounced increase of DNA methylation in memory lymphocytes was observed for the *Etv5* gene ($p \leq 0.002$), in a region located approximately 2.0 kb upstream of the cognate TSS (region 1, Figure 4-12). However, consistent hypermethylation in memory cells is not a general phenomenon, as decrease of DNA methylation in *c-MAF* ($p \leq 0.001$, region 3 and 4) and *TBX21* ($p \leq 0.002$, region 1) in the memory lymphocytes as compared to the naive lymphocytes was measured. For *c-MAF*, the region of differential methylation was spatially limited: homogenous hypermethylation was measured in regions further upstream (region 1 and to some extend region 2). The CpGs of the annotated CpG island in the 5'-UTR of *c-MAF* (region 5) were unmethylated throughout lymphopoiesis. Interestingly, the T-helper1 specific transcription factor *TBX21* displayed differential methylation within the analyzed region located in intron 1 but not in the putative promoter region (Figure 4-3 C).

Figure 4-13 B displays averaged methylation rates of analyzed regions of genes that were not differentially methylated such as *FOG-1*, *Notch-1, Hlx1, Eomes, Th-POK* and *STAT1*. These gene regions were either unmethylated or displayed rather low methylation (<40%) with the exception of an intragenic region of *STAT6* that was homogenously hypermethylated (Figure 4-13 B). A number of the analyzed genes have a CpG island (CGI) within their 5'-UTR which were all unmethylated, consistent with the notion that the majority of CGIs in the human genome are unmethylated (153).

4.2.2. Methylation - expression correlation of TF genes in cell lines

A number of genes, including tumor suppressor genes, are regulated via DNA methylation in the promoter and other regulatory regions (6). In some cases, promoter hypermethylation leads to gene silencing, while unmethylated promoters are associated with transcription of the cognate gene. To

further examine the functional implications of the observed differential methylation, real–time PCR expression (RT-PCR) analysis was performed for several of the transcription factors using two B-cell lymphoma (Z-138 and SU-DHL) cell lines, one T-cell leukaemia (Jurkat) and one T-cell lymphoma (Karpas-299) cell line. For the RT analysis, intron-spanning assays were used with GAPDH mRNA as a relative reference for expression normalization. The relative expression was calculated according to Muller et al. (134) by averaging normalized expression values of three independent RT measurements. All four cell lines were analyzed for DNA methylation in several of the regions described above, some of them are shown in Figure 4-14. The averaged methylation level of differentially methylated regions was plotted against the normalized expression in Figure 4-15.

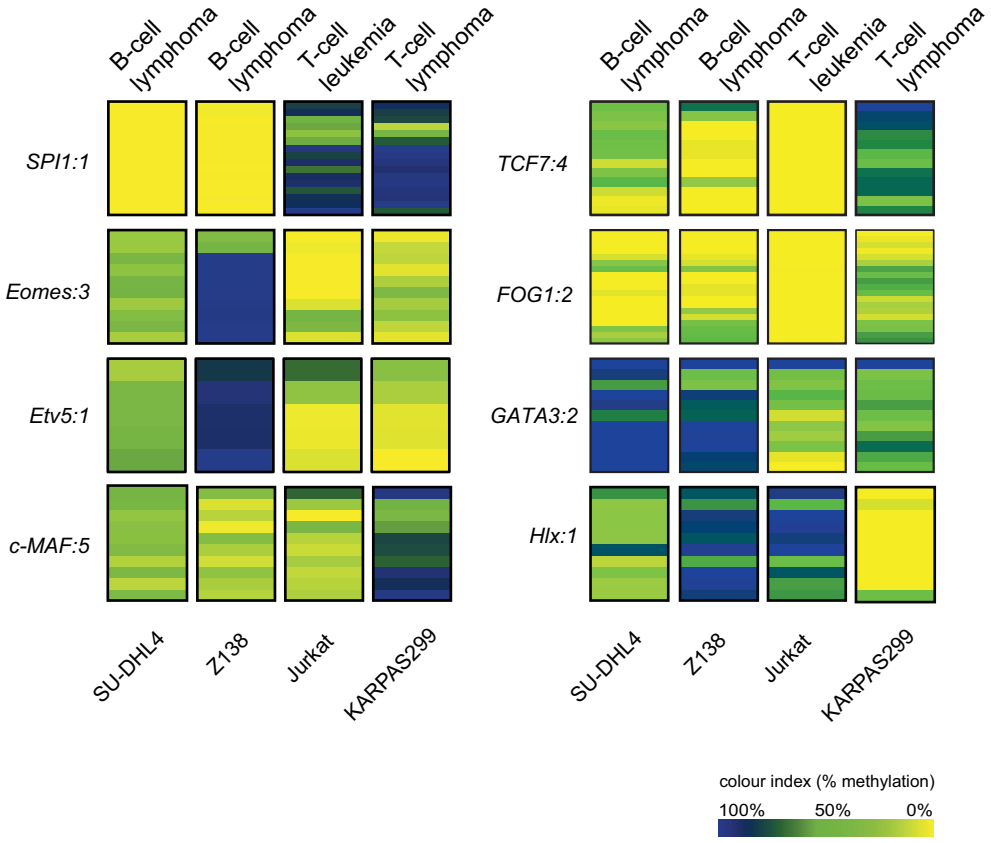

Figure 4-14 Methylation profiles of selected 5'-UTR regions in B- and T-cell cancer cell lines. In total, two B-cell lymphoma cell lines (SUDHL4, Z138), one T-cell leukaemia cell line (Jurkat) and one T-cell lymphoma cell line (KARPAS 299) were analyzed.

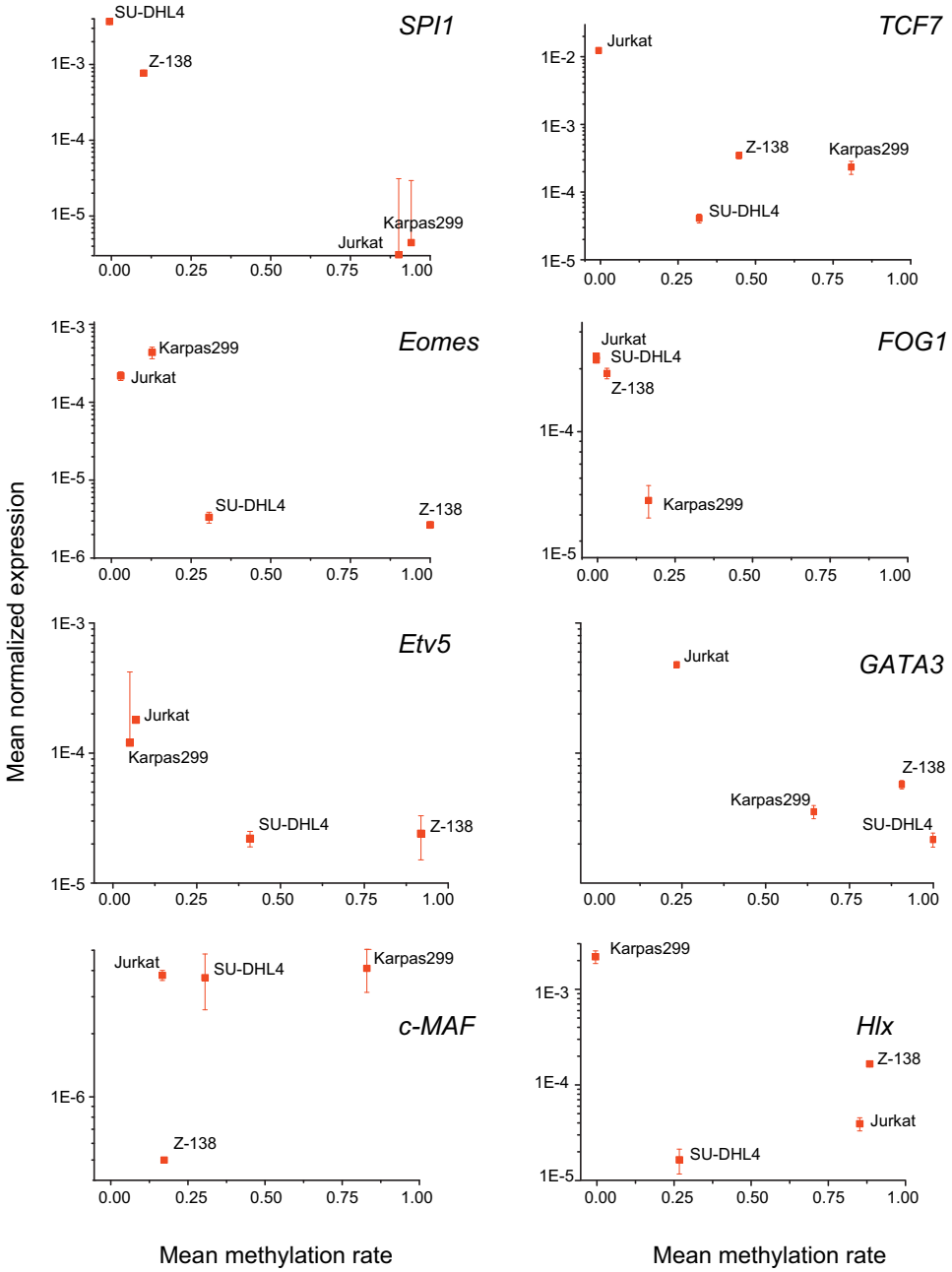

Figure 4-15 Averaged DNA methylation and mRNA expression for selected transcription factor genes. Averaged methylation values of amplicons located within the 5'-UTR of each gene and cell line are shown (x-axis). Gene expression was measured by real-time PCR and normalized against GAPDH (y-axis). The expression values shown are mean values derived from three independent experiments; the error bars indicate the standard deviation (SD).

The strictest correlation between methylation pattern and expression was found for the *SPI1* gene. Here, the hypermethylated CpGs of the T-cell cell lines (Jurkat and Karpas299) correlates with no expression, while hypomethylation in the B-cell lines correlates with an elevated level of SPI1 mRNA (Figure 4-15). A cell-type independent pattern was observed for the *TCF7* gene: relevant expression was measured only in the T-cell Jurkat clone, where the average methylation level of *TCF7:4* was measured with 0%, while the T-cell Karpas line (90% methylation) shows more than ten times lower

relative expression. Expression of *TCF7* in the B-cell lines is very low, regardless of the methylation pattern (Figure 4-15).

Etv5 was differentially methylated between B-cell lines and T-cell lines in both analyzed regions. The upstream region *Etv5:1* is hypermethylated in the B-cell lines (100% in Z-138 and 60% in SU-DHL) and hypomethylated in the T-cells (0% in both) (Figure 4-14), a pattern which is inversed in the intragenic *Etv5:2* (data not shown). The highest expression of *Etv5* was found in both T-cell lines suggesting *Etv5:1* as more likely to harbor a regulatory region (Figure 4-15). *Etv5:1*, in contrast to *Etv5:2*, also shows differential methylation in the hematopoietic cascade data, underlining the above assumption.

Relatively high levels of *Eomes* mRNA were measured in both T-cell lines, while the expression dropped in the B-cell lines. Differential methylation between T-cells and B-cells was measured only within *Eomes:3*, where the T-cell lines were found to be hypomethylated, while the B-cell lines showed an increased level of average methylation (100% in Z-138 and 40% in SU-DHL4).

GATA3 mRNA was detected only in the Jurkat T-cell line (25% average methylation for *GATA3:2*) but not in the two B-cell lines and in Karpas-299 (>50% average methylation) suggesting here, too, a correlation between hypomethylation and expression.

Similarly, Hlx mRNA level is highest in the Karpas T-cell line (0% average methylation). An increased level of methylation as measured in the other cell lines correlates with a drastic decrease of the mRNA level (Figure 4-15). *FOG1* expression is also highest in the hypomethylated cell lines (Jurkat, SU-DHL and Z-138) regardless of the cell type, while it quickly drops for the case of Karpas-299 where the average level exceeds 20% methylation (Figure 4-15).

No significant correlation between differentially methylated regions and measured expression could be determined for *Th-POK*, *NOTCH1*, *c-MAF* and *TBX21* (Figure 4-15 and data not shown).

Overall, these results suggest that specific CpGs within the analyzed regions might be responsible for the drastic pattern of expression changes between the individual samples. The approach of averaging the methylation levels over larger stretches of DNA is a rather rough quantification of the real methylation events occurring in the cell at a certain locus and possibly having an influence on the expression phenotype. The impact of methylation on the expression can be limited to as few as 1 CpG as shown recently for the *IL2* gene (57), which may explain in part some of the weak correlations detected here.

4.3. Targeted approach to biomarker identification by means of differentially methylated regions

4.3.1. T-helper cell imbalances in the peripheral blood of patients with rheumatoid arthritis detectable by DNA methylation

In order to determine a potential diagnostic application for a strongly differentially methylated marker as represented by the IFN-γ locus, a quantitative measurement of methylation was performed on memory and naive CD4+ cell compartments obtained from six healthy volunteers and nine patients with rheumatoid arthritis (RA). CD4+CD45RA+ (naive) and CD4+CD45RO+ (memory) cells were isolated as described in chapter 3.1.4. Equal cell numbers from each sample type were used for DNA extraction. All nine RA patients were within an acute phase of disease during sample extraction and had not yet undergone any immunosuppressive treatment.

The methylation pattern of all samples was determined within the *IFNγ* regions 1, 2, and 3, and the individual methylation levels obtained for each CpG were averaged per patient / donor within each region, assuming an equal level of methylation for adjacent CpGs. The results are displayed as box plots in Figure 4-16.

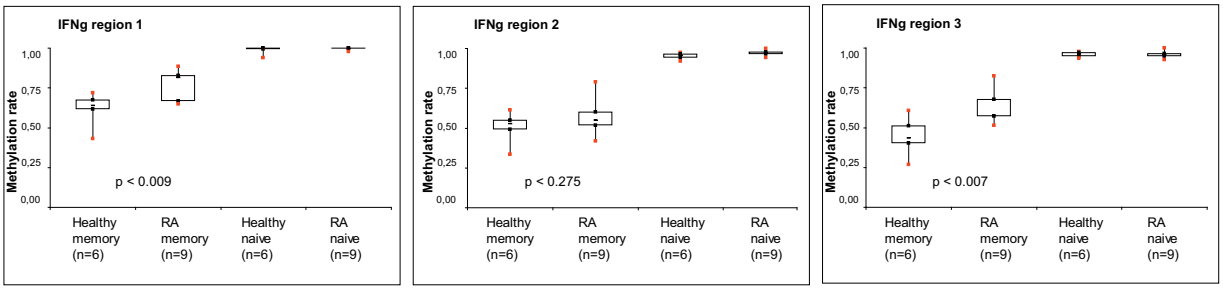

Figure 4-16 Box plots of averaged methylation levels for rheumatoid arthritis patients (RA) and healthy volunteers. Genomic regions 1, 2, and 3 of the *IFNγ* were analyzed within naive and memory CD4+ T-cell subsets and compared between patients and healthy donors. Two-sided t-test p-values were calculated to quantify the significance of the differentially methylated region within the memory cell compartments of healthy donors and RA patients.

The averaged methylation levels of the naive cell compartment are for both, RA patients and healthy donors and within every investigated region higher than 95% (Figure 4-16). This finding is in agreement with the high methylation levels observed in IFN-γ- cells (Figure 4-9). The averaged methylation levels for the more differentiated memory cells, however, differ significantly between RA patients and healthy donors for the *IFNγ* regions 1 and 3, respectively (Figure 4-16). No significant difference was seen within region 2. *IFNγ* region 1 is an enhancer element approx. 4.0 kb upstream of the TSS while region 3 is part of the proximal promoter covering the TSS and exon1. Within region 1, the mean average

methylation value in CD4+ memory cells of healthy individuals is approx. 60% while that of RA patient reaches approx. 85%. Similarly, within region 3 the mean average methylation value of healthy individuals is of approx. 45% and that of RA patients of 60%. Thus, both regions show slightly elevated levels of methylation within the RA patient group.

Statistical significance of the data was confirmed by a t-test: highly significant shift towards a more methylated status of these regions exists within RA patients ($p < 0.009$ for region 1 and of $p < 0.007$ for region 2). The question imposed by this data is: (1) do memory Th1 cells of RA patients have in general higher methylation levels than those of healthy individuals or (2) is the Th1/Th2 peripheral blood balance within RA patients shifted towards an increased number of Th2 cells? To address this question, IFN-γ+ were separated from IFN-γ- CD45RO+ memory cells from a subset of patients and from two healthy individuals for control purposes. The determined methylation levels are displayed qualitatively as heat charts in Figure 4-17.

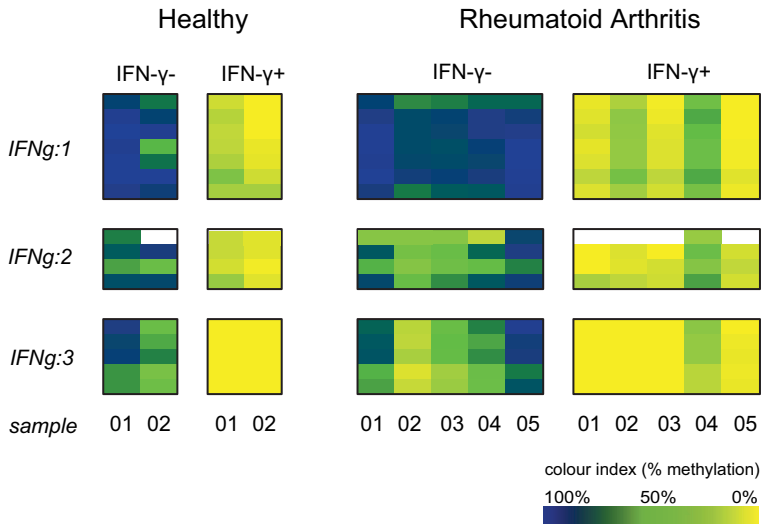

Figure 4-17 DNA methylation levels in IFN-γ- and IFN-γ+ memory cells of patient with RA and healthy individuals

As previously shown for the *IFNγ* gene locus (Figure 4-9), IFN-γ+ and IFN-γ- cells show here too significant differential methylation for several CpGs in the analyzed regions 1, 2, and 3 regardless of the health status ($p < 0.003$ for healthy and $p < 0.0005$ for RA patients respectively). However, no significant difference in methylation could be determined between the IFN-γ+ cells of patients with RA and healthy individuals ($p < 0.89$). Apart from slightly elevated methylation levels measured in individual samples (e.g. sample 04 in the RA IFN-γ+ group), the general methylation of both IFN-γ+ and IFN-γ- cells does not differ in RA patients and healthy individuals at the *IFNγ* gene locus.

Taken together, these results indicate that peripheral blood of patients with RA harbors an increased number of Th2 cells and thus sustains previously published findings by (122) and (123). Moreover, a DNA methylation marker was for the first time successfully applied to quantify cell balances within a mixed cell population.

4.3.2. Methylation profiles of the *IFNγ* and *IL10* gene in endometriosis

For many years, the immune system was considered to be involved in the development of endometriosis. Many women with endometriosis display certain immunologic defects or dysfunctions. Whether this is a cause or effect of the disease remains unknown. Endometriosis is associated with changes in both cell-mediated and humoral immunity. As an example, macrophages, which would be expected to clear endometrial cells from the peritoneal cavity seem to enhance their proliferation by secreting growth factors and cytokines (154).

It has also been shown that reactive T- and NK-cells are frequently found in the endometrium of women with endometriosis as compared to their healthy counterparts and that the eutopic endometrium in women with endometriosis tends to express a large variety of cytokine genes (155).

The data presented here is part of a large candidate gene project aimed at identification of defects in DNA methylation detectable in the endometrial tissue of affected women. However, due to current efforts to ensure the intellectual property, not all data can be shown here.

Since inflammatory parameters (cytokines, chemokines, etc.) were reported to be present in the peritoneum of woman with endometriosis and in the endometrium (156), DNA methylation for these factors was profiled in the endometrial cells of ten non- endometriosis women and ten endometriosis patients. The results are displayed as methylation heat charts in Figure 4-18.

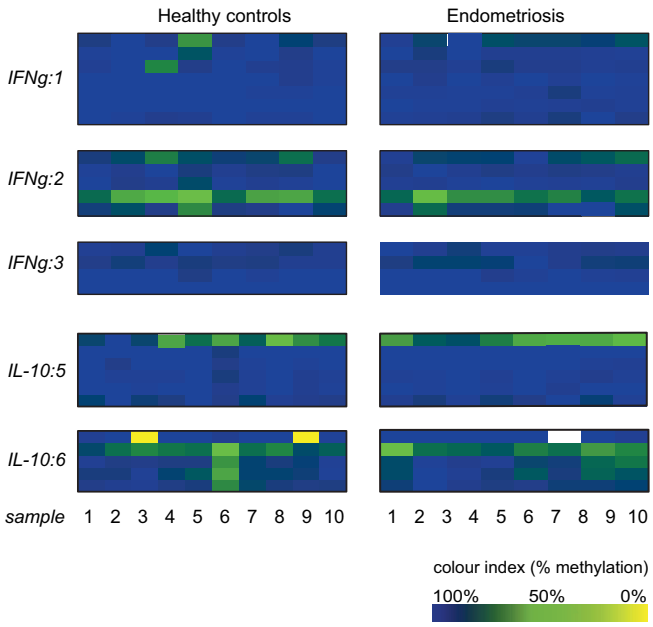

Figure 4-18 DNA methylation profiles in endometrial biopsies of patients with endometriosis (right column) versus non – endometriosis controls (left column). Selected regions within the *IL10* and *IFNγ* gene were profiled. Region numbering and genomic position is according to Figure 4-4 B and 4-9 respectively.

As for the two cytokines of relevance in this work, IFN-γ and IL-10, no significant differential methylation pattern could be detected within the two groups for none of the two genes.
Although there is considerable inter – individual variance within the groups, as seen for example in region 6 of the *IL10* gene, the pattern did not show the desired discrimination between healthy and disease. The *IFNγ* locus is strongly upmethylated for all three investigated regions suggesting a tissue specific silencing of this gene in the analyzed endometrial stromal cell. Eventual IFN-γ secreting residual T-lymphocytes in the endometrium could not be quantitatively detected by the used sequencing technique. Interestingly, the most 5' CpG of the IL-10 region 5 located at position -86, which has been intensively discussed in chapter 4.1.3.2 is methylated at about 50% in most endometrial samples as seen in the IL-10- lymphocytes (Figure 4-4 B).
Since endometrial stromal cells do not express IL-10, a monoallelic expression mechanism could be proposed regarding the importance of the methylation information carried by this specific CpG.

4.3.3. Testing selective methylation marker in tissue biopsies of T- and B-cell lymphomas

As aberrant methylation is a frequent phenomenon in cancer development and progression, the methylation profiles of the described transcription factors in T- and B-cell lymphomas were analyzed. For this analysis, samples from patients diagnosed with either diffuse large B-cell lymphoma (DLBCL, n=20) or T-cell non-Hodgkin lymphoma (n=14) were included and normal lymph nodes (n=18) were used as controls. For each tissue sample, histological examination was performed and only those samples with a confirmed tumor content of greater than 85% were included in the study, thus ensuring a relatively homogenous tumor composition.
Significant methylation differences at several genomic loci in DLBCL samples as compared to either normal lymph nodes or T-cell NHL samples were measured. Figure 4-19 shows the measured methylation levels for each CpG in selected genes and regions. A broader overview of DNA methylation in the tumor samples versus controls is given by Figure 4-20 where averaged methylation of co-methylated CpGs per sample is shown in box plots with each box plot summarizing one disease entity. Statistical significance for the measured methylation difference was determined by assessing the difference in the means and the variance for each displayed disease entity (Wilcoxon test).

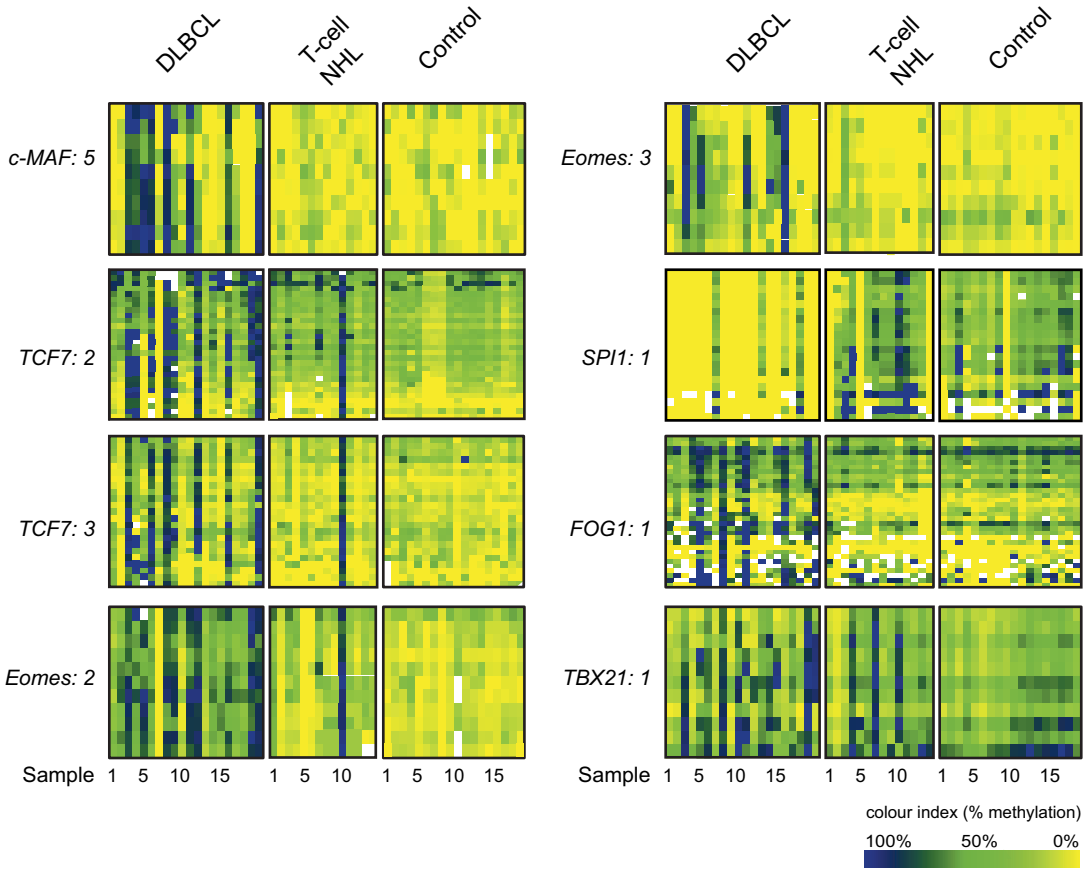

Figure 4-19 Methylation profiles of selected TF regions in diffuse large B-cell lymphoma (DLBCL), T-cell non-Hodgkin lymphomas (NHL) and control (healthy) lymph node samples. Rows show the methylation levels of individual CpGs. Samples and disease states are represented in columns.

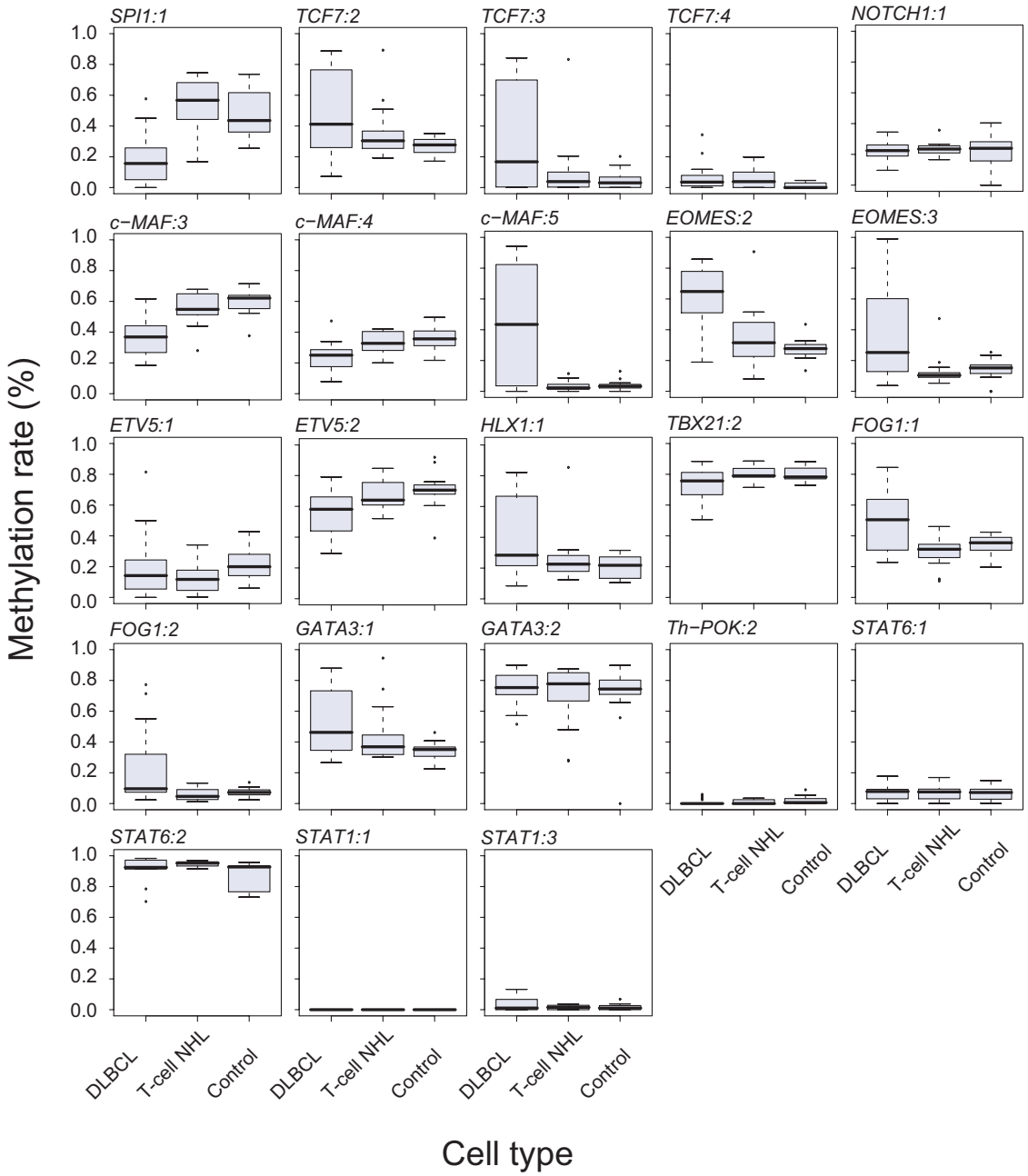

Figure 4-20 Box plots displaying averaged methylation levels for several analyzed genes and regions. Each box plot contains data from several samples analyzed within the respective disease entity. The median is shown as black bar.

The genes showing the most prominent differences in DLBCL samples were *c-MAF*, *TCF7*, *Eomes* and *SPI1* (Figure 4-19 and Figure 4-20. Hypermethylation of two CGIs associated with *c-MAF* (c-MAF:5, Figure 4-19) and *TCF7* (TCF7:3, Figure 4-19) was observed. The *c-MAF* associated CGI was hypermethylated (>90% methylation) compared to the methylation of normal lymph nodes (0%) in more than 50% (11 out of 20) of the DLBCL patient samples. Similarly, the *TCF7* associated CGI (TCF7:3, Figure 4-19) showed increased methylation (>60%) in 50% of the analyzed DLBCL samples (10 out of 20). Most of the DLBCL samples with a hypermethylated *TCF7* CGI were hypermethylated within the *c-*

MAF CGI as well. Interestingly, the CGIs of both genes were hypomethylated in normal B-cells (Figure 4-13) indicating that hypermethylation of these two CGIs is a specific event in DLBCL.

Eomes region 2, located approximately 1.0 kb upstream of the TSS (Figure 4-12), was specifically hypermethylated (>60%, p ≤ 0,001) in 90% of the DLBCL samples compared to normal lymph nodes (Figure 4-19). Although the *Eomes* TSS is located within a CGI, this CGI remained unmethylated in most cases (region 3) but the adjacent region 2 (Figure 4-19) was consistently hypermethylated in DLBCL samples. In contrast to the *Eomes* methylation in DLBCL, normal naive and memory B-cells displayed an average methylation (below 30%) in this region. Hypermethylation was often detected in the same samples at several gene loci, e.g. DLBCL samples # 3, 4, 5, 6, 8, 11, 12 and 20 were consistently hypermethylated within *c-MAF, TCF7*, *Eomes* and *FOG1*.

The 5'-UTR of *SPI1* was unmethylated in almost 80% of the DLBCL samples (Figure 4-19). This methylation status corresponds well with the profile observed for healthy B-cells and the two cancer B-cell lines analyzed (Figure 4-13 and Figure 4-14). In contrast, normal lymph nodes and the T-cell NHL samples showed hypermethylation (>50%) in this region. This methylation difference might reflect the differing cell type compositions present in healthy peripheral lymph nodes as compared to lymph nodes from DLBCL patients. The CGI of *FOG1* (region 2, Figure 4-19) showed increased methylation levels (>50%) in some DLBCL samples (6 out of 20) as compared to those measured in normal lymph nodes and the T-cell NHL group (<10%). Other analyzed genes, such as *TBX21* (Figure 4-19), *Hlx* and *GATA3* (Figure 4-19) showed no statistically significant methylation differences between the analyzed groups, although methylation heterogeneity was measured in some DLBCL cancer samples and not in normal lymph nodes. Similar to the methylation profiles derived from healthy cells of the hematopoietic cascade samples, no methylation alterations for *Th-POK*, *NOTCH1*, *STAT1* and *STAT6* could be identified in any of the lymphoma samples analyzed (Figure 4-19).

In contrast to the aberrant methylation observed in the DLBCL group, no recurring methylation differences between T-cell NHL samples and normal lymph nodes could be measured for the genes analyzed in the study. In the T-cell NHL group, only one sample (# 10, Figure 4-19) showed hypermethylation in some regions, however this observation did not reach statistical significance. In other analyzed samples and loci, T-cell NHL and normal lymphatic tissue showed indistinguishable methylation profiles (Figure 4-19 and Figure 4-20).

5. Discussion

In the current study, the DNA methylation profiles of major cytokine genes and transcription factors relevant during lymphopoiesis were determined at several CpGs spanning the respective gene loci.
The predominant method used to quantify methylation was the direct bisulfite sequencing.
For the *IL10* gene, epigenetic features beyond DNA methylation, specifically histone modifications were assessed, thus allowing a deeper insight of the chromatin status at this gene locus.
The aims of this profiling were twofold: (1) to gain insights into the epigenetic effects participating in the cell-specific regulation of these genes and (2) to identify differentially methylated regions that may allow the use of these markers directly or indirectly as surrogate markers in clinical diagnostic. To obtain accurate and robust methylation data from each of the analyzed cell types and for each investigated region, a direct PCR bisulfite sequencing technique with subsequent methylation – specific software analysis was applied.
As DNA methylation is a tissue specific feature in metazoan, different cell types of the human immune system were analyzed and the methylation levels were compared between cell types according to the defined biological question. A major cell type in which DNA methylation of cytokine genes was interrogated are CD4+ T-lymphocytes and their naive and memory subsets. Differentially methylated regions discovered in the *IFNγ* and *IL10* gene were used to interrogate their methylation status in indications like rheumatoid arthritis and endometriosis and to evaluate their potential as diagnostic biomarkers in these diseases.
Transcription factor gene methylation was analyzed in hematopoietic progenitor cells, in naive and mature B-cells as well as CD8+ cells, and in the T-helper cell subpopulation of CD4+ lymphocytes. Further, differentially methylated markers obtained for the transcription factor comparisons within hematopoietic cellular differentiation were investigated in two human hematopoietic neoplasias, T-cell and B-cell non Hodgkin lymphoma, and compared to non – affected, “normal” lymph node methylation.
During cell differentiation processes, several epigenetic modifications at the loci of effector cytokine genes such as *IFNγ*, *IL4* / *IL13*, and *IL2* were demonstrated in Th-cells. These included effects like DNA demethylation, histone hyperacetylation, development of characteristic DNAseI hypersensitivity patterns, increased restriction enzymes accessibility, and rearrangement of the chromatin within the nucleus (157), (158), (159), (160). An emerging view is that helper T cells use the above mentioned epigenetic mechanisms to allow dividing cells to memorize, signalling events that occurred earlier in their development (35, 161). As the only epigenetic modification for which an inheritance mechanism is known (maintenance methylation), DNA methylation is likely to mediate the restoration of DNAseI hypersensitivity sites following replication (162).
Differentiation of precursor naive T cells into mature cytokine producing cells is initiated by stimulation of naive T cells through the T cell antigen receptor (TCR) and influenced by a large number of genetic and environmental variables including the cytokine milieu (163), (164). Mature Th1 and Th2 cells are characterized by their specific, non-overlapping pattern of cytokine expression. The “poised” chromatin

state apparent in effector/memory Th-cells is thought to allow rapid secretion of effector cytokines when re-challenged by invading pathogens.

It has been shown for IL-4 and IFN-γ that DNA demethylation is not required for the transcription per se but that demethylation at the specific loci promotes high levels of cytokine production in fully differentiated, mature T-helper lymphocytes (146), (56).

The demethylation events in cytokine competent cells occurs in the proximal 5' promoter region, further upstream at specific locus control regions (LCRs) and within the gene body (140), (102), (103). In the case of IL-2, as few as one single CpG was shown to confer competency for efficient IL-2 production (57).

5.1. Quantitative direct bisulfite sequencing: advantages and shortcomings

The major method used to characterize DNA methylation in the in the present study was the quantitative sequencing of PCR products obtained after amplification of bisulfite converted DNA (84). It is based on the calculation of methylation signals by quantifying the cytosine/thymine proportions at CpG dinucleotides in the pre-processed sequence traces.

The method was developed at the Epigenomics AG to meet the requirements of the Human Epigenome Project (HEP). There, it has been successfully applied to generate high resolution methylation profiles of the human chromosomes 6, 20, and 22, where approximately 1.9 million individual CpG methylation values were measured in a total of 12 different human tissues (33).

The direct bisulfite sequencing is especially useful in generating high resolution profiles of methylation levels at individual CpGs located *in cis* on stretches no longer than 500 bp on the DNA sequence.

It is a high throughput method, which bypasses laborious cloning and sequencing of PCR products. There is no restriction regarding the sample DNA origin, which can be analyzed by this method, and the analysis can be performed on as little as 100 ng initial DNA due to the amplification step immediately following bisulfitation.

Thus, the method allows parallel screening of large numbers of CpGs in several different tissues at the same time. Subsequent computed data analysis helps to generate comparisons between individual genomic regions and between DNA originating from different tissue types.

The results of the sequencing are usually displayed in this work as methylation levels of individual CpGs in the heat charts. In some cases, when adjacent CpGs have similar methylation levels, the individual levels were averaged to obtain the methylation pattern of an entire region (Figure 4-11, Figure 4-13 B, Figure 4-15, Figure 4-16 and Figure 4-20). This averaged quantification makes the data more robust to small variations between individual CpG levels resulting from incorrect level quantification.

Like every other laboratory method, the direct bisulfite sequencing also has its limitations, especially when it comes to accurate quantification of methylation levels with error rates lower than 15%-20%.

First, the efficiency of the bisulfite reaction is of crucial importance for the successful approximation of the methylation level at any given CpG. The efficient bisulfite conversion of genomic DNA is not only dependent on adequate reaction conditions. Factors like the chromatin status at a certain region affect the conversion rate substantially. It has been observed that methylation levels of CpGs located in heterochromatin are more difficult to quantify than CpGs located in active chromatin. Incomplete conversion of DNA results in incorrect normalisation and finally leads to inaccurate quantification of the methylation signal.

The normalisation information is derived from the conversion rates of cytosines outside of CpG dinucleotides, calculated from the area under the sequence trace curve. This rate is usually calculated by two different methods and overall conversion rates below 85% led to the exclusion of the respective sequence trace from the analysis.

The primers used to amplify the bisulfited DNA are positioned on regions depleted of CpGs in order to avoid inefficient amplification due to the C/T polymorphism generated after bisulfite conversion at unmethylated CpGs. However, for not yet entirely clear reasons, some primer assays tend to amplify specific methylation conformations out of the heterogeneously methylated DNA stretch. This phenomenon, known as “PCR bias”, leads to wrong assignment of the methylation composition of a given sample (165). In order to determine the bias introduced by any of the primer assays used in this study, every assay was used to sequence artificially generated up- and downmethylated DNA as well as 50% mixtures of the upper two DNA types. Assays, failing to calculate the expected levels, especially in the mixed DNA sample, were discarded from the study. Nevertheless, at some CpGs located at the periphery of the analyzed regions, the methylation signal is difficult to quantify mainly due to the high proportion of mixed signals. This resulted too in inaccurate quantification of these loci.

The average level of discrimination for all employed assays was 30% methylation differences between individual samples.

In order to account for much of the noise derived from the described method inaccuracy, replica biologic samples were employed and repeated PCR amplification and sequencing reactions were performed.

Altogether, the method helped to characterize consistent methylation differences between sets of samples and to discover previously uncharacterized DNA methylation markers.

5.2. Methylation profiling at the *IL4*, *IL13*, *GATA3* and *TBX21* loci in CD4+ subsets

The genes encoding the cytokines IL-4 and IL-13 as well as the transcription factor GATA-3 are predominantly expressed in Th2 cellular subsets of the CD4+ cells (140). *IL4* and *IL13* are part of a locus of co-regulated cytokines which also contains the *IL5* and *RAD50* genes (Figure 4-3 A). In this work, the methylation profiling of a large number of CpGs located near and within these gene loci were analyzed in T-cells that do not express IL-4 and IL-13.

Differentially methylated regions were observed in the previously described locus control region (LCR) between the *IL4* and *IL13* gene (Figure 4-3 A, region 3) as well as within the exon 1 and exon 2 of the *IL4* gene (Figure 4-3 A, region 5 - 9). In contrast to the naive precursor cells, depicted as IL-10-/IFN-γ-, where the methylation levels of nearly every measured CpG exceeded 90%, methylation of the memory cell subsets IL-10+ / IFN-γ+ and IFN-γ+ drops to levels of about 50% - 60%. IL-10+ memory subsets show intermediate levels, usually higher than 60%. It is known, that low-level non selective transcription of the *IFNγ*, *IL4* and *IL13* genes occurs in naive T-cells following stimulation with antigen, indicating that these genes are poised to respond to the signals that induce differentiation (166). Thus, DNA methylation information can be overridden to induce transcription and is later used as a “lock in”-mechanism to maintain stable transcription in fully differentiated cells. Although the current analysis was not performed in Th2 cells, where complete demethylation is known to occur following stable transcription establishment, the reduced methylation levels in the memory cell subsets are remarkable. They suggest that epigenetic modifications of the loci towards complete demethylation occurs gradually and sporadic rather than from one cell division to the other or directly by a targeted DNA demethylation event. The hypothesis could be set up, that upmethylated, antigen-inexperienced naive cells become gradually demethylated at the cytokine gene loci, ultimately leading to very low methylation levels for the expressed cytokines. The loci of the other cytokines remain at an intermediate level of methylation allowing a “mixed lineage” status. Definitive cell fate determination towards Th1 or Th2 lineage occurs therefore later during differentiation and not after first antigen contact of the naive T-cell.

The cell populations used for methylation analysis within this study have been sorted to a purity of greater that 90% and the analysis of methylation by bisulfite sequencing has a resolution capacity of 20% methylation differences (data not shown). It cannot be excluded that phenotypically identical cells obtained by a defined purification method have different methylation patterns and constitute a mixed cell population. However, the methylation pattern at a specific genomic locus of a cell population that has been purified according to expression of the respective region is expected to be the same in the targeted cells.

Interestingly, the intermediate methylation state does not allow the cell to return to transcription at the respective loci since studies are available where it was shown that once committed memory cells are not able to return to the point before definitive commitment.

However, more profound studies of the methylation dynamics are required to fully demonstrate the upper statements.

The methylation of the *GATA3* gene showed the same pattern in all of the analyzed cell types. At this point of differentiation, DNA methylation is not correlated to the gene transcription as its expression was significantly up-regulated in IL-10^{+}IFN-γ^{-} versus IL-10^{+}IFN-γ^{+} Th-cells. The zinc finger transcription factor GATA-3, apart from its key role as Th 2 cytokine regulator, is known to be expressed already in hematopoietic progenitor cells (36). As frequently described for CpG islands, the island associated to the *GATA-3* gene is demethylated at several analyzed CpGs and within the conserved regions located within and outside the island (Figure 4-3 B). The low degree of methylation is correlated to the high degree of sequence conservation found in the CpG island (Figure 4-3 B, CNS row).

A clearer differentially methylated pattern is displayed by the *TBX21* locus. As the transcriptional regulator TBX21 is essential for transcription of the *IFN-γ* gene in Th1 cells (137), its methylation pattern correlates with the TBX21 expression in IFN-γ+ cells. Interestingly, the regions of low methylation in *TBX21* expressing cells are both located within the first intron, suggesting an as yet unknown regulatory role within the conserved elements they are covering (Figure 4-3 C, region 2 and 3).

Again, the CpG island located at the 5' end of the *TBX21* gene and harboring a large conserved DNA region is demethylated in all analyzed samples underlining the role of demethylation for the evolutionary conservation of DNA sequences.

5.3. Absence of differential methylation at the *IL10* gene locus: consequences for the functional memory

Although the immunoregulatory role of IL-10 has been extensively studied for decades, little information is available on the molecular mechanism of its transcriptional regulation in humans. Aspects of epigenetically related expression memory, conferring rapid reactivation of the *IL10* gene in committed Th1 and Th2 cells have not yet been addressed.

As an approach to this question, the methylation of 48 CpGs encompassing the *IL10* locus was measured in IL-10+ and IL-10- CD4+ memory cells obtained directly from the peripheral blood of healthy donors. Simultaneously, Th1 and Th2 cell lines with IL-10 expressing and non-expressing properties were analyzed for methylation. The methylation results from both *ex vivo* cells and cell lines showed similar methylation patterns. In contrast to the findings of extensive locus demethylation for e.g. the *IFN-γ* gene in IFN-γ+ cells, no such clear pattern emerged for the *IL10* gene. The *IL10* locus is rather CpG poor and most of the CpGs located upstream of the annotated transcription start site were upmethylated regardless of IL-10 transcription (Figure 4-4 A, B) suggesting no regulative role for DNA methylation in the analyzed T-cell subtypes. A more interesting region with respect to differential methylation between the cell types is region 5, located in close vicinity to the TSS and within a highly conserved DNA sequence. The two most 3' analyzed CpGs within these region, located at positions -161 and -86 display slight methylation differences between the IL-10+ and IL-10- cells in both analyzed systems, the *ex vivo* cells and the Th cell lines. IL-10 expressing cells tend to be demethylated at these two CpG positions, a finding that could be strengthened by the sequencing of cloned PCR products obtained from region-specific amplification of the bisulfited DNA (Figure 4-5). The histone modification data obtained for region 5 sustains the notion of an open chromatin state in the region (Figure 4-6). Previous studies investigating DNAseI hypersensitivity sites (HS) in naive and differentiating murine T-cells identified this conserved region as a Th2 specific, constitutive HS and also found the corresponding murine CpG at position -86 to be demethylated in IL-10 expressing cells (99). Taken together, these data suggest a regulative role of this proximal promoter region in T-cells expressing IL-10 in the human immune system.

Next, we addressed the relevance of methylation level of the two conspicuous CpGs in memorizing the ability of IL-10 expression. Answering this question becomes easier when comparing expression in view of the methylation pattern for the two cytokines IL-10 and IFN-γ. Clonal *in vitro* expansion for two weeks of CD4+ T-cells expressing IL-10, IFN-γ or both cytokines revealed a strong tendency of IL-10 expression loss upon restimulation (Figure 4-7). Simultaneously, the two promoter CpGs maintain the lower methylation status observed previously (Figure 4-8). At the same time, IFN-γ expressing cells being extensively demethylated at the entire gene locus maintain the expression of this cytokine throughout the incubation time. Thus, the promoter DNA methylation of the *IL10* gene might not harbor the "locked in" expression memory for this cytokine as it does in the case of IFN-γ.

The unique role of IL-10 with its broad immunoregulatory functions might be a major reason for these differences in expression and regulation. Recent studies have demonstrated that IL-10 produced by the human Th1 cells has a regulative effect of limiting exaggerated inflammation in animals infected with *Toxoplasma gondii* (167), (168). It has been suggested that the *IL10* locus might be in a reversible histone deacetlyase – responsive state in Th1 cells that allows its reactivation upon continuous stimulation by chronic infection. A constitutive expression, conferred by an epigenetic memory mechanism, would prevent the appropriate inflammatory response and hence reduce immune system efficacy.

In conclusion, IL-10 is excluded from the functional cytokine memory in human Th-cells, preventing the generation of memory Th-cells with an inherited program to secrete IL-10.

5.4. Differential DNA methylation at the *IFNγ* locus and its role as epigenetic memory

In the current study, the CpG methylation of 28 CpGs located within the *IFNγ* gene body, the proximal promoter and up to 4.0kb upstream of the TSS were profiled in IFN-γ expressing and non expressing CD4+ lymphocyte subsets. The analyzed regions are highly conserved between man and mouse as revealed by interspecies sequence comparisons. In agreement with previously reported data, strong demethylation was found at the 4.0 kb upstream enhancer element and at the CpG located -53 bp upstream the TSS in IFN-γ competent cells (169). Upmethylation of the latter CpG was shown to be sufficient for transcriptional silencing of the *IFN-γ* gene in Th2 cells (55).

The results in the current study reveal an extensive demethylation of several CpGs across the *IFNγ* locus including a number of CpGs within the gene body up to exon 3. As the methylation levels of IFN-γ expressing cells were determined at about 0 %-10% methylation and of IFN-γ non expressing cells at 80 – 100% methylation (Figure 4-9), demethylation of both alleles seems to be required for stable expression competence. The DNA demethylation at the IFN-γ locus confers the cell the stable property to rapidly express IFN-γ upon restimulation as seen in the *in vitro* cultivation and restimulation

experiment (Figure 4-7). Over 95% of the cells were still able to express IFN-γ after one week of cultivation.

The *in vitro* experiments performed to induce differentiation of naive cells towards the Th1 IFN-γ expressing phenotype (chapter 4.1.4.2) revealed a strong dependency of the demethylation on the externally applied stimulus and a region specific dynamic of this process (Figure 4-10). Cells co-cultured with allogeneic dendritic cells (stimulus III), secrete themselves several cytokines and growth stimulating factors and thus induce the lowest degree in methylation within both, IFN-γ producing and non-producing cells. Regions to be first and most prominently demethylated are obviously those located in the proximal promoter (region 2 and region 3) and in the enhancer element (region1).

The stimuli I and II consisting mainly of T-cell stimulatory molecules and one respectively two Th1 polarisation priming conditions (anti IL-4 and anti IL-4 / IFN-γ for stimulus I and II respectively), only induce slight demethylation at the genomic regions 2 and 3 (both located in the proximal promoter) suggesting a relative importance of these regions regarding chromatin accessibility. IFN-γ expression despite a hypermethylated locus (as seen in region 1 of IFN-γ + cells stimulated with the stimuli I and II) was demonstrated to occur through transactivation mediated by the Th1 key transcriptional regulator TBX21 (146). However, during the cultivation period of six days none of the stimuli induced total demethylation at both alleles within the investigated cells.

The strong effect in inducing DNA methylation-mediated accessibility at the *IFNγ* locus conferred by the allogeneic dendritic cells in contrast to the cytokine cocktails stimulation may be explained by a probabilistic view of cellular polarisation and gene expression. Following this concept, a complex promoter as that of *IFNγ*, requiring several transcriptional initiation molecules, is most likely to be activated and made accessible for transcriptional complexes, the higher the number of external stimuli that influence the cell to differentiate or to produce the respective cytokine. The probability of expression is thus multiplicatively enhanced by each individual stimulus (170). A typical dendritic cell presents several antigens on its MHC complexes and releases several stimulatory molecules into its cellular surrounding. This increases the probability of the presence of all required factors for inducing a stable, accessible configuration at the targeted gene locus.

To fully elucidate the role of the external stimulus on the cytokine locus accessibility and associated expression, a quantification of the produced IFN-γ in the IFN-γ+ cells and individual cell numbers obtained in the individual stimulation experiment is necessary.

5.5. DNA methylation of transcription factor genes changes during differentiation

The results presented in chapter 4.2 reflect the DNA methylation profiles of a number of candidate transcription factor (TF) genes that are key for the development of specific cell lineages in the lymphopoietic system. It could be shown that differential DNA methylation of several TF genes such as *SPI1*, *TCF7*, *c-maf*, *Etv5*, *TBX21* and *GATA3* is an accompanying feature during development and

lineage commitment. For *SPI1*, *Eomes* and *Etv5*, an inverse correlation between 5'-UTR methylation and the respective gene expression was demonstrated, suggesting that these genes are regulated in part by DNA methylation. A specific role of the differentially methylated regions in transcription initiation has yet to be elucidated.

The lack of an inverse correlation between 5'-UTR methylation and the respective gene expression that has been observed for the other genes is consistent with previous reports (38), (33). These groups found an inverse correlation with the transcription of the cognate gene for only about 1/3 of all differentially methylated 5'-UTRs.

Since the current study does not claim a comprehensive screen of all putative regulatory sequences of the genes, it cannot be excluded that the methylation of other, adjacent CpGs might also affect gene transcription. Methylation of a single CpG as opposed to an entire region might be sufficient to silence expression of these TF genes. Indeed, Murayama *et al.* showed recently for the *IL2* gene that methylation at a single CpG within the *IL2* promoter is sufficient to regulate IL-2 expression (57). Alternatively, the differential methylation observed might not directly regulate transcription, but might rather reflect a different accessibility of the chromatin (171).

The 5'-UTR of *SPI1* was unmethylated in undifferentiated progenitor cells and naive and memory B-cells while being hypermethylated in CD4+ and CD8+ lymphocytes. This methylation profile, combined with the presented evidence that *SPI1* is regulated in part via 5'-UTR methylation, is consistent with the reported expression of this TF. *SPI1* is highly expressed in early hematopoietic development and expression persists in differentiated B-cells but not in T-cells (172), (173). Furthermore, the vast methylation profiling data presented here complements the data from Amaravadi and Klemsz, who described the tissue specific methylation in B-, T- and macrophage cell lines of three CpGs flanking exon 1 of *SPI1* (174). In summary, the presented results point to an epigenetic regulation of *SPI1* during hematopoiesis.

The observed differential methylation profiles of *TCF7*, *c-maf*, *TBX21*, *Etv5* and *GATA3* indicate that there are lineage and differentiation-specific methylation profiles that in turn might help to "lock" and memorize a specific state. Furthermore, the observed methylation profiles correlate well with reported expression patterns of these genes. Although *TCF7* expression did not correlate with its methylation status in the cell lines used, the observed low methylation in the primary cells ($CD34^+$ progenitor cells, naive CD4+ and CD8+ lymphocytes) correlates with the reported expression of TCF7 in hematopoietic progenitor cells (175) and during T cell development (176).

For *c-maf* and *TBX21*, regions located within their 5'-UTR were specifically unmethylated in memory Th1 CD4+ lymphocytes and CD8+ lymphocytes. In turn, c-maf is expressed in Th2 CD4+ lymphocytes (177) and in CD8+ lymphocytes (178) and TBX21 is expressed in Th1 CD4+ lymphocytes (179) and in CD8+ lymphocytes (180). In all examined hematopoietic cells, the Etv5 5'-UTR displayed a low methylation, with only Th1 CD4+ and CD8+ memory cells being slightly higher methylated. Etv5 is expressed at low levels in both naive and memory Th1 CD4+ cells but is highly expressed in activated Th1 CD4+ cells (118) suggesting that DNA methylation might only play a permissive regulatory role in these cells. GATA-3, which has been implicated in both early T cell development and the transition of a

mature Th precursor cell to the Th2 lineage, is expressed at higher levels in CD4+ as compared to CD8+ lymphocytes (181). In the samples used within this study, the 5'-UTR of the *GATA3* gene showed reduced methylation in CD4+ naive and memory cells as compared to B-cell and CD8+ lymphocytes.

In conclusion, the current study provides evidence for DNA methylation changes throughout healthy lymphocyte development in transcription factor genes that are restricted in their expression to particular lineages.

5.6. Differentially methylated regions as diagnostic biomarkers

A biomarker is an endogenous molecule or process that is a specific indicator for the presence of a given disease condition in the body. It might be either derived from the disease area itself or the response of the body to the abnormal state.

Within the current study, several regions found to be differentially methylated in the analyzed cell types have been tested for their discrimination potential between disease and healthy state.

Three different disease entities were exemplarily analyzed in the fields of autoimmune disease and hematologic cancer. Differentially methylated regions within the cytokine gene *IFNγ* were used to quantify differences in the composition of the memory T –cell compartments of patients with rheumatoid arthritis (RA) and healthy individuals. In the field of endometriosis, none of the applied markers derived from the *IFNγ* and *IL10* gene was able to detect significant differences between the analyzed disease tissue and its healthy counterpart. In contrast, several markers based on the transcription factor genes were found to be differentially methylated between healthy lymph node and cancerous lymphatic tissue in the analyzed B-cell neoplasm. Concomitantly, none of them was aberrantly methylated in the analyzed T-cell neoplasm when compared to the correspondent healthy tissue.

A controversially discussed topic in the etiology of rheumatoid arthritis is that of a disturbed Th1/Th2 balance in the peripheral blood. The synovial membrane of patients with rheumatoid arthritis is invaded by activated Th1 lymphocytes that locally induce a strong inflammatory environment. It has been therefore hypothesised, that accumulation of Th1 cells in the joints of patients with RA results in a general depletion of these cell subset in the periphery (122). Figure 4-1 shows schematically the hypothesized view regarding the composition of the peripheral blood memory Th cell subsets in healthy individuals and RA patients.

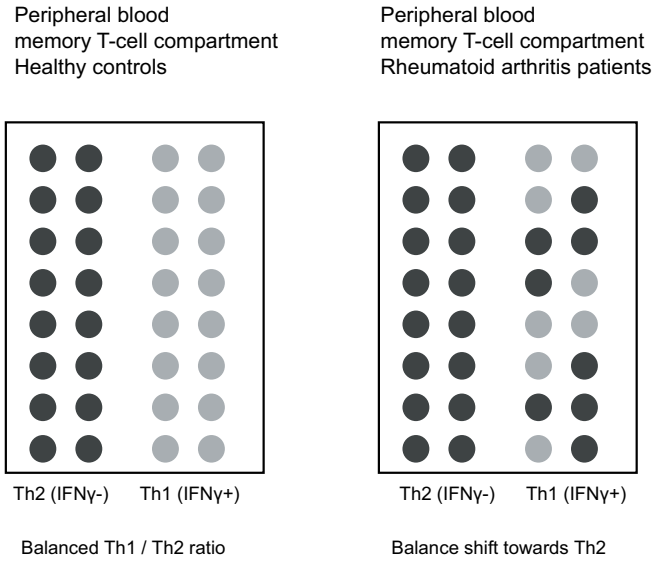

Figure 5-1 Hypothesized composition of the Th - memory cell compartment in healthy individuals and Rheumatoid Arthritis patients. The diminished number of IFN-γ+ Th1 cells in the peripheral blood is possibly the consequence of massive Th1 cell migration into the synovial membrane of the affected individuals.

However, controversial results led to a critical view of this hypothesis (182), (183). The methylation-based measurement performed in the current study is strengthening the hypothesis of diminished Th1 cell numbers in the peripheral blood of individuals carrying the disease.

Since the methylation in the *IFNγ* gene promoter region is strogly discriminating between IFN-γ producers and non-producers and thus between Th1 and Th2 cells (Figure 4-9, Figure 4-17), this marker was chosen to quantify the cell balance in isolated memory Th-cell compartments. The resulting methylation value is a mixed signal obtained from the proportion of unmethylated Th1 cells and upmethylated Th2 cells. The analysis was focused on the promoter regions 1, 2 and 3 (Figure 4-9). After determining the methylation level for each individual CpG in the respective regions, the averaged value was determined for each region and patient. The medians of the two groups (healthy and RA patients) were compared and statistically significant differences were determined for the regions 1 and 3, consisting specifically in a higher methylation level in patients with RA. Since FACS separation of the twoTh cell types revealed no irregularities in the methylation of IFN-γ producing Th1 cells (Figure 4-17), a possible conclusion is that of a cell balance shift towards Th2 cells within the six RA affected individuals analysed in this study.

However, before putting this data into a clinical context two limitations of the study need to be considered: first, the small sample numbers especially in the control group and second, the measurement method of averaged bisulfite sequencing methylation values.

The limitations of the measurement method is discussed in detail in chapter 5.1. In order to minimize the data background obtained from a single CpG measurement, the methylation values across a DNA stretch of the size of e.g. region 1, 2 or 3 were averaged for each sample. The averaged data were used for the comparison of the means between the two defined groups.

In order to obtain a homogenous group of RA patients, a set of criteria had to be defined, such as heterogenous gender distribution, disease stage and most important, the patient therapyat the time of blood withdrawal. The nine patient samples included in the study were obtained from individuals suffering an acute RA phase and prior to any anti-inflammatory drug treatment.

The disease phase at the time point of sample withdrawal was determined by physical symptom classification rather than by evaluation of clinical parameters such as the C-reactive protein (CRP) level. Literature data shows a strong direct correlation between high CRP levels (and thus strong disease activity) and the depletion of Th1 cells in the peripheral blood (123). Hence, the information on the respective CRP level of each patient would have been a useful parameter in the further classification of the nine patient samples.

Especially the last mentioned condition (no previous medication), is essential since anti-inflammatory drugs may have an influence on the cell composition in the peripheral blood. At the same time, this prerequisite is rendering sample collection difficult since most patients have a long history of non steroidal antiinflammatory drug (NSAID) or corticosteroid drug treatment. Thus, we had to limit our study to the available nine patient and six control samples.

The results obtained with the current patient cohort point to a shifted balance of Th cells in the peripheral blood of RA patients towards Th2 cells.

An incomplete demethylation and thus maturation of Th1 cells at the *IFNγ* locus is improbable, since IFN-γ+ CD4+ cells sorted by FACS from the blood of RA patients showed the usual low methylation levels as described in healthy individuals for this cell type. Thus, the observed increase in methylation is most likely to be derived from a shift in the Th1/Th2 balance.

Until now, relatively few studies have been addressing this issue, mainly because clinical diagnosis of RA is increasingly performed by the identification of specific antibodies present in patients carrying the disease. In addition, shifts in the balance of cellular compartments may be an unspecific event accompanying the course of the disease rather than the cause.

However, the quantification of cell compartments via DNA methylation performed in the current study is useful for two reasons: first, it simplifies the general procedure of FACS cell counting, intracellular cytokine staining and/or mRNA measurement that are currently used to determine cellular ratios. Second, it could be used to monitor the efficacy of a given therapy in restoring the natural cellular balance.

Cell specific methylation patterns could be further used in several applications. For example, Saito at al described a significantly higher Th1/Th2 ratio in patients with preeclampsia, a severe pregnancy disorder which results in premature birth (184). The development of a methylation based test to determine the cell ratios would help to carefully monitor the pregnancy and to evaluate the risk of preeclampsia at early stage.

Although not for the use in peripheral blood, another possible application of T-cell specific methylation markers is the assessment of the number of infiltrating lymphocytes in tumors. High levels of specific CD4+ lymphocytes (Treg cells) in tumor tissue of ovarian cancer have been reported to be associated with a poor disease prognosis (185). Since immune surveillance plays a significant role in cancer

development, the presence and the quantification of lymphocytes in the environment of solid tumors might be of crucial importance for prognosis and even therapeutic prediction.

As for the two markers tested in endometriosis (*IL10* and *IFNγ*) no significant methylation differences could be detected that enable discrimination between patients and healthy individuals. These lymphocyte markers were tested in endometrial tissue with the expectation of detecting infiltrates that are indicative of an inflammatory process in the endometrium. For the failure to detect difference two possible explanations were considered. First, the methylation detection method of direct bisulfite sequencing could be too insensitive to detect small proportions of differentially methylated cells among a strong background (see chapter 0 for details). Second, the presence of lymphocyte infiltrates in the endometrium was hypothesised upon the finding of severe inflammation in the peritoneum of woman with endometriosis. However, the inflammatory reaction at established peritoneal lesions may not be present already in the pre-menstrual endometrial tissue thus resulting in the absence of detectable numbers of immune cells.

The third disease class that has been analyzed to detect discriminating methylation markers belongs to the field of cancer, where methylation was already abundantly shown to be an important contributor in disease establishment (71). DNA methylation biomarkers, which currently possess the most clinical relevance, have been developed in the field of tumor classification, disease and therapy prognosis.

In this study, candidate methylation tags used to assess patterns in the healthy hematopoietic cascade were employed to analyse patterns of differential methylation in malignancies of the lymph node.

Profound changes in the DNA methylation profile of several transcription factor genes (*SPI1*, *TCF7*, *c-maf* and *eomes*) were found in diffuse large B-cell lymphoma (DLBCL).

Compared to normal lymph nodes and T-cell derived lymphomas, *SPI1* was unmethylated in most of the DLBCL samples. It is possible that this observation reflects the increased number of B-cells in lymph nodes derived from DLBCL patients. Alternatively, it is possible that the 5'-UTR of *SPI1* is specifically unmethylated in DLBCL lymph nodes and contributes to tumorigenesis. Regulation of *SPI1* is crucial for effective cell proliferation control, as Rosenbauer *et al.* recently reported that mice, carrying a deletion of a regulatory element (URE) approximately 14.0 kb upstream of *SPI1,* developed acute myeloid leukemias (106). In conclusion, the presented data suggest a tight epigenetic control of *SPI1* during hematopoiesis and point to a role of aberrant *SPI1* methylation in DLBCL tumorigenesis.

Although the expression status of these genes was not measured in DLBCL, promiscuous expression of TF genes appears to be a common feature of lymphomas. Dorfman *et al.* found that T-cell transcription factors are aberrantly expressed in B-cell lymphoproliferative disorders (186), and conversely B-cell transcription factors are aberrantly expressed in T-cell lymphoproliferative disorders (187). Additionally, a number of DLBCL patients showed consistent hypermethylation of several genes that could point to distinct methylation signatures potentially defining molecular subgroups within these patients. Interestingly, a number of genes (e.g. *SPI1*, *TCF7* and *c-maf*) that were differentially methylated in healthy cells were also aberrantly methylated in lymphoma samples, thus potentially indicating increased susceptibility of aberrant methylation of these genes during tumorigenesis. Currently, the mechanisms that lead to aberrant methylation in tumors are largely unknown, but further

genome-wide studies will help determine if tissue-specific methylated genes are more likely to become aberrantly methylated in diseased tissues.

6. References

1. Holliday, R. 1990. DNA methylation and epigenetic inheritance. *Philosophical transactions of the Royal Society of London* 326:329-338.
2. Holliday, R. 1994. Epigenetics: an overview. *Developmental Genetics* 15:453-457.
3. Egger, G., G. Liang, A. Aparicio, and P.A. Jones. 2004. Epigenetics in human disease and prospects for epigenetic therapy. *Nature* 429:457-463.
4. Jenuwein, T. 2001. Re-SET-ting heterochromatin by histone methyltransferases. *Trends in cell biology* 11:266-273.
5. Clark, S.J., J. Harrison, and M. Frommer. 1995. CpNpG methylation in mammalian cells. *Nature Genetics* 10:20-27.
6. Bird, A. 2002. DNA methylation patterns and epigenetic memory. *Genes and Development* 16:6-21.
7. Antequera, F., and A. Bird. 1993. Number of CpG islands and genes in human and mouse. *Proceedings of the National Academy of Sciences of the United States of America* 90:11995-11999.
8. Razin, A., and H. Cedar. 1977. Distribution of 5-methylcytosine in chromatin. *Proceedings of the National Academy of Sciences of the United States of America* 74:2725-2728.
9. McClelland, M., and R. Ivarie. 1982. Asymmetrical distribution of CpG in an 'average' mammalian gene. *Nucleic Acids Research* 10:7865-7877.
10. Takai, D., and P.A. Jones. 2002. Comprehensive analysis of CpG islands in human chromosomes 21 and 22. *Proceedings of the National Academy of Sciences of the United States of America* 99:3740-3745.
11. Saxonov, S., P. Berg, and D.L. Brutlag. 2006. A genome-wide analysis of CpG dinucleotides in the human genome distinguishes two distinct classes of promoters. *Proceedings of the National Academy of Sciences of the United States of America* 103:1412-1417.
12. Ehrlich, M., M.A. Gama-Sosa, L.H. Huang, R.M. Midgett, K.C. Kuo, R.A. McCune, and C. Gehrke. 1982. Amount and distribution of 5-methylcytosine in human DNA from different types of tissues of cells. *Nucleic Acids Research* 10:2709-2721.
13. Okano, M., D.W. Bell, D.A. Haber, and E. Li. 1999. DNA methyltransferases Dnmt3a and Dnmt3b are essential for de novo methylation and mammalian development. *Cell* 99:247-257.
14. Weber, M., I. Hellmann, M.B. Stadler, L. Ramos, S. Paabo, M. Rebhan, and D. Schubeler. 2007. Distribution, silencing potential and evolutionary impact of promoter DNA methylation in the human genome. *Nature Genetics* 39:457-466.
15. Pradhan, S., A. Bacolla, R.D. Wells, and R.J. Roberts. 1999. Recombinant human DNA (cytosine-5) methyltransferase. I. Expression, purification, and comparison of de novo and maintenance methylation. *The Journal of Biological Chemistry* 274:33002-33010.
16. Bhattacharya, S.K., S. Ramchandani, N. Cervoni, and M. Szyf. 1999. A mammalian protein with specific demethylase activity for mCpG DNA. *Nature* 397:579-583.
17. Vairapandi, M., D.A. Liebermann, B. Hoffman, and N.J. Duker. 2000. Human DNA-demethylating activity: a glycosylase associated with RNA and PCNA. *Journal of Cellular Biochemistry* 79:249-260.
18. Kapoor, A., F. Agius, and J.K. Zhu. 2005. Preventing transcriptional gene silencing by active DNA demethylation. *Federation of European Biochemical Societies letters* 579:5889-5898.
19. Gaudet, F., J.G. Hodgson, A. Eden, L. Jackson-Grusby, J. Dausman, J.W. Gray, H. Leonhardt, and R. Jaenisch. 2003. Induction of tumors in mice by genomic hypomethylation. *Science* 300:489-492.
20. Florl, A.R., R. Lower, B.J. Schmitz-Drager, and W.A. Schulz. 1999. DNA methylation and expression of LINE-1 and HERV-K provirus sequences in urothelial and renal cell carcinomas. *British Journal of Cancer* 80:1312-1321.
21. Reik, W., and W. Dean. 2001. DNA methylation and mammalian epigenetics. *Electrophoresis* 22:2838-2843.
22. Wutz, A., and R. Jaenisch. 2000. A shift from reversible to irreversible X inactivation is triggered during ES cell differentiation. *Molecular Cell* 5:695-705.
23. Lee, J.T., L.S. Davidow, and D. Warshawsky. 1999. Tsix, a gene antisense to Xist at the X-inactivation centre. *Nature Genetics* 21:400-404.
24. Reik, W., and A. Lewis. 2005. Co-evolution of X-chromosome inactivation and imprinting in mammals. *Nature Reviews Genetics* 6:403-410.

25. Robertson, K.D. 2005. DNA methylation and human disease. *Nature Reviews Genetics* 6:597-610.
26. Feinberg, A.P., M. Oshimura, and J.C. Barrett. 2002. Epigenetic mechanisms in human disease. *Cancer Research* 62:6784-6787.
27. Moulton, T., T. Crenshaw, Y. Hao, J. Moosikasuwan, N. Lin, F. Dembitzer, T. Hensle, L. Weiss, L. McMorrow, T. Loew, and et al. 1994. Epigenetic lesions at the H19 locus in Wilms' tumour patients. *Nature Genetics* 7:440-447.
28. Steenman, M.J., S. Rainier, C.J. Dobry, P. Grundy, I.L. Horon, and A.P. Feinberg. 1994. Loss of imprinting of IGF2 is linked to reduced expression and abnormal methylation of H19 in Wilms' tumour. *Nature Genetics* 7:433-439.
29. Woodcock, D.M., C.B. Lawler, M.E. Linsenmeyer, J.P. Doherty, and W.D. Warren. 1997. Asymmetric methylation in the hypermethylated CpG promoter region of the human L1 retrotransposon. *The Journal of Biological Chemistry* 272:7810-7816.
30. Yoder, J.A., C.P. Walsh, and T.H. Bestor. 1997. Cytosine methylation and the ecology of intragenomic parasites. *Trends in Genetics* 13:335-340.
31. Bird, A., P. Tate, X. Nan, J. Campoy, R. Meehan, S. Cross, S. Tweedie, J. Charlton, and D. Macleod. 1995. Studies of DNA methylation in animals. *Journal of Cell Science* 19:37-39.
32. Rodriguez, J., J. Frigola, E. Vendrell, R.A. Risques, M.F. Fraga, C. Morales, V. Moreno, M. Esteller, G. Capella, M. Ribas, and M.A. Peinado. 2006. Chromosomal Instability Correlates with Genome-wide DNA Demethylation in Human Primary Colorectal Cancers. *Cancer Research* 66:8462-9468.
33. Eckhardt, F., J. Lewin, R. Cortese, V.K. Rakyan, J. Attwood, M. Burger, J. Burton, T.V. Cox, R. Davies, T.A. Down, C. Haefliger, R. Horton, K. Howe, D.K. Jackson, J. Kunde, C. Koenig, J. Liddle, D. Niblett, T. Otto, R. Pettett, S. Seemann, C. Thompson, T. West, J. Rogers, A. Olek, K. Berlin, and S. Beck. 2006. DNA methylation profiling of human chromosomes 6, 20 and 22. *Nature Genetics* 38:1378-1385.
34. Ivascu, C., R. Wasserkort, R. Lesche, J. Dong, H. Stein, A. Thiel, and F. Eckhardt. 2007. DNA methylation profiling of transcription factor genes in normal lymphocyte development and lymphomas. *International Journal of Biochemistry and Cell Biology* 39:1523-1538.
35. Reiner, S.L. 2005. Epigenetic control in the immune response. *Human Molecular Genetics* 14 Spec No 1:R41-46.
36. Orkin, S.H. 2000. Diversification of haematopoietic stem cells to specific lineages. *Nature Reviews Genetics* 1:57-64.
37. De Smet, C., C. Lurquin, B. Lethe, V. Martelange, and T. Boon. 1999. DNA methylation is the primary silencing mechanism for a set of germ line- and tumor-specific genes with a CpG-rich promoter. *Molecular and Cellular Biology* 19:7327-7335.
38. Song, F., J.F. Smith, M.T. Kimura, A.D. Morrow, T. Matsuyama, H. Nagase, and W.A. Held. 2005. Association of tissue-specific differentially methylated regions (TDMs) with differential gene expression. *Proceedings of the National Academy of Sciences of the United States of America* 102:3336-3341.
39. Shiota, K. 2004. DNA methylation profiles of CpG islands for cellular differentiation and development in mammals. *Cytogenetic and genome research* 105:325-334.
40. Reik, W., K. Davies, W. Dean, G. Kelsey, and M. Constancia. 2001. Imprinted genes and the coordination of fetal and postnatal growth in mammals. *Novartis Foundation symposium* 237:19-31; discussion 31-42.
41. Oswald, J., S. Engemann, N. Lane, W. Mayer, A. Olek, R. Fundele, W. Dean, W. Reik, and J. Walter. 2000. Active demethylation of the paternal genome in the mouse zygote. *Current Biology* 10:475-478.
42. Santos, F., B. Hendrich, W. Reik, and W. Dean. 2002. Dynamic reprogramming of DNA methylation in the early mouse embryo. *Developmental Biology* 241:172-182.
43. Holliday, R., and J.E. Pugh. 1975. DNA modification mechanisms and gene activity during development. *Science* 187:226-232.
44. Ferguson, A.T., R.G. Lapidus, S.B. Baylin, and N.E. Davidson. 1995. Demethylation of the estrogen receptor gene in estrogen receptor-negative breast cancer cells can reactivate estrogen receptor gene expression. *Cancer Research* 55:2279-2283.
45. Boyes, J., and A. Bird. 1992. Repression of genes by DNA methylation depends on CpG density and promoter strength: evidence for involvement of a methyl-CpG binding protein. *The EMBO Journal* 11:327-333.
46. Iguchi-Ariga, S.M., and W. Schaffner. 1989. CpG methylation of the cAMP-responsive enhancer/promoter sequence TGACGTCA abolishes specific factor binding as well as transcriptional activation. *Genes and development* 3:612-619.

47. Prendergast, G.C., and E.B. Ziff. 1991. Methylation-sensitive sequence-specific DNA binding by the c-Myc basic region. *Science* 251:186-189.
48. Nan, X., H.H. Ng, C.A. Johnson, C.D. Laherty, B.M. Turner, R.N. Eisenman, and A. Bird. 1998. Transcriptional repression by the methyl-CpG-binding protein MeCP2 involves a histone deacetylase complex. *Nature* 393:386-389.
49. Glimcher, L.H., and K.M. Murphy. 2000. Lineage commitment in the immune system: the T helper lymphocyte grows up. *Genes and Development* 14:1693-1711.
50. Carbone, A.M., P. Marrack, and J.W. Kappler. 1988. Demethylated CD8 gene in CD4+ T cells suggests that CD4+ cells develop from CD8+ precursors. *Science* 242:1174-1176.
51. Lee, P.P., D.R. Fitzpatrick, C. Beard, H.K. Jessup, S. Lehar, K.W. Makar, M. Perez-Melgosa, M.T. Sweetser, M.S. Schlissel, S. Nguyen, S.R. Cherry, J.H. Tsai, S.M. Tucker, W.M. Weaver, A. Kelso, R. Jaenisch, and C.B. Wilson. 2001. A critical role for Dnmt1 and DNA methylation in T cell development, function, and survival. *Immunity* 15:763-774.
52. Zou, Y.R., M.J. Sunshine, I. Taniuchi, F. Hatam, N. Killeen, and D.R. Littman. 2001. Epigenetic silencing of CD4 in T cells committed to the cytotoxic lineage. *Nature Genetics* 29:332-336.
53. Fitzpatrick, D.R., K.M. Shirley, L.E. McDonald, H. Bielefeldt-Ohmann, G.F. Kay, and A. Kelso. 1998. Distinct methylation of the interferon gamma (IFN-gamma) and interleukin 3 (IL-3) genes in newly activated primary CD8+ T lymphocytes: regional IFN-gamma promoter demethylation and mRNA expression are heritable in CD44(high)CD8+ T cells. *The Journal of Experimental Medicine* 188:103-117.
54. Yano, S., P. Ghosh, H. Kusaba, M. Buchholz, and D.L. Longo. 2003. Effect of promoter methylation on the regulation of IFN-gamma gene during in vitro differentiation of human peripheral blood T cells into a Th2 population. *Journal of Immunology* 171:2510-2516.
55. Jones, B., and J. Chen. 2006. Inhibition of IFN-gamma transcription by site-specific methylation during T helper cell development. The *EMBO Journal* 25:2443-2452.
56. Lee, D.U., S. Agarwal, and A. Rao. 2002. Th2 lineage commitment and efficient IL-4 production involves extended demethylation of the IL-4 gene. *Immunity* 16:649-660.
57. Murayama, A., K. Sakura, M. Nakama, K. Yasuzawa-Tanaka, E. Fujita, Y. Tateishi, Y. Wang, T. Ushijima, T. Baba, K. Shibuya, A. Shibuya, Y. Kawabe, and J. Yanagisawa. 2006. A specific CpG site demethylation in the human interleukin 2 gene promoter is an epigenetic memory. The *EMBO Journal* 25:1081-1092.
58. Holliday, R. 1979. A new theory of carcinogenesis. *British Journal of Cancer* 40:513-522.
59. Gama-Sosa, M.A., V.A. Slagel, R.W. Trewyn, R. Oxenhandler, K.C. Kuo, C.W. Gehrke, and M. Ehrlich. 1983. The 5-methylcytosine content of DNA from human tumors. *Nucleic Acids Research* 11:6883-6894.
60. Eden, A., F. Gaudet, A. Waghmare, and R. Jaenisch. 2003. Chromosomal instability and tumors promoted by DNA hypomethylation. *Science* 300:455.
61. Pogribny, I.P., B.J. Miller, and S.J. James. 1997. Alterations in hepatic p53 gene methylation patterns during tumor progression with folate/methyl deficiency in the rat. *Cancer letters* 115:31-38.
62. Hanada, M., D. Delia, A. Aiello, E. Stadtmauer, and J.C. Reed. 1993. bcl-2 gene hypomethylation and high-level expression in B-cell chronic lymphocytic leukemia. *Blood* 82:1820-1828.
63. Feinberg, A.P., and B. Vogelstein. 1983. Hypomethylation distinguishes genes of some human cancers from their normal counterparts. *Nature* 301:89-92.
64. Herman, J.G., and S.B. Baylin. 2003. Gene silencing in cancer in association with promoter hypermethylation. *The New England Journal of Medicine* 349:2042-2054.
65. Feinberg, A.P., and B. Tycko. 2004. The history of cancer epigenetics. *Nature Reviews Cancer* 4:143-153.
66. Fraga, M.F., M. Herranz, J. Espada, E. Ballestar, M.F. Paz, S. Ropero, E. Erkek, O. Bozdogan, H. Peinado, A. Niveleau, J.H. Mao, A. Balmain, A. Cano, and M. Esteller. 2004. A mouse skin multistage carcinogenesis model reflects the aberrant DNA methylation patterns of human tumors. *Cancer Research* 64:5527-5534.
67. Keshet, I., Y. Schlesinger, S. Farkash, E. Rand, M. Hecht, E. Segal, E. Pikarski, R.A. Young, A. Niveleau, H. Cedar, and I. Simon. 2006. Evidence for an instructive mechanism of de novo methylation in cancer cells. *Nature Genetics* 38:149-153.
68. Esteller, M., P.G. Corn, S.B. Baylin, and J.G. Herman. 2001. A gene hypermethylation profile of human cancer. *Cancer Research* 61:3225-3229.
69. Saito, Y., G. Liang, G. Egger, J.M. Friedman, J.C. Chuang, G.A. Coetzee, and P.A. Jones. 2006. Specific activation of microRNA-127 with downregulation of the proto-oncogene BCL6 by chromatin-modifying drugs in human cancer cells. *Cancer Cell* 9:435-443.

70. Lujambio, A., S. Ropero, E. Ballestar, M.F. Fraga, C. Cerrato, F. Setien, S. Casado, A. Suarez-Gauthier, M. Sanchez-Cespedes, A. Gitt, I. Spiteri, P.P. Das, C. Caldas, E. Miska, and M. Esteller. 2007. Genetic unmasking of an epigenetically silenced microRNA in human cancer cells. *Cancer Research* 67:1424-1429.
71. Laird, P.W. 2003. The power and the promise of DNA methylation markers. *Nature Reviews Cancer.* 3:253-266.
72. Gowher, H., O. Leismann, and A. Jeltsch. 2000. DNA of Drosophila melanogaster contains 5-methylcytosine. *The EMBO Journal* 19:6918-6923.
73. Fraga, M.F., E. Uriol, L. Borja Diego, M. Berdasco, M. Esteller, M.J. Canal, and R. Rodriguez. 2002. High-performance capillary electrophoretic method for the quantification of 5-methyl 2'-deoxycytidine in genomic DNA: application to plant, animal and human cancer tissues. *Electrophoresis* 23:1677-1681.
74. Stach, D., O.J. Schmitz, S. Stilgenbauer, A. Benner, H. Dohner, M. Wiessler, and F. Lyko. 2003. Capillary electrophoretic analysis of genomic DNA methylation levels. *Nucleic Acids Research* 31:E2.
75. Sano, H., H.D. Royer, and R. Sager. 1980. Identification of 5-methylcytosine in DNA fragments immobilized on nitrocellulose paper. *Proceedings of the National Academy of Sciences of the United States of America* 77:3581-3585.
76. Gonzalgo, M.L., G. Liang, C.H. Spruck, 3rd, J.M. Zingg, W.M. Rideout, 3rd, and P.A. Jones. 1997. Identification and characterization of differentially methylated regions of genomic DNA by methylation-sensitive arbitrarily primed PCR. *Cancer Research* 57:594-599.
77. Toyota, M., C. Ho, N. Ahuja, K.W. Jair, Q. Li, M. Ohe-Toyota, S.B. Baylin, and J.P. Issa. 1999. Identification of differentially methylated sequences in colorectal cancer by methylated CpG island amplification. *Cancer Research* 59:2307-2312.
78. Costello, J.F., D.J. Smiraglia, and C. Plass. 2002. Restriction landmark genome scanning. *Methods* 27:144-149.
79. Huang, T.H., M.R. Perry, and D.E. Laux. 1999. Methylation profiling of CpG islands in human breast cancer cells. *Human Molecular Genetics* 8:459-470.
80. Feltus, F.A., E.K. Lee, J.F. Costello, C. Plass, and P.M. Vertino. 2003. Predicting aberrant CpG island methylation. *Proceedings of the National Academy of Sciences of the United States of America* 100:12253-12258.
81. Frommer, M., L.E. McDonald, D.S. Millar, C.M. Collis, F. Watt, G.W. Grigg, P.L. Molloy, and C.L. Paul. 1992. A genomic sequencing protocol that yields a positive display of 5-methylcytosine residues in individual DNA strands. *Proceedings of the National Academy of Sciences of the United States of America* 89:1827-1831.
82. Xiong, Z., and P.W. Laird. 1997. COBRA: a sensitive and quantitative DNA methylation assay. *Nucleic Acids Research* 25:2532-2534.
83. Eads, C.A., K.D. Danenberg, K. Kawakami, L.B. Saltz, C. Blake, D. Shibata, P.V. Danenberg, and P.W. Laird. 2000. MethyLight: a high-throughput assay to measure DNA methylation. *Nucleic Acids Research* 28:E32.
84. Lewin, J., A.O. Schmitt, P. Adorjan, T. Hildmann, and C. Piepenbrock. 2004. Quantitative DNA methylation analysis based on four-dye trace data from direct sequencing of PCR amplificates. *Bioinformatics.* 20:3005-3012.
85. Bluestone, J.A., and A.K. Abbas. 2003. Natural versus adaptive regulatory T cells. *Nature Reviews Immunology* 3:253-257.
86. Moore, K.W., R. de Waal Malefyt, R.L. Coffman, and A. O'Garra. 2001. Interleukin-10 and the interleukin-10 receptor. *Annual Review of Immunology* 19:683-765.
87. Kuhn, R., J. Lohler, D. Rennick, K. Rajewsky, and W. Muller. 1993. Interleukin-10-deficient mice develop chronic enterocolitis. *Cell* 75:263-274.
88. Murray, P.J., L. Wang, C. Onufryk, R.I. Tepper, and R.A. Young. 1997. T cell-derived IL-10 antagonizes macrophage function in mycobacterial infection. *Journal of Immunology* 158:315-321.
89. Ding, W., S. Beissert, L. Deng, E. Miranda, C. Cassetty, K. Seiffert, K.L. Campton, Z. Yan, G.F. Murphy, J.A. Bluestone, and R.D. Granstein. 2003. Altered cutaneous immune parameters in transgenic mice overexpressing viral IL-10 in the epidermis. *The Journal of Clinical Investigation* 111:1923-1931.
90. Hill, J.A., K. Polgar, and D.J. Anderson. 1995. T-helper 1-type immunity to trophoblast in women with recurrent spontaneous abortion. *The Journal of the American Medical Association* 273:1933-1936.
91. Ng, S.C., A. Gilman-Sachs, P. Thaker, K.D. Beaman, A.E. Beer, and J. Kwak-Kim. 2002. Expression of intracellular Th1 and Th2 cytokines in women with recurrent spontaneous

abortion, implantation failures after IVF/ET or normal pregnancy. *American Journal of Reproductive Immunology* 48:77-86.

92. Ziegler-Heitbrock, L., M. Lotzerich, A. Schaefer, T. Werner, M. Frankenberger, and E. Benkhart. 2003. IFN-alpha induces the human IL-10 gene by recruiting both IFN regulatory factor 1 and Stat3. *Journal of Immunology* 171:285-290.
93. Brightbill, H.D., S.E. Plevy, R.L. Modlin, and S.T. Smale. 2000. A prominent role for Sp1 during lipopolysaccharide-mediated induction of the IL-10 promoter in macrophages. *Journal of Immunology* 164:1940-1951.
94. Tone, M., M.J. Powell, Y. Tone, S.A. Thompson, and H. Waldmann. 2000. IL-10 gene expression is controlled by the transcription factors Sp1 and Sp3. *Journal of Immunology* 165:286-291.
95. Saraiva, M., J.R. Christensen, A.V. Tsytsykova, A.E. Goldfeld, S.C. Ley, D. Kioussis, and A. O'Garra. 2005. Identification of a macrophage-specific chromatin signature in the IL-10 locus. *Journal of Immunology* 175:1041-1046.
96. Kitani, A., I. Fuss, K. Nakamura, F. Kumaki, T. Usui, and W. Strober. 2003. Transforming growth factor (TGF)-beta1-producing regulatory T cells induce Smad-mediated interleukin 10 secretion that facilitates coordinated immunoregulatory activity and amelioration of TGF-beta1-mediated fibrosis. *Journal of Experimental Medicine* 198:1179-1188.
97. Cao, S., J. Liu, L. Song, and X. Ma. 2005. The protooncogene c-Maf is an essential transcription factor for IL-10 gene expression in macrophages. *Journal of Immunology* 174:3484-3492.
98. Wang, Z.Y., H. Sato, S. Kusam, S. Sehra, L.M. Toney, and A.L. Dent. 2005. Regulation of IL-10 gene expression in Th2 cells by Jun proteins. *Journal of Immunology* 174:2098-2105.
99. Im, S.H., A. Hueber, S. Monticelli, K.H. Kang, and A. Rao. 2004. Chromatin-level regulation of the IL10 gene in T cells. *Journal of Biological Chemistry* 279:46818-46825.
100. Jones, E.A., and R.A. Flavell. 2005. Distal enhancer elements transcribe intergenic RNA in the IL-10 family gene cluster. *Journal of Immunology* 175:7437-7446.
101. Shankaran, V., H. Ikeda, A.T. Bruce, J.M. White, P.E. Swanson, L.J. Old, and R.D. Schreiber. 2001. IFNgamma and lymphocytes prevent primary tumour development and shape tumour immunogenicity. *Nature.* 410:1107-1111.
102. Lee, D.U., O. Avni, L. Chen, and A. Rao. 2004. A distal enhancer in the interferon-gamma (IFN-gamma) locus revealed by genome sequence comparison. *Journal of Biological Chemistry* 279:4802-4810.
103. Bream, J.H., D.L. Hodge, R. Gonsky, R. Spolski, W.J. Leonard, S. Krebs, S. Targan, A. Morinobu, J.J. O'Shea, and H.A. Young. 2004. A distal region in the interferon-gamma gene is a site of epigenetic remodeling and transcriptional regulation by interleukin-2. *Journal of Biological Chemistry* 279:41249-41257.
104. Young, H.A., P. Ghosh, J. Ye, J. Lederer, A. Lichtman, J.R. Gerard, L. Penix, C.B. Wilson, A.J. Melvin, M.E. McGurn, and et al. 1994. Differentiation of the T helper phenotypes by analysis of the methylation state of the IFN-gamma gene. *Journal of Immunology* 153:3603-3610.
105. Melvin, A.J., M.E. McGurn, S.J. Bort, C. Gibson, and D.B. Lewis. 1995. Hypomethylation of the interferon-gamma gene correlates with its expression by primary T-lineage cells. *European Journal of Immunology* 25:426-430.
106. Rosenbauer, F., B.M. Owens, L. Yu, J.R. Tumang, U. Steidl, J.L. Kutok, L.K. Clayton, K. Wagner, M. Scheller, H. Iwasaki, C. Liu, B. Hackanson, K. Akashi, A. Leutz, T.L. Rothstein, C. Plass, and D.G. Tenen. 2006. Lymphoid cell growth and transformation are suppressed by a key regulatory element of the gene encoding PU.1. *Nature Genetics* 38:27-37.
107. Rasmussen, T., L.M. Knudsen, I.M. Dahl, and H.E. Johnsen. 2003. C-MAF oncogene dysregulation in multiple myeloma: frequency and biological relevance. *Leukemia and Lymphoma.* 44:1761-1766.
108. Morito, N., K. Yoh, Y. Fujioka, T. Nakano, H. Shimohata, Y. Hashimoto, A. Yamada, A. Maeda, F. Matsuno, H. Hata, A. Suzuki, S. Imagawa, H. Mitsuya, H. Esumi, A. Koyama, M. Yamamoto, N. Mori, and S. Takahashi. 2006. Overexpression of c-Maf contributes to T-cell lymphoma in both mice and human. *Cancer Research* 66:812-819.
109. Kuehl, W.M., and P.L. Bergsagel. 2002. Multiple myeloma: evolving genetic events and host interactions. *Nature Reviews Cancer* 2:175-187.
110. Ho, I.C., and L.H. Glimcher. 2002. Transcription: tantalizing times for T cells. *Cell.* 109 Suppl:S109-120.
111. Tenen, D.G., R. Hromas, J.D. Licht, and D.E. Zhang. 1997. Transcription factors, normal myeloid development, and leukemia. *Blood.* 90:489-519.

112. Hinrichs, C.S., L. Gattinoni, and N.P. Restifo. 2006. Programming CD8+ T cells for effective immunotherapy. *Current Opinion in Immunology* 18:363-370.
113. Singh, H., and J.M. Pongubala. 2006. Gene regulatory networks and the determination of lymphoid cell fates. *Current Opinion in Immunology* 18:116-120.
114. Pearce, E.L., A.C. Mullen, G.A. Martins, C.M. Krawczyk, A.S. Hutchins, V.P. Zediak, M. Banica, C.B. DiCioccio, D.A. Gross, C.A. Mao, H. Shen, N. Cereb, S.Y. Yang, T. Lindsten, J. Rossant, C.A. Hunter, and S.L. Reiner. 2003. Control of effector CD8+ T cell function by the transcription factor Eomesodermin. *Science.* 302:1041-1043.
115. He, X., X. He, V.P. Dave, Y. Zhang, X. Hua, E. Nicolas, W. Xu, B.A. Roe, and D.J. Kappes. 2005. The zinc finger transcription factor Th-POK regulates CD4 versus CD8 T-cell lineage commitment. *Nature.* 433:826-833.
116. He, X., and D.J. Kappes. 2006. CD4/CD8 lineage commitment: light at the end of the tunnel? *Current Opinion in Immunology* 18:135-142.
117. Tsang, A.P., Y. Fujiwara, D.B. Hom, and S.H. Orkin. 1998. Failure of megakaryopoiesis and arrested erythropoiesis in mice lacking the GATA-1 transcriptional cofactor FOG. *Genes and Development* 12:1176-1188.
118. Cousins, D.J., T.H. Lee, and D.Z. Staynov. 2002. Cytokine coexpression during human Th1/Th2 cell differentiation: direct evidence for coordinated expression of Th2 cytokines. *Journal of Immunology.* 169:2498-2506.
119. Korz, C., A. Pscherer, A. Benner, D. Mertens, C. Schaffner, E. Leupolt, H. Dohner, S. Stilgenbauer, and P. Lichter. 2002. Evidence for distinct pathomechanisms in B-cell chronic lymphocytic leukemia and mantle cell lymphoma by quantitative expression analysis of cell cycle and apoptosis-associated genes. *Blood.* 99:4554-4561.
120. Jahr, S., H. Hentze, S. Englisch, D. Hardt, F.O. Fackelmayer, R.D. Hesch, and R. Knippers. 2001. DNA fragments in the blood plasma of cancer patients: quantitations and evidence for their origin from apoptotic and necrotic cells. *Cancer Research* 61:1659-1665.
121. Sidransky, D. 2002. Emerging molecular markers of cancer. *Nature Reviews Cancer* 2:210-219.
122. Mangge, H., P. Felsner, J. Herrmann, Y. el-Shabrawi, P. Liebmann, and K. Schauenstein. 1999. Early rheumatoid arthritis is associated with diminished numbers of TH1 cells in stimulated peripheral blood. *Immunobiology.* 200:290-294.
123. Kawashima, M., and P. Miossec. 2005. mRNA quantification of T-bet, GATA-3, IFN-gamma, and IL-4 shows a defective Th1 immune response in the peripheral blood from rheumatoid arthritis patients: link with disease activity. *Journal of Clinical Immunology* 25:209-214.
124. Burmester, G.-R., and A. Pezzutto. 2003. Color Atlas of Immunology. Stuttgart - New York.
125. Foss, H.D., T. Marafioti, and H. Stein. 2000. [Hodgkin lymphoma. Classification and pathogenesis]. *Der Pathologe* 21:113-123.
126. Alizadeh, A.A., M.B. Eisen, R.E. Davis, C. Ma, I.S. Lossos, A. Rosenwald, J.C. Boldrick, H. Sabet, T. Tran, X. Yu, J.I. Powell, L. Yang, G.E. Marti, T. Moore, J. Hudson, Jr., L. Lu, D.B. Lewis, R. Tibshirani, G. Sherlock, W.C. Chan, T.C. Greiner, D.D. Weisenburger, J.O. Armitage, R. Warnke, R. Levy, W. Wilson, M.R. Grever, J.C. Byrd, D. Botstein, P.O. Brown, and L.M. Staudt. 2000. Distinct types of diffuse large B-cell lymphoma identified by gene expression profiling. *Nature.* 403:503-511.
127. Rosenbauer, F., K. Wagner, J.L. Kutok, H. Iwasaki, M.M. Le Beau, Y. Okuno, K. Akashi, S. Fiering, and D.G. Tenen. 2004. Acute myeloid leukemia induced by graded reduction of a lineage-specific transcription factor, PU.1. *Nature Genetics* 36:624-630.
128. Brugnolo, F., S. Sampognaro, F. Liotta, L. Cosmi, F. Annunziato, C. Manuelli, P. Campi, E. Maggi, S. Romagnani, and P. Parronchi. 2003. The novel synthetic immune response modifier R-848 (Resiquimod) shifts human allergen-specific CD4+ TH2 lymphocytes into IFN-gamma-producing cells. *Journal of Allergy and Clinical Immunology* 111:380-388.
129. Parronchi, P., F. Brugnolo, F. Annunziato, C. Manuelli, S. Sampognaro, C. Mavilia, S. Romagnani, and E. Maggi. 1999. Phosphorothioate oligodeoxynucleotides promote the in vitro development of human allergen-specific CD4+ T cells into Th1 effectors. *Journal of Immunology.* 163:5946-5953.
130. Estrov, Z., M. Talpaz, S. Ku, D. Harris, Q. Van, M. Beran, C. Hirsch-Ginsberg, Y. Huh, G. Yee, and R. Kurzrock. 1998. Z-138: a new mature B-cell acute lymphoblastic leukemia cell line from a patient with transformed chronic lymphocytic leukemia. *Leukemia Research* 22:341-353.
131. Dean, F.B., S. Hosono, L. Fang, X. Wu, A.F. Faruqi, P. Bray-Ward, Z. Sun, Q. Zong, Y. Du, J. Du, M. Driscoll, W. Song, S.F. Kingsmore, M. Egholm, and R.S. Lasken. 2002. Comprehensive human genome amplification using multiple displacement amplification. *Proceedings of the National Academy of Sciences of the United States of America* 99:5261-5266.

132. Berlin, K., M. Ballhause, and K. Cardon. 2005. Improved bisulfite conversion of DNA. Patent number: PCT/WO/2005/038051
133. Sanger, F., S. Nicklen, and A.R. Coulson. 1977. DNA sequencing with chain-terminating inhibitors. *Proceedings of the National Academy of Sciences of the United States of America* 74:5463-5467.
134. Muller, P.Y., H. Janovjak, A.R. Miserez, and Z. Dobbie. 2002. Processing of gene expression data generated by quantitative real-time RT-PCR. *Biotechniques.* 32:1372-1374, 1376, 1378-1379.
135. Pai, S.Y., M.L. Truitt, and I.C. Ho. 2004. GATA-3 deficiency abrogates the development and maintenance of T helper type 2 cells. *Proceedings of the National Academy of Sciences of the United States of America* 101:1993-1998.
136. Zheng, W., and R.A. Flavell. 1997. The transcription factor GATA-3 is necessary and sufficient for Th2 cytokine gene expression in CD4 T cells. *Cell* 89:587-596.
137. Szabo, S.J., S.T. Kim, G.L. Costa, X. Zhang, C.G. Fathman, and L.H. Glimcher. 2000. A novel transcription factor, T-bet, directs Th1 lineage commitment. *Cell* 100:655-669.
138. Shoemaker, J., M. Saraiva, and A. O'Garra. 2006. GATA-3 directly remodels the IL-10 locus independently of IL-4 in CD4+ T cells. *Journal of Immunology* 176:3470-3479.
139. Loots, G.G., R.M. Locksley, C.M. Blankespoor, Z.E. Wang, W. Miller, E.M. Rubin, and K.A. Frazer. 2000. Identification of a coordinate regulator of interleukins 4, 13, and 5 by cross-species sequence comparisons. *Science.* 288:136-140.
140. Lee, G.R., P.E. Fields, T.J. Griffin, and R.A. Flavell. 2003. Regulation of the Th2 cytokine locus by a locus control region. *Immunity* 19:145-153.
141. Grosveld, F., G.B. van Assendelft, D.R. Greaves, and G. Kollias. 1987. Position-independent, high-level expression of the human beta-globin gene in transgenic mice. *Cell* 51:975-985.
142. Kelly, B.L., and R.M. Locksley. 2000. Coordinate regulation of the IL-4, IL-13, and IL-5 cytokine cluster in Th2 clones revealed by allelic expression patterns. *Journal of Immunology* 165:2982-2986.
143. Kitamura, N., O. Kaminuma, A. Mori, T. Hashimoto, F. Kitamura, M. Miyagishi, K. Taira, and S. Miyatake. 2005. Correlation between mRNA expression of Th1/Th2 cytokines and their specific transcription factors in human helper T-cell clones. *Immunology and Cell Biology* 83:536-541.
144. Zhang, Y., and D. Reinberg. 2001. Transcription regulation by histone methylation: interplay between different covalent modifications of the core histone tails. *Genes and development* 15:2343-2360.
145. Bulger, M. 2005. Hyperacetylated chromatin domains: lessons from heterochromatin. *The Journal of Biological Chemistry* 280:21689-21692.
146. Tong, Y., T. Aune, and M. Boothby. 2005. T-bet antagonizes mSin3a recruitment and transactivates a fully methylated IFN-gamma promoter via a conserved T-box half-site. *Proceedings of the National Academy of Sciences of the United States of America.* 102:2034-2039.
147. Rothenberg, E.V., and T. Taghon. 2005. Molecular genetics of T cell development. *Annual Reviews Immunology* 23:601-649.
148. Anderson, M.K. 2006. At the crossroads: diverse roles of early thymocyte transcriptional regulators. *Immunological Reviews.* 209:191-211.
149. Orkin, S.H. 2000. Diversification of haematopoietic stem cells to specific lineages. *Nat Rev Genet.* 1:57-64.
150. Hatton, R.D., and C.T. Weaver. 2003. Immunology. T-bet or not T-bet. *Science.* 302:993-994.
151. Kurata, H., H.J. Lee, T. McClanahan, R.L. Coffman, A. O'Garra, and N. Arai. 2002. Friend of GATA is expressed in naive Th cells and functions as a repressor of GATA-3-mediated Th2 cell development. *Journal of Immunology* 168:4538-4545.
152. Woolfe, A., M. Goodson, D.K. Goode, P. Snell, G.K. McEwen, T. Vavouri, S.F. Smith, P. North, H. Callaway, K. Kelly, K. Walter, I. Abnizova, W. Gilks, Y.J. Edwards, J.E. Cooke, and G. Elgar. 2005. Highly conserved non-coding sequences are associated with vertebrate development. *Public Library of Science Biology* 3:e7.
153. Smiraglia, D.J., and C. Plass. 2002. The study of aberrant methylation in cancer via restriction landmark genomic scanning. *Oncogene.* 21:5414-5426.
154. Seli, E., and A. Arici. 2003. Endometriosis: interaction of immune and endocrine systems. *Seminars in reproductive medicine* 21:135-144.
155. Ulukus, M., H. Cakmak, and A. Arici. 2006. The role of endometrium in endometriosis. *Journal of the Society for Gynecologic Investigation* 13:467-476.

156. Arici, A. 2002. Local cytokines in endometrial tissue: the role of interleukin-8 in the pathogenesis of endometriosis. *Annals of the New York Academy of Sciences* 955:101-109; discussion 118, 396-406.
157. Agarwal, S., O. Avni, and A. Rao. 2000. Cell-type-restricted binding of the transcription factor NFAT to a distal IL-4 enhancer in vivo. *Immunity* 12:643-652.
158. Avni, O., D. Lee, F. Macian, S.J. Szabo, L.H. Glimcher, and A. Rao. 2002. T(H) cell differentiation is accompanied by dynamic changes in histone acetylation of cytokine genes. *Nature Immunology* 3:643-651.
159. Fields, P.E., S.T. Kim, and R.A. Flavell. 2002. Cutting edge: changes in histone acetylation at the IL-4 and IFN-gamma loci accompany Th1/Th2 differentiation. *Journal of Immunology* 169:647-650.
160. Yamashita, M., M. Ukai-Tadenuma, M. Kimura, M. Omori, M. Inami, M. Taniguchi, and T. Nakayama. 2002. Identification of a conserved GATA3 response element upstream proximal from the interleukin-13 gene locus. *The Journal of Biological Chemistry* 277:42399-42408.
161. Reiner, S.L., A.C. Mullen, A.S. Hutchins, and E.L. Pearce. 2003. Helper T cell differentiation and the problem of cellular inheritance. *Immunological Research* 27:463-468.
162. Gruenbaum, Y., H. Cedar, and A. Razin. 1982. Substrate and sequence specificity of a eukaryotic DNA methylase. *Nature* 295:620-622.
163. O'Garra, A. 1998. Cytokines induce the development of functionally heterogeneous T helper cell subsets. *Immunity* 8:275-283.
164. Murphy, K.M., W. Ouyang, J.D. Farrar, J. Yang, S. Ranganath, H. Asnagli, M. Afkarian, and T.L. Murphy. 2000. Signaling and transcription in T helper development. *Annual review of immunology* 18:451-494.
165. Warnecke, P.M., C. Stirzaker, J.R. Melki, D.S. Millar, C.L. Paul, and S.J. Clark. 1997. Detection and measurement of PCR bias in quantitative methylation analysis of bisulphite-treated DNA. *Nucleic Acids Research* 25:4422-4426.
166. Grogan, J.L., M. Mohrs, B. Harmon, D.A. Lacy, J.W. Sedat, and R.M. Locksley. 2001. Early transcription and silencing of cytokine genes underlie polarization of T helper cell subsets. *Immunity* 14:205-215.
167. Jankovic, D., M.C. Kullberg, C.G. Feng, R.S. Goldszmid, C.M. Collazo, M. Wilson, T.A. Wynn, M. Kamanaka, R.A. Flavell, and A. Sher. 2007. Conventional T-bet(+)Foxp3(-) Th1 cells are the major source of host-protective regulatory IL-10 during intracellular protozoan infection. *The Journal of Experimental Medicine* 204:273-283.
168. Anderson, C.F., M. Oukka, V.J. Kuchroo, and D. Sacks. 2007. CD4(+)CD25(-)Foxp3(-) Th1 cells are the source of IL-10-mediated immune suppression in chronic cutaneous leishmaniasis. *The Journal of Experimental Medicine* 204:285-297.
169. Bream, J.H., D.L. Hodge, R. Gonsky, R. Spolski, W.J. Leonard, S. Krebs, S. Targan, A. Morinobu, J.J. O'Shea, and H.A. Young. 2004. A distal region in the interferon-gamma gene is a site of epigenetic remodeling and transcriptional regulation by interleukin-2. *Journal of Biological Chemistry* 279:41249-41257.
170. Hume, D.A. 2000. Probability in transcriptional regulation and its implications for leukocyte differentiation and inducible gene expression. *Blood* 96:2323-2328.
171. Bonifer, C., P. Lefevre, and H. Tagoh. 2006. The regulation of chromatin and DNA-methylation patterns in blood cell development. *Current Topics in Microbiology and Immunology* 310:1-12.
172. Klemsz, M.J., S.R. McKercher, A. Celada, C. Van Beveren, and R.A. Maki. 1990. The macrophage and B cell-specific transcription factor PU.1 is related to the ets oncogene. *Cell.* 61:113-124.
173. Hromas, R., A. Orazi, R.S. Neiman, R. Maki, C. Van Beveran, J. Moore, and M. Klemsz. 1993. Hematopoietic lineage- and stage-restricted expression of the ETS oncogene family member PU.1. *Blood.* 82:2998-3004.
174. Amaravadi, L., and M.J. Klemsz. 1999. DNA methylation and chromatin structure regulate PU.1 expression. *DNA and Cell Biology* 18:875-884.
175. Reya, T., and H. Clevers. 2005. Wnt signalling in stem cells and cancer. *Nature.* 434:843-850.
176. Willinger, T., T. Freeman, M. Herbert, H. Hasegawa, A.J. McMichael, and M.F. Callan. 2006. Human naive CD8 T cells down-regulate expression of the WNT pathway transcription factors lymphoid enhancer binding factor 1 and transcription factor 7 (T cell factor-1) following antigen encounter in vitro and in vivo. *Journal of Immunology.* 176:1439-1446.
177. Ho, I.C., D. Lo, and L.H. Glimcher. 1998. c-maf promotes T helper cell type 2 (Th2) and attenuates Th1 differentiation by both interleukin 4-dependent and -independent mechanisms. *Journal of Experimental Medicine.* 188:1859-1866.

178. Chen, X.P., D.H. Falkner, and P.A. Morel. 2005. Impaired IL-4 production by CD8+ T cells in NOD mice is related to a defect of c-Maf binding to the IL-4 promoter. *European Journal of Immunology.* 35:1408-1417.
179. Szabo, S.J., B.M. Sullivan, C. Stemmann, A.R. Satoskar, B.P. Sleckman, and L.H. Glimcher. 2002. Distinct effects of T-bet in TH1 lineage commitment and IFN-gamma production in CD4 and CD8 T cells. *Science.* 295:338-342.
180. Intlekofer, A.M., N. Takemoto, E.J. Wherry, S.A. Longworth, J.T. Northrup, V.R. Palanivel, A.C. Mullen, C.R. Gasink, S.M. Kaech, J.D. Miller, L. Gapin, K. Ryan, A.P. Russ, T. Lindsten, J.S. Orange, A.W. Goldrath, R. Ahmed, and S.L. Reiner. 2005. Effector and memory CD8+ T cell fate coupled by T-bet and eomesodermin. *Nature Immunology* 6:1236-1244.
181. Hernandez-Hoyos, G., M.K. Anderson, C. Wang, E.V. Rothenberg, and J. Alberola-Ila. 2003. GATA-3 expression is controlled by TCR signals and regulates CD4/CD8 differentiation. *Immunity.* 19:83-94.
182. Berner, B., D. Akca, T. Jung, G.A. Muller, and M.A. Reuss-Borst. 2000. Analysis of Th1 and Th2 cytokines expressing CD4+ and CD8+ T cells in rheumatoid arthritis by flow cytometry. *The Journal of Rheumatology* 27:1128-1135.
183. van der Graaff, W.L., A.P. Prins, T.M. Niers, B.A. Dijkmans, and R.A. van Lier. 1999. Quantitation of interferon gamma- and interleukin-4-producing T cells in synovial fluid and peripheral blood of arthritis patients. *Rheumatology (Oxford, England)* 38:214-220.
184. Saito, S., M. Sakai, Y. Sasaki, K. Tanebe, H. Tsuda, and T. Michimata. 1999. Quantitative analysis of peripheral blood Th0, Th1, Th2 and the Th1:Th2 cell ratio during normal human pregnancy and preeclampsia. *Clinical and Experimental Immunology* 117:550-555.
185. Sato, E., S.H. Olson, J. Ahn, B. Bundy, H. Nishikawa, F. Qian, A.A. Jungbluth, D. Frosina, S. Gnjatic, C. Ambrosone, J. Kepner, T. Odunsi, G. Ritter, S. Lele, Y.T. Chen, H. Ohtani, L.J. Old, and K. Odunsi. 2005. Intraepithelial CD8+ tumor-infiltrating lymphocytes and a high CD8+/regulatory T cell ratio are associated with favorable prognosis in ovarian cancer. *Proceedings of the National Academy of Sciences of the United States of America.* 102:18538-18543.
186. Dorfman, D.M., E.S. Hwang, A. Shahsafaei, and L.H. Glimcher. 2004. T-bet, a T-cell-associated transcription factor, is expressed in a subset of B-cell lymphoproliferative disorders. *American Journal of Clinical Pathology* 122:292-297.
187. Marafioti, T., S. Ascani, K. Pulford, E. Sabattini, M. Piccioli, M. Jones, P.L. Zinzani, G. Delsol, D.Y. Mason, and S.A. Pileri. 2003. Expression of B-lymphocyte-associated transcription factors in human T-cell neoplasms. *American Journal of Pathology* 162:861-871.

7. Appendix

7.1. Materials and Devices

7.1.1. Buffers

Buffer	Components
TE	10 mM Tris, 1 mM EDTA
Sanger buffer	320 mM Tris-HCl (pH 9), 6mM MgCl2 und 10 % [v/v] Sulfolane

7.1.2. Molecular biology reagents

Molecular biology reagents	Supplier
Agarose	Eurogentec, Cologne, Germany
Brefeldin A (C16H24O4, MW = 280.36)	Sigma-Aldrich, Dorset, UK
Bovine serum albumin (BSA)	Fermentas, St. Leon-Rot, Germany
DEPC treated water	Fluka Chemie, Buchs, Swiss
Dinucleotidetriphosphates (dNTPs)	Fermentas, St. Leon-Rot, Germany
1,3-Dioxane (C4H8O2, MW = 88.11)	Merck KGaA, Darmstadt, Germany
Dulbecco's Modified Eagle Medium (DMEM) (culture media)	PAA Laboratories GmbH, Innsbruck, Austria
Ethidiumbromid (C21H20BrN3, MW = 394.31)	Merck KGaA, Darmstadt, Germany
EDTA ((HO2CCH2)2NCH2CH2N(CH2CO2H)2, MW = 292.24)	Sigma-Aldrich Chemie GmbH, Deisenhofen, Germany
Fetal calf serum (FCS)	Gibco-BRL, Karlsruhe, Germany
Formaldehyde (HCHO, MW = 30.03)	Merck KGaA, Darmstadt, Germany
Glycine (NH2CH2COOH, MW = 75.07)	Merck KGaA, Darmstadt, Germany
Granulocye macrophage - colony stimulating factor (GM-CSF)	Roche Diagnostics, Mannheim, Germany
HEPES (C8H18N2O4S, MW = 238,3)	Gibco-BRL, Karlsruhe, Germany
Hi-Di formamide	Applied Biosystems, Foster City, USA
HotStart Taq polymerase	Qiagen, Hilden, Germany
Human Genomic DNA	Promega, WI, USA
Hydrochloric acid (HCl, MW = 36,46)	Merck KGaA, Darmstadt, Germany
Ionomycin (I) (C41H72O9, MW= 709.00)	Sigma-Aldrich Chemie GmbH, Deisenhofen, Germany
L-glutamine (H2NCOCH2CH2CH(NH2)CO2H, MW = 146.14)	Gibco-BRL, Karlsruhe, Germany
Lithiumchloride (LiCl, MW = 42.39)	Sigma-Aldrich Chemie GmbH, Deisenhofen, Germany
Natriumdodecylsulphat (SDS) (CH3(CH2)10CH2SO3Na, MW = 288.38)	Fluka GmbH, Buchs, Germany
Oligonucleotides for PCR amplification and sequencing	MWG Biotech AG, Ebersberg, Germany
10xPCR buffer	Qiagen, Hilden, Germany
Phorbol 12 -myristat 13-acetat (PMA), (C36H56O8, MW = 616.8)	Sigma-Aldrich Chemie GmbH, Deisenhofen, Germany
Phosphate buffered saline (PBS)	Fluka GmbH, Buchs, Germany
polyT primer	MWG Biotech AG, Ebersberg,

	Germany
Proteinase K	Qiagen, Hilden, Germany
Random hexamers (oligonucleotides)	MWG Biotech AG, Ebersberg, Germany
RNAse A	Qiagen, Hilden, Germany
RNAse Inhibitor	Ambion, Foster City, USA
RPMI 1640 (culture media)	PAA Laboratories GmbH, Innsbruck, Austria
S-adenosylmethionine (SAM)	New England Biolabs, MA, USA
Sodium bisulfite (Na2S2O5, MW = 190.11)	Merck KGaA, Darmstadt, Germany
Sodium sulfite (Na2SO3, MW = 126.04)	Merck KGaA, Darmstadt, Germany
Sodiumchloride (NaCl, MW = 58.44)	Merck KGaA, Darmstadt, Germany
Sodiumhydrogencarbonat (NaHCO3, MW = 84.01)	Sigma-Aldrich Chemie GmbH, Deisenhofen, Germany
Sodiumhydroxid (NaOH, MW = 40.0)	Merck KGaA, Darmstadt, Germany
Sodiumpyruvate (CH3COCOONa, MW = 110.04)	Gibco-BRL, Karlsruhe, Germany
*Sss*I methylase	New England Biolabs, Ipswich, USA
Sulfolane (C4H8O2S, MW = 120.17)	Merck KGaA, Darmstadt, Germany
Trishydroxymethylaminomethane, Tris (NH2C(CH2OH)3, MW = 121.14)	Carl Roth GmbH & Co., Karlsruhe, Germany
Triton-X-100 (t-Oct-C6H4-(OCH2CH2)xOH, x= 9-10)	Sigma-Aldrich Chemie GmbH, Deisenhofen, Germany
Water, sterile, filtered 0,2 µm, DEPC treated	Fluka GmbH, Buchs, Germany
6-hydroxy-2,5,7,8-tetramethylchromane-2-carboxylic acid (C14H18O4, MW = 250.29)	Fluka GmbH, Buchs, Germany

7.1.3. Cytokines and antibodies

Antibodies and Cytokines	Supplier
antiCD8 FITC conjugated	PharMingen via Becton Dickinson, Heidelberg, Germany
antiCD4 FITC conjugated	PharMingen via Becton Dickinson, Heidelberg, Germany
antiCD14 FITC conjugated	BD Biosciences, San Jose, USA
antiCD19 FITC conjugated	BD Biosciences, San Jose, USA
antiIFN-γ PerCP Cy5.5 conjugated	BD Biosciences, San Jose, USA
antiIL-10 APC conjugated	BD Biosciences, San Jose, USA
anti H3K4me3	Abcam, Cambridge, UK
anti H3AcK9/14	Abcam, Cambridge, UK
BD Tritest (antiCD4/CD8/CD3 conjugated with FITC, PE, and PerCP respectively)	BD Biosciences, San Jose, USA
mouse IgG	Caltag, Burlingame, USA
anti CD80 PE conjugated	BD Biosciences, San Jose, USA
anti CD83 PE conjugated	BD Biosciences, San Jose, USA
anti CD86 PE conjugated	BD Biosciences, San Jose, USA
anti-CD28	Upstate Biotechnology, Charlottesville, VA, USA
anti-CD3	Upstate Biotechnology, Charlottesville, VA, USA
anti-IL4	Upstate Biotechnology, Charlottesville, VA, USA
rIL-12	Upstate Biotechnology, Charlottesville, VA, USA

7.1.4. Kits

Kit	Supplier
BigDye Terminator V3.1	Applied Biosystems, Foster City, USA
CD14 MicroBeads	Miltenyi Biotec, Bergisch Gladbach, Germany
CD19 MicroBeads	Miltenyi Biotec, Bergisch Gladbach, Germany
CD27 MicroBeads	Miltenyi Biotec, Bergisch Gladbach, Germany
CD4 MicroBeads	Miltenyi Biotec, Bergisch Gladbach, Germany
CD45RA MicroBeads	Miltenyi Biotec, Bergisch Gladbach, Germany
CD45RO MicroBeads	Miltenyi Biotec, Bergisch Gladbach, Germany
CD8 MicroBeads	Miltenyi Biotec, Bergisch Gladbach, Germany
ExoSAP IT	USB Corporation, Cleveland, USA
FASTStart SYBR Green Master Mix	Roche Diagnostics, Penzberg, Germany
GenomiPhi® DNA Amplification Kit	Amersham Biosciences, Piscataway, NJ, USA
human Th1/Th2 cytokine CBA Kit	Miltenyi Biotec, Bergisch Gladbach, Germany
Human Th1/Th2 Cytokine Cytometric Bead Array Kit	BD Biosciences, San Jose, USA
IFN-γ capture assays	Miltenyi Biotec, Bergisch Gladbach, Germany
Omniscript Reverse Transcription Kit	Qiagen, Hilden, Germany
Plasmid Mini Kit	Qiagen, Hilden, Germany
Protein A microbeads	Miltenyi Biotec, Bergisch Gladbach, Germany
QIAamp DNA Mini Kit	Qiagen, Hilden, Germany
RNeasy Kit	Qiagen, Hilden, Germany
SYBR Green PCR master mix	Applied Biosystems, Foster City, USA
TOPO TA Cloning	Invitrogen, Carlsbad, USA

7.1.5. Instruments and devices

Device	Supplier
ABI Prism 7900HT	Applied Biosystems, Foster City, USA
Balance BL 600	Sartorius AG, Göttingen, Germany
Centrifuge MiniSpin	Eppendorf-Nethler-Hinz GmbH, Cologne, Germany
DNA Engine Tetrad® thermocycler	BioRad, Hercules, USA
DyeEx™ 96	Qiagen, Hilden, Germany
Eppendorf UV spectrophotometer	Eppendorf AG, Hamburg, Gemany
FACScalibur	BD Biosciences, San Jose, USA
Ficoll - Hypaque	Sigma-Aldrich, St. Louis, Missouri, US
Gelelectrophoresis chambers	Biozym Diagnostik GmbH, Oldendorf, Germany
LightCycler instrument 2.0	Roche Diagnostics, Mannheim, Germany
Microcon Centrifugal Filter Units YM30	Millipore, Billerica USA
NanoDrop® ND-1000 spectrophotometer	Nanodrop Technologies, Wilmington, USA
NucleoSpin Extract II	Macherey-Nagel, Düren, Germany
Pipets	Eppendorf-Nethler-Hinz GmbH, Cologne, Germany
Plate centrifuge Eppendorf 5810 R and 5417 R	Eppendorf-Nethler-Hinz GmbH, Cologne, Germany
Sonicator	Bandelin, Berlin, Germany
Thermomixer 5355 Comfort	Eppendorf-Nethler-Hinz GmbH, Cologne, Germany
µ columns	Miltenyi Biotec, Bergisch Gladbach, Germany
3730 DNA Analyser	Applied Biosystems, Foster City, USA
96 well microtiter plates (PCR and sequencing)	ABgene, Epsom, UK

7.1.6. Software

Software	Supplier
ABI KB basecaller	Applied Biosystems, Foster City, USA
CELLQuest™	BD Biosciences, San Jose, USA
FACSDiva	BD Biosciences, San Jose, USA
ESME	Lewin, J et al., Bioinformatics, 2004
ABI SDS 2.2	Applied Biosystems, Foster City, USA
Q-gene	Muller, P.Y. et al., Biotechniques, 2002 http://www.gene-quantification.de/download.html#qgene

7.2. Bisulfite primer assays

Cytokine and transcription factors analysed for DNA methylation in CD4+ T-cell subsets

Gene	Accession number	Chromosomal location	Primer orientation	Bisulfite primer	Position relative to TSS (upstream)	Position relative to TSS (downstream)	No. of CpG's	Region
GATA3	NM_002051	10p14	S	GGGAAGAGAGTGATATTTATTGATT	-9623	-9154	25	1
			A	TTAATCCCAACCCTACCAA				
			S	TTTGGTTGTTGGGTTGAT	-7112	-6680	23	2
			A	ACTCCATTCAAATCTTAAAAACA				
			S	TTGGGGATGGTATGTGAT	-6004	-5513	23	3
			A	TTTCCACTCACCCTCAAAA				
			S	GGGAAAAGGTGGTAGTGG	-5808	-5329	25	4
			A	CTCTTCAAACAAAACCCAAAA				
			S	GGAGGGGTAAAGGAGAGATT	-5364	-4881	37	5
			A	CCCAAATTCCCTACTCTCTAAA				
			S	GGGGGAGGAGAAGTTTTT	-4618	-4162	40	6
			A	CCCTTTACAATTCCCACA				
			S	GGAATGGGAAGGGATTTT	-4188	-3696	52	7
			A	CCACCAAAACCAAACAAC				
			S	TTTTAGGGTTGAGTTTTAGAAAG	-3655	-3214	30	8
			A	CTCCCTCACCAAAATAAAAA				
			S	GTTTGGGGTTGGATGTTT	-2728	-2495	17	9
			A	CTCCCATCCTTTTCCCTT				
			S	GGTTGGGAAGTAAAGGTGA	382	818	32	10
			A	CCTAAAACTTACCCTCCAAATTA				
			S	AATTTTAAGGGAGAGGAAGG	2215	2530	11	11
			A	AAAACTTTCTAAATCCAACCAA				
			S	AATGAGTTGGGATAGGAAAAA	4375	4848	11	12
			A	CCCCTAACTACACTAAAAACTCTAAA				
			S	GAGGGAGTATTTTGGGAGTTT	5362	5752	7	13
			A	TACACCCCACTTCTTAATCCT				

TBX21	NM_013351	17q21.32	S	TGGGATGGGTAGGGAGTA	-42	139	17	1
			A	ACTTCATAAAACCACAACAAAA				
			S	ATGGGGTTGTTAGGAGGAT	838	1258	14	2
			A	CCATATCACCAAATCCCA				
			S	AGATTTGGGAAATTAGTGGTT	3458	3842	9	3
			A	CAACCCCATCTAAACTACCTT				
IFN-γ	NM_000619.2	12q15	S	AAGTAGGATTATGAATTTTTGGA	-4560	-4200	7	1
			A	CCCTTTTCCTCTATCATCAA				
			S	TGGGTGTTGTAGTTAGAGTTTTT	-479	-300	4	2
			A	CCTCACCAAATTATTCTTTTAAC				
			S	TTTGAATGGTGTGAAGTAAAAG	-299	0	5	3
			A	ATCCTAACAATAACAACCAAAAA				
			S	TTTTTGGATTTGATTAGTTTGA	0	481	4	4
			A	TACCCATATTATACCCATCTTTTA				
			S	AGAGTGTGGAGATTATTAAGGAA	1740	2161	8	5
			A	ACAACCTCTCATTCAAAATAAAAA				
IL-10	NM_000572	1q32.2	S	ATGAGTTAAGAGGGGTATATGTAAA	-9192	-8999	2	1
			A	AAACATCATCCTACCCATTCTA				
			S	GTTTGGGGTGTAAGGAGATA	-5865	-5462	7	2
			A	ATAACCAAAACTCAAACACCTAA				
			S	GGAGTTGTAGAGGGAAGGTTT	-5479	-5067	8	3
			A	TCTCCTTACACCCCAAACTAA				
			S	AAATAGGGTTGAGGTTAGGATT	-3011	-2858	13	4
			A	ACTTACCCATAATTCTCTCCAA				
			S	TTTATATTGTAAGTTTAGGGAGGTT	-400	-25	6	5
			A	AACCCAATTATTTCTCAATCC				
			S	AGAGGATTTAATAGTGATGGGA	550	932	5	6
			A	CTCCCCATACCTTACAACAAA				
			S	TGGGAATTGATATTTTTAGGTATT	2748	3196	7	7
			A	AACTCAATAAACCCCATTCTT				
IL-13	NM_002188.2	5q23.3	S	TGGTTATGGGGGATAAGG	-1606	-1357	11	1
			A	ACTTCCCAACCCAACTACTAA				
			S	TGTTATAGGTAAAATTGTTGGAAT	-298	160	10	2
			A	CTCCTCAATAAACTCCCTAAAAA				
			S	GGGTAGGGAGTTGTGGAT	5847	6337	10	3

			A	CTCATAAAACCCCATTATCTTC				
IL-4	NM_172348	14p12.1	S	AAGTAGTTGGGAGGTGAGATT	-62	393	5	5
			A	TTACTCTATCTTTCCCCAAAAA				
			S	TTGTGTGTTTTGGATTGTTATT	235	631	7	6
			A	CCAATATAAACTCATTTTCCCT				
			S	GAGAAGTTGGAATTGGTGG	589	1073	9	7
			A	TTCTTTAACCAAAATCTAAATCAAA				
			S	TTTGATTTAGATTTTGGTTAAAGA	1049	1512	10	8
			A	CTATCTCCTCCCACTACAAATAA				
			S	ATGAAGTAGGATGGGTTTTGT	1306	1772	10	9
			A	CCACCTAACAACCCTCTAAA				
			S	TTGGGTAGGGTTATATTTTAGTATTT	1716	1865	3	10
			A	ATTTACCCTTCAAAATCTCATC				
			S	TTTGGGTAGGATGGGAGA	3468	3844	8	11
			A	TCCTAAAAACAACTTTAATACAAAAC				
			S	TTATTAAGGTTTGTGGTAAAAGAA	4026	4355	7	12
			A	CCCCTTTCCCCTATAAAA				
			S	TGGTATTAGAGAATATGGGATTG	4242	4426	8	13
			A	TCTTACATTTCCAACTAAAATCAAA				
			S	GATAAGATGTTTAGGGGTTTTTATT	4835	4875	3	14
			A	CAACTCTCAATCCCATATTCTC				
			S	AGAGTTTAGGTTAAAGGATGTGTAT	5520	5855	6	15
			A	TATCAACAACCTCTCCCAATTA				
			S	TGAATGGGTTGATTAAGGG	5976	6317	11	16
			A	TCTCCCATCCTCCAAATAA				
			S	GGAAATGTGAGTTGTATTTTGTT	11381	11736	2	17
			A	ACTTCAAATCTCACCCTAACC				

Table 1 Cytokine and transcription factor gene regions: genomic locations, bisulfite primer assays and the position of the analyzed amplicons relative to the transcription start site as well as the number of analyzed CpG per amplicons, S : sense primer, A : antisense primer

Transcription factors analysed for DNA methylation in the hematopoietic cascade model

Gene	Accession number	Chromosomal location	Primer orientation	Bisulfite primer	Position relative to TSS (upstream)	Position relative to TSS (downstream)	No. of CpG's	Region
MAF	NM_005360	16q23.1	S	AGGGTTGAATGTTTTTGAGAT	-5306	-4932	6	1
			A	ATACCAACCTTCTTCTCTTTCTT				
			S	TTTAGATTATGGATGTTTGATTTT	-3777	-3333	4	2
			A	TTTATTTCACTTCTATCCAAACC				
			S	TTTAGTGATAAATGAGATGTTTTTAGT	-2482	-1994	7	3
			A	TAACATAATCTTCACTCTTTCTTCC				
			S	ATTAAGGATTTTTGGGTTTGT	-2276	-1797	5	4
			A	AATCATTTTTACCCCTCCTCT				
			S	GTTGATAGTTAGTTGATTGGGTT	-201	188	14	5
			A	CTCTACCTCTATACAAAATACAAAACA				
EOMES	NM_005442	3p24.1	S	TTTTTGGTTATTTTATTTGTTGTG	-1646	-1160	27	1
			A	AAACAATCACTTTTATTCCCC				
			S	GGTTGGAGTAGATTTTAGAGGTT	-1103	-726	11	2
			A	CACTCTTATCCTATCCCCAATA				
			S	TAAGTTTAATTTTTGAGGAGAGG	-61	160	14	3
			A	TAACTCCCCCATCCTACC				
ETV5	NM_004454	3q27.2	S	ATTTGGTTTGAGGTAAAGGTTAT	-2144	-1843	5	1
			A	CAATTTTATCTACCCCCACTC				
			S	AGGGAGAAGATAGGGAAGAAT	3126	3545	6	2
			A	CTCCCAAATTCATATTACAAAAA				
FOG1	NM_153813	16q24.2	S	AGATGATATAATTTAGTTGGGAGTGG	-1137	-592	33	1
			A	TAATCCCTCCCTAAACCCC				
			S	GGGGTTTAGTTTAGGAGGGG	565	854	23	2
			A	CTCTACCTCCCAAATCTCTCTC				
GATA3	NM_002051	10p14	S	TTTGGTTGTTGGGTTGAT	-7112	-6680	23	1
			A	ACTCCATTCAAATCTTAAAAACA				
			S	AATGAGTTGGGATAGGAAAAA	4375	4848	11	2
			A	CCCCTAACTACACTAAAAACTCTAAA				

HLX1	NM_021958	1q41	S	TTTTGGTTTTGAAGAGTGGG	-2402	-1906	42	1
			A	CTCTCTTAAAAAATAAAACTCCCC				
			S	GTAGTTTGTTTTGTAGTTTTTGAGG	-748	-484	15	2
			A	CCCTCATCTTTCCTAAACCC				
NOTCH1	NM_017617	9q34.3	S	AAGAGGTGTGTTAGGAAAGGT	-1402	-941	23	1
			A	CCTACCTAAAATAACCCCAAA				
SPI1	NM_003120	11p11.2	S	TTTTATTGATAGTAAGTTAGGAGGG	-349	122	22	1
			A	TAAACACCACCTACCCCAA				
STAT1	NM_007315	2q32.2/2q32.3	S	AATGAAAATGAAGGAAAGAAAAT	-6232	-5981	27	1
			A	TCCTCTCAATCCCAATCC				
			S	TGTTAAAGGGAGTTTTTAGAATG	-341	-145	10	2
			A	CTAAATAAACTACAACCCAATCC				
			S	GTTATTTTGTGTTTTAATAAGGGTT	453	683	10	3
			A	AACACTACACCTTCCCATTTAC				
STAT6	NM_003153	12q13.3	S	AGTTTTTTGAAGGGGAAGGG	715	1055	20	1
			A	TTTCCCCCTCAAAACTACTCC				
			S	GTGGGGAGAGGGAAGTAG	2542	3030	7	2
			A	CCTATCTCCTAAAACAACCAAAA				
TBX21	NM_013351	17q21.32	S	AGATTTGGGAAATTAGTGGTT	3458	3842	9	1
			A	CAACCCCATCTAAACTACCTT				
TCF7	NM_003202	5q31.1	S	CAACAACTCCCCTAACAAATTTC	-1346	-1092	10	1
			A	GATAGGATTTGAATATAGGGAAGTATGG				
			S	GGGAGTTGTTGTTGATTGTAT	-727	-1102	28	2
			A	CAACCCCTATAACTCTCCCA				
			S	GGGTTAGAGGGTTAGTTAGGTT	-526	-916	23	3
			A	CCCTATACCAATCAAAAACTTC				
			S	TGGAGGATGGGGTAAGAGT	-188	-524	19	4
			A	AACCTAAAAATAATCACCCTTCT				
Th-POK	NM_015872	1q22	S	GGGGGAATGAGGTTTTTA	-3297	-2817	40	1
			A	TCCCCTAAACTTCCTAAAACTA				
			S	GGTGGGAGTTAGGTGAATGTA	56	467	25	2
			A	TCAATTAAAACCAATTCCAAAA				

Table 2 Transcription factor gene regions: genomic locations, bisulfite primer assays and the position of the analyzed amplicons relative to the transcription start site as well as the number of analyzed CpG per amplicons, S : sense primer, A : antisense primer

7.3. mRNA primer assays

Gene	Primer orientation	Primer sequence
GAPDH	S	GAAATCCCATCACCATCTTCC
	A	ATGAGTCCTTCCACGATACC
MAF	S	GGACGCGTACAAGGAGAAAT
	A	GCTTCCAAAATGTGGCGTAT
EOMES	S	CGCCACCAAACTGAGATGAT
	A	CAGCACCACCTCTACGAACA
ETV5	S	TGCAGATGCCAAAGATGATG
	A	GATGGTAACTGGGGCGATTA
FOG1	S	ATGTCCAGGCGGAAACAG
	A	GTGGCCTTTTGCTCCATGT
GATA3	S	TACAGCTCCGGACTCTTCCC
	A	GTTGCCCCACAGTTCACAC
HLX1	S	CCTCCAGCAAAGACCTCAAA
	A	CGGTTAGCAGGGAAGTGAGA
NOTCH1	S	GTCCAACCCATGTCTGAACC
	A	GGCAGACACAGGAGAAGCTC
SPI1	S	GTGCAAAATGGAAGGGTTTC
	A	GGGGTAATACTCGTGCGTTT
TBX21	S	CCACCTGTTGTGGTCCAAGT
	A	ACCACGTCCACAAACATCCT
TCF7	S	TCTGCTCATGCATTACCCAC
	A	GATGTGGGCTGTTGAAATGTT
Th-POK	S	GTCTGCCACAAGATCATCCA
	A	TGTGGATCTTCAGCTTGTCG
IFN-γ	S	GACCAGAGCATCCAAAAGA
	A	CTCTTCGACCTCGAAACAGC
IL-10	S	CCAAGCTGAGAACCAAGACC
	A	AAGGCATTCTTCACCTGCTC

Table 3 Intron spanning primer assays for quantitative real – time PCR

7.4. Chromatin immunoprecipitation primer assays

Gene	Region	Primer orientation	Primer sequence
IL10	*1*	S	GACATCATCCTGCCCATTCT
		A	AGGGGCACATGTAAATGACAG
	2	S	TGGTGGGCCAGAAGTTTAAG
		A	GCCTGATTTGGTGCCATAGT
	4	S	TCTCAGCTCACTGCAAGCTC
		A	ACACAGTGAAACCCCGTCTC
	5	S	AGGGAGGCCTCTTCATTCAT
		A	AGCTGTTCTCCCCAGGAAAT

Table 4 Primer assays used for amplification of chromatin crosslinked DNA

7.5. Sample details

7.5.1. Donors included in the T-cell pools

Donor	Age (y)	Gender (m: male, f: female)	Pool
1	36	f	1
2	45	f	1
3	54	m	1
4	41	f	1
5	40	f	1
6	24	m	1
7	59	f	1
8	28	f	1
9	20	m	1
10	44	f	1
11	49	m	2
12	59	m	2
13	41	f	2
14	68	f	2
15	53	m	2
16	52	m	2
17	38	m	2
18	28	m	2
19	33	f	2
20	26	f	2
21	23	f	3
22	51	m	3
23	49	m	3
24	35	f	3
25	35	f	3
26	34	f	3
27	67	m	3
28	38	m	3
29	28	m	3
30	39	m	3

Table 5 Age and gender of the healthy PBMC donors. Four different Th-cell subsets were obtained from each donor and individual subsets were collected in pools. The right column (pool) shows the pool composition.

7.5.2. Donor DNA used for bisulfite PCR cloning experiments

	Analyzed clones
IL-10- / IFN-γ-	
Donor1 age : 54 gender : m	**19**
Donor2 age : 68 gender : f	**17**
IL-10- / IFN-γ+	
Donor1 age : 44 gender : f	**19**
Donor2 age : 59 gender : m	**19**
IL-10+ / IFN-γ+	
Donor1 age : 53 gender : m	**15**
Donor2 age : 67 gender : m	**15**
IL-10+ / IFN-γ-	
Donor1 age : 44 gender : f	**20**
Donor2 age : 23 gender : f	**14**

Table 6 Age and gender of the individuals selected for clone sequencing. The number of clones per individual and cell type is given in the right column.

7.5.3. Lymph node tumor and healthy tissue samples

Sample	Main diagnosis	Anatomical origin	Amount of tumor cells in smear	Pathological Staging Lymphoma (WHO)	Age at extraction	Gender
1	DLBCL	Lymphoid tissue / Lymph node	90	I	56	M
2	DLBCL	Lymphoid tissue / Lymph node	90	I	62	M
3	DLBCL	Lymphoid tissue / Lymph node	90	I	69	M
4	DLBCL	Lymphoid tissue / Lymph node	40	IE	74	F
5	DLBCL	Lymphoid tissue / Lymph node	90	I	75	F
6	DLBCL	Lymphoid tissue / Lymph node	90	I	74	M
7	DLBCL	Lymphoid tissue / Lymph node	85	I	75	M
8	DLBCL	Lymphoid tissue / Lymph node	80	IE	65	M
9	DLBCL	Lymphoid tissue / Lymph node	80	IV	72	M
10	DLBCL	Lymphoid Tissue/ Groin	95	I	69	M
11	DLBCL	Lymph Node	90	I	75	F
12	DLBCL	Lymph Node	90	IIE	72	M
13	DLBCL	Lymph Node	90	I	62	M
14	DLBCL	Lymphoid tissue / Spleen	90	IV	61	M
15	DLBCL	Lymph Node	90	I	61	M
16	DLBCL	Lymph Node	90	I	65	M
17	DLBCL	Lymphoid tissue / Spleen	90	IV	55	M
18	DLBCL	Lymph Node	90	I	56	M
19	DLBCL	Lymphoid Tissue / Abdominal cavity	90	IIE	74	F
20	DLBCL	Testis / Brain	75	IV	66	M
1	T-cell NHL	Lymph Node	100	Not Reported	74	F
2	T-cell NHL	Lymph Node	100	Not Reported	56	M
3	T-cell NHL	Lymph Node	100	Not Reported	35	M
4	T-cell NHL	Lymph Node	95	Not Reported	62	M
5	T-cell NHL	Lymph Node	90	Not Reported	58	M
6	T-cell NHL	Lymph Node	85	Not Reported	68	M
7	T-cell NHL	Lymph Node	90	Not Reported	75	M
8	T-cell NHL	Lymph Node	90	Not Reported	69	M
9	T-cell NHL	Lymph Node	90	Not Reported	60	F
10	T-cell NHL	Lymph Node	90	Not Reported	52	F
11	T-cell NHL	Lymph Node	90	Not Reported	52	F
12	T-cell NHL	Lymph Node	85	Not Reported	73	M
13	T-cell NHL	Lymph Node	85	Not Reported	75	M
14	T-cell NHL	Lymph Node	100	Not Reported	89	M
1	normal	Lymph node	NA	NA	50	M
2	normal	Lymph node	NA	NA	50	M
3	normal	Lymph Node	NA	NA	63	F
4	normal	Lymph Node	NA	NA	74	F
5	normal	Lymph Node	NA	NA	75	M
6	normal	Lymph Node	NA	NA	76	M
7	normal	Lymph Node	NA	NA	74	F
8	normal	Lymph Node	NA	NA	75	M
9	normal	Lymph Node	NA	NA	73	F
10	normal	Para-aortal lymph node	NA	NA	68	F
11	normal	lymph node, Inguinal	NA	NA	89	M
12	normal	lymph node, Inguinal	NA	NA	75	F
13	normal	lymph node, Inguinal	NA	NA	65	M

14	normal	lymph node, Inguinal	NA	NA	72	M
15	normal	Normal lymph node	NA	NA	NA	F
16	normal	Normal lymph node	NA	NA	NA	M
17	normal	Normal lymph node	NA	NA	NA	M
18	normal	lymph node, Inguinal	NA	NA	67	M

Table 7 Lymph node biopsy samples used for methylation measurement of hematopoietic transcription factors. In the second column, the main diagnosis of the patient is given (DLBCL : diffuse large B-cell Non Hodgkin Lymphoma, T-cell NHL: T-cell Non Hodgkin Lymphoma).

7.6. Abbreviation list

aIL4	Anti IL4 antibody
allo DC	Allogeneic dendritic cell
APC	Allophycocyanin
B-cell NHL	B-cell Non Hodgkin lymphoma
bp	Base pairs
BSA	Bovine serum albumine
℃	Celsius degree
CD4	Cluster of differentiation, 4 (surface antigen of helper T -lymphocytes)
CD45RA	Cluster of differentiation, 45, RA isoform, (surface antigen, naive CD4+ T-lymphocytes)
CD45RO	Cluster of differentiation, 45, RO isoform, (surface antigen, memory CD4+ T-lymphocytes)
CD8	Cluster of differentiation, 8 (surface antigen of cytotoxic T -lymphocytes)
CD8	Cluster of differentiation, 8 (surface antigen, T -lymphocytes)
CGI	CpG island
ChIP	Chromatin Immunoprecipitation
c-MAF	c-maf musculoaponeurotic fibrosarcoma oncogene homolog
CNS	Conserved non coding sequence
CpG	5'-CG-3'-Dinucleotide
DC	Dendritic cell
ddNTPs	Di-deoxy-nucleotide triphosphate
DEPC	Diethylpyrocarbonate
DLBCL	Diffuse large B-cell lymphoma
DMEM	Dulbecco's Modified Eagle Medium
dNTPs	Deoxy-nucleotide triphosphate
dsDNA	Double stranded DNA
EDTA	Ethylenediaminetetraacetic acid
EOMES	Eomesodermin
ETV5	Ets variant gene 5
FACS	Flourescence activated cell sorting
FITC	Fluorescein isothiocyanat
FL	Fluorescence
FOG1	Friend of GATA1
GAPDH	Glycerol aldehyd-3-phosphate dehydrogenase
GAPDH	Glyceraldehyde-3-phosphate dehydrogenase
GATA3	GATA binding protein 3
GM-CSF	Granulocyte Macrophage Colony Stimulating Factor
HEPES	4-(2-hydroxyethyl)-1-piperazineethanesulfonic acid
HLX1	H2.0-like homeo box 1
I	Ionomycin
IFN-γ	Interferon gamma gene
IFN-γ	Interferon gamma
IL10	Interleukin 10 gene
IL-10	Interleukin 10
IL13	Interleukin 13 gene
IL-13	Interleukin 13
IL2	Interleukin 2 gene
IL-2	Interleukin 2
IL4	Interleukin 4 gene
IL-4	Interleukin 4

IL5	Interleukin 5 gene
IL-5	Interleukin 5
λ	Wavelength
LOI	Loss of imprinting
LPS	Lipopolysacharide
MACS	Magnetic activated cell sorting
mg	Milligramm
MHC	Multihistocompatibility complex
µl	Microliter
mm	Milimeters
ng	Nanogramm
nm	Nanometers
NOTCH1	Notch homolog 1, translocation-associated
P/I	Phorbol 12-myristate 13-acetate / ionomycin
PBMC	Peripheral blood mononucleated cells
PBS	Phosphate buffered saline
PCR	Polymerase chain reaction
PE	Phycoerythrin
PMA	Phorbol 12-myristate 13-acetate
RA	Rheumatoid Arthritis
rIL-12	Recombinant IL-12
rIL-4	Recombinant IL-4
RPMI	Roswell Park Memorial Institute
SAM	S-adenosylmethionine
SPI1	Spleen focus forming virus (SFFV) proviral integration oncogene
ssDNA	Single stranded DNA
TBX21	T-box protein 21
T-cell NHL	T-cell Non Hodgkin lymphoma
TCF7	Transcription factor 7 (T-cell specific)
TCR	T - cell receptor
TE	Tris - EDTA buffer
Th	helper T-cells
Th-POK	T-helper-inducing POZ/Krüppel-like factor
Treg	regulatory T-cells
TSS	Transcription start site

7.7. Eidesstattliche Erklärung

Hiermit versichere ich, dass die vorliegende Arbeit eigenständig und ohne jede unerlaubte Hilfe angefertigt wurde. Alle von mir verwendeten Hilfsmittel und Quellen sind als solche gekennzeichnet.